

# **Renewable Thermoplastic Composites for Environmentally Friendly and Sustainable Applications**

by

Sungho Park

A thesis  
presented to the University of Waterloo  
in fulfillment of the  
thesis requirement for the degree of  
Master of Applied Science  
in  
Chemical Engineering

Waterloo, Ontario, Canada, 2013

© Sungho Park 2013

## **AUTHOR'S DECLARATION**

I hereby declare that I am the sole author of this thesis. This is a true copy of the thesis, including any required final revisions, as accepted by my examiners.

I understand that my thesis may be made electronically available to the public.

## Abstract

Thermoplastic composites using natural fibres are studied intensively and widely used in applications including automotive, packaging, consumer goods and construction. Good balance of mechanical properties, processability and low cost are great advantages of these materials on top of the environmental benefits. Recently, there have been various efforts to amplify the positive effects on the environment by replacing the conventional polymers by bio-derived renewable polymers in the composites.

Recent studies conducted from our research group showed competitiveness of plant fibre-thermoplastic composites. Implementing the promising results and experience, a new composite design using renewable polyethylene as the matrix material was studied. This polyethylene is a renewable thermoplastic that was derived from sugar cane ethanol. The objectives of this study were to employ renewable high density polyethylene (HDPE) into composites using wheat straw and flax fibre to extend the range of properties of the HDPE while keeping the amount of renewable content to nearly 100%. The chemical resistance of these materials has not been reported before and it was investigated here by measuring and comparing the properties before and after accelerated chemical ageing.

Both wheat straw and flax fibre had two different grades in size. Each of them was compounded with HDPE and additives (antioxidant and coupling agent) in a co-rotating twin screw extruder. The concentrations of fibres were varied from 0 to 30 wt-%. Then, injection molded samples were prepared for measurement of properties: tensile, flexural, impact tests.

The effects of reinforcing fibre size were studied first. Both length and aspect ratio were considered. For both types of fibre composites, a general trend was observed. There was no clear evidence of improvements in flexural (strength and modulus) and tensile (strength, percentage elongation at break) properties with respect to the change in fibre size. However, impact (IZOD impact strength, Gardner impact failure energy) properties showed some improvements. This result was due to no substantial difference in size and aspect ratios in post-processed fibres that were actually residing in the matrix.

There were remarkable improvements in flexural strength and modulus when the fibre content increased. However, minor decreases in tensile properties were observed. Furthermore, the impact properties were very sensitive to the concentration of fibres. As the fibre concentration went up, there were significant decreases in both IZOD impact strength and Gardner impact failure energy.

Chemical resistance of these composites was studied by exposing them in six different chemical solutions (hydrochloric acid, acetic acid, sodium hydroxide, ethyl alcohol, industrial detergent, water) for up to thirty days. The increase in weight and leaching behaviour was observed. As the fibre content increased within the composites, the weight gain was more rapid during chemical ageing. Because there were more fibres exposed on the surface after chemical ageing, it is likely that they contributed to the higher flux of liquids (used for chemical ageing) inside the sample. Among the physical properties, tensile properties were most susceptible to the chemical ageing. One possible reason could be due to the exposed surface area to volume ratio, which was the highest in tensile bars and therefore faster mass transfer taking place into the matrix per volume.

Finally, morphological study using scanned electron spectroscopy (SEM) revealed the damage on the surface when exposed to the chemicals. The fibres on the surface had been leached out in the sodium hydroxide solution leaving empty spaces. The fractured surface was also monitored via SEM. Though there was not enough evidence of strong interfacial interactions between the fibre and the polymer, good dispersions were observed.

## **Acknowledgements**

Foremost, I would like to express the sincere gratitude to my supervisor, Professor Leonardo Simon, for the continuous support of my study and research, for his motivation, enthusiasm and immense knowledge.

I would like to thank Professor Ali Elkamel and Professor João Soares, my thesis committee members, for accepting to be the reader of my thesis, and for all their help and guidance.

I would like to thank all my colleagues, especially Arathi Sharma and Dr. Muhammad Arif for their time and assistance during my research work.

A special thanks to my co-op student Justin Raimbault for his valuable help and support.

I would also like to thank my friends, Heywoong, TaeJung, Hoonsub, Larry, Dongun, Kihun and Baejung, who supported and understood me throughout the time I spent in Waterloo.

Finally, I would like to express the deepest love to Sujin Kwon, who always supported and had confidence in me all the time.

## **Dedication**

존경하고 사랑하는 부모님께 이 논문을 바칩니다.

I would like to dedicate this thesis to my parents, Jukuk Park and Domi Seo, and my little sister, Sanghee for the love and support throughout my life.

## Table of Contents

AUTHOR'S DECLARATION .....	ii
Abstract .....	iii
Acknowledgements .....	v
Dedication .....	vi
Table of Contents .....	vii
List of Figures .....	x
List of Tables.....	xiii
List of Abbreviations.....	xiv
Chapter 1 Introduction.....	1
1.1 Motivation and Objectives.....	1
1.2 Thesis Layout .....	2
1.3 Experimental Plan .....	4
Chapter 2 Literature Review.....	5
2.1 Thermoplastic Composites .....	5
2.2 Renewable Polyethylene.....	6
2.3 Renewable Fibre .....	9
2.3.1 Wheat Straw .....	11
2.3.2 Flax Fibre .....	13
2.4 Additives .....	15
2.4.1 Antioxidant.....	15
2.4.2 Coupling Agent .....	15
2.5 Environmental Impact of Renewable Composite Materials .....	16
2.6 Properties of Interest.....	18
2.6.1 Pre- and Post-Process Fibre Particle Size .....	19
2.6.2 Density .....	19
2.6.3 Flexural Properties.....	20
2.6.4 Tensile Properties .....	22
2.6.5 Impact Properties .....	23
2.6.6 Chemical Ageing and Absorption.....	24
2.6.7 Scanning Electron Microscopy .....	25
Chapter 3 Materials and Methods.....	27

3.1 Materials .....	27
3.2 Sample Preparations.....	29
3.3 Characterization .....	31
3.3.1 Pre- and Post-Processing Fibre Particle Size Analysis .....	31
3.3.2 Density .....	32
3.3.3 Mechanical Properties .....	33
3.3.4 Chemical Ageing and Chemical Absorptions.....	34
3.3.5 Scanned Electron Microscopy.....	35
Chapter 4 Results and Discussions: Wheat Straw-Renewable Polyethylene Composites .....	37
4.1 Fibre Particle Size Analysis .....	37
4.2 Density .....	40
4.3 Mechanical Properties.....	40
4.3.1 Effects of Fibre Size.....	40
4.3.2 Effects of Fibre Concentration .....	42
4.4 Chemical Aging .....	44
4.5 Water and Chemical Absorptions.....	47
4.6 Scanned Electron Microscopy.....	47
4.6.1 Cut Surface from IZOD Impact Test.....	47
4.6.2 Chemically Aged Surface.....	49
Chapter 5 Results and Discussions: Flax Fibre-Renewable Polyethylene Composites .....	51
5.1 Pre- and Post-Processing Fibre Particle Size Analysis .....	51
5.2 Density .....	54
5.3 Mechanical Properties.....	54
5.3.1 Effects of Fibre Size.....	55
5.3.2 Effects of Fibre Concentration .....	56
5.4 Chemical Ageing .....	58
5.5 Water and Chemical Absorptions.....	64
5.6 Scanned Electron Microscopy.....	65
5.6.1 Cut Surface from IZOD Impact Test.....	65
5.6.2 Chemically Aged Surface.....	69
Chapter 6 Conclusion and Recommendation .....	73
6.1 Contributions and Summary .....	73



6.2 Main Conclusions .....	73
6.3 Recommendations .....	75
Bibliography.....	76
Appendix.....	80

## List of Figures

Figure 1.1 Thesis Layout with contents .....	3
Figure 1.2 Experimental Plan.....	4
Figure 2.1 Schematics of Thermoplastic Composite.....	5
Figure 2.2 Types of matrix and dispersed filler materials for thermoplastic composites.....	6
Figure 2.3 Schematics of high density polyethylene (top) and low density polyethylene (bottom) .....	7
Figure 2.4 Process of manufacturing renewable polyethylene from sugar cane .....	8
Figure 2.5 The belly pan of a hybrid-electric experimental vehicle will be made from renewable PE..	9
Figure 2.6 Chemical structure of cellulose (top) and hemicellulose (bottom) .....	11
Figure 2.7 Uses of wheat .....	12
Figure 2.8 Wheat straw-polymer composite as interior part material in Ford Flex 2010 .....	13
Figure 2.9 Sterically hindered phenolic antioxidant IRGANOX 1010 (Ciba).....	15
Figure 2.10 Polyethylene grafted maleic anhydride .....	16
Figure 2.11 Energy requirement, CO <sub>2</sub> emissions and approximate prices to produce 1kg of petrochemical derived low density polyethylene, polyethylene terephthalate, renewable Green polyethylene and its wheat straw composites.....	18
Figure 2.12 (a) Three-point flexural test; (b) tensile test.....	22
Figure 2.13 Illustration of Gardner impact test .....	24
Figure 2.14 Simple schematic image of scanned electron microscope (SEM) .....	26
Figure 3.1 Differential Scanning Calorimetry (DSC) graphics of pure renewable polyethylene resin used in this study .....	27
Figure 3.2 Fourier Transform Infrared spectroscopy of Braskem resin used in this study .....	28
Figure 3.3 Flexural (left, rectangular), Tensile (centre, dumbbell) and Gardner Impact (right, circular) Specimens for Characterizations and Testing .....	31
Figure 3.4 Collecting fibres after processing using a Soxhlet extractor system .....	32
Figure 3.5 Surfaces investigated under SEM. (a) Fractured surface from IZOD impact test; (b) Regular smooth surface of flexural bar .....	36
Figure 4.1 Length in mm of medium wheat straw (MW) and fine wheat straw (FW) particles before processing .....	37
Figure 4.2 Aspect ratio of medium wheat straw (MW) and fine wheat straw (FW) particles before processing .....	38
Figure 4.3 Medium Size Wheat Straw (a) before and (b) after processing .....	38

Figure 4.4 Average length and aspect ratio comparisons of pre- and post-processed wheat straw particles .....	39
Figure 4.5 Density of pure polyethylene and WS composites .....	40
Figure 4.6 Flexural strength, flexural modulus, tensile strength, percentage elongation at break, IZOD impact strength and Gardner impact failure energy of PE-fws20 and PE-mws20 .....	42
Figure 4.7 Flexural strength, flexural modulus, tensile strength, percentage elongation at break, IZOD impact strength and Gardner impact failure energy of PE, PE-fws10, PE-fws20 and PE-fws30 .....	43
Figure 4.8 Property retention in tensile strength, elongation at break, flexural strength, flexural modulus and IZOD impact strength of PE-fws10 at 0, 7, 14 and 30 days of exposure to chemical reagents .....	46
Figure 4.9 Weight change comparison of composites with PE, PE-10fws and PE-20fws. Exposure to HCl, HAc, NaOH, EtOH, IGEPAL, and Water for 0, 7, 14 and 30 days .....	47
Figure 4.10 SEM image of cut surface of (a) pure PE and (b) PE-fws10 composite .....	48
Figure 4.11 Surface of (a) untreated and (b) NaOH treated PE-fws10 composite .....	50
Figure 5.1 Length in mm of medium flax (MF) and fine flax (FF) fibre particles before processing .	51
Figure 5.2 Aspect ratio of medium flax (MF) and fine flax (FF) particles before processing .....	52
Figure 5.3 Average length and aspect ratio comparisons of pre- and post-processed flax fibre particles .....	53
Figure 5.4 Density of pure polyethylene and flax fibre composites .....	54
Figure 5.5 Flexural strength, flexural modulus, tensile strength, percentage elongation at break, IZOD impact strength and Gardner impact failure energy of PE-ff20 and PE-mf20 .....	56
Figure 5.6 Flexural strength, flexural modulus, tensile strength, percentage elongation at break, IZOD impact strength and Gardner impact failure energy of PE, PE-ff10, PE-ff20 and PE-ff30 .....	57
Figure 5.7 Property retention in tensile strength, elongation at break, flexural strength, flexural modulus and IZOD impact strength of PE-ff10 at 0, 7, 14 and 30 days of exposure to chemical reagents .....	60
Figure 5.8 Weight change comparison of composites with PE, PE-10ff and PE-20ff. Exposure to HCl, HAc, NaOH, EtOH, IGEPAL, and Water for 0, 7, 14 and 30 days .....	65
Figure 5.9 SEM image (100x, 5kV) of the fractured surface of PE-ff10 .....	66
Figure 5.10 SEM images of the fractured surface of PE-ff20 at (a) 100x and 5kV, and (b) 500x, 5kV with broken fibre (in the red dotted circle) .....	67
Figure 5.11 SEM image (100x, 5kV) of the fractured surface of PE-ff30 .....	68

Figure 5.12 SEM image (100x, 5kV) of fractured surface of PE-ff20 with air pockets .....	69
Figure 5.13 SEM image (50x, 5kV) of the surface of PE-ff10.....	70
Figure 5.14 SEM image (50x, 5kV) of the surface of PE-ff30.....	70
Figure 5.15 SEM images of the surface of PE-ff10 aged in 10% NaOH solution for 30 days. (a) 50x and 5kV; (b) 500x and 5kV; Red circles highlight empty spaces where fibres leached out .....	72

## List of Tables

Table 2.1 Applications of glass-fibre plastic composites in Europe in 2010 (Witten 2010) .....	10
Table 2.2 Physical properties of glass and some plant fibres (Zini 2011).....	10
Table 2.3 Flax production statistics in year 2010-2012 (Ministry of Agriculture and Agri-Food Canada 2012) .....	14
Table 2.4 Density of commodity polymers, glass, water and ethanol at room temperature .....	20
Table 3.1 Concentrations of Diluted Chemical Reagents .....	29
Table 3.2 Samples prepared with different wheat straw sizes and concentrations, and different polymer concentrations .....	29
Table 3.3 Samples prepared with different flax fibre sizes and concentrations, and different polymer concentrations .....	30
Table 4.1 Tensile strength, elongation at break, flexural strength and modulus, IZOD impact strength, and Gardner impact failure energy of pure PE and WS composites .....	41
Table 4.2 Tensile strength, elongation at break, flexural strength, modulus and IZOD impact strength of pure PE and PE-fws10 composite samples after 30 days of exposure to various chemical reagents .....	45
Table 5.1 Average length and aspect ratio of post-processed fibres .....	53
Table 5.2 Tensile strength, elongation at break, flexural strength and modulus, IZOD impact strength, and Gardner impact failure energy of flax composites .....	55
Table 5.3 Tensile strength, elongation at break, flexural strength, modulus and IZOD impact strength of 10% fine flax composite (PE-ff10) samples after 30 days of exposure to various chemical reagents .....	58
Table 5.4 Tensile strength, elongation at break, flexural strength, modulus and IZOD impact strength of 10, 20 and 30% fine flax composite samples after 7, 14 and 30 days of exposure to various chemical reagents .....	61
Table 5.5 Tensile strength, elongation at break, flexural strength, modulus and IZOD impact strength of 10, 20 and 30% medium flax composite samples after 7, 14 and 30 days of exposure to various chemical reagents .....	63

## List of Abbreviations

%	Percentage
cm	Centimeter
CO <sub>2</sub>	Carbon Dioxide
DSC	Differential Scanning Calorimeter
EtOH	Ethyl Alcohol
FF	Fine Flax
ft	feet
FTIR	Fourier Transform Infrared Spectroscopy
FWS	Fine Wheat Straw
g	gram
GPa	Gigapascal
H <sub>2</sub> O	Water
HAc	Acetic Acid
HCl	Hydrochloric Acid
HDPE	High Density Polyethylene
in	Inch
J	Joule
kg	kilogram
lb	Pound
LDPE	Low Density Polyethylene
LLDPE	Linear Low Density Polyethylene
m	metre
MF	Medium Flax
mg	Milligram
MJ	Megajoule
mm	Millimetre
MPa	Megapascal
MWS	Medium Wheat Straw
NaOH	Sodium Hydroxide
nm	Nanometre
PA	Polyamide
Pa	Pascal
PC	Polycarbonate
PE	Polyethylene
PE-10ff	10 Weight Percent Fine Flax-Polyethylene Composite
PE-10fws	10 Weight Percent Fine Wheat Straw-Polyethylene Composite
PE-10mf	10 Weight Percent Medium Flax-Polyethylene Composite
PE-10mws	10 Weight Percent Medium Wheat Straw-Polyethylene Composite

PE-20ff	20 Weight Percent Fine Flax-Polyethylene Composite
PE-20fws	20 Weight Percent Fine Wheat Straw-Polyethylene Composite
PE-20mf	20 Weight Percent Medium Flax-Polyethylene Composite
PE-20mws	20 Weight Percent Medium Wheat Straw-Polyethylene Composite
PE-30ff	30 Weight Percent Fine Flax-Polyethylene Composite
PE-30fws	30 Weight Percent Fine Wheat Straw-Polyethylene Composite
PE-30mf	30 Weight Percent Medium Flax-Polyethylene Composite
PE-30mws	30 Weight Percent Medium Wheat Straw-Polyethylene Composite
PEMA	Polyethylene Grafted Maleic Anhydride
PET	Polyethylene Terephthalate
PLA	Poly(lactic acid)
PMMA	Polymethyl Methacrylate
PP	Polypropylene
SEM	Scanning Electron Microscopy
UV	Ultraviolet
wt-%	Weight Percent





# Chapter 1

## Introduction

### 1.1 Motivation and Objectives

Thermoplastic composites using natural fibres are widely used in applications including automotive, packaging, consumer goods and construction. Good balance of mechanical properties, processability and low cost are great advantages of these materials on top of the environmental benefits. Conventional petrochemical derived thermoplastics including high and low density polyethylene and polypropylene are some widely used matrix polymers in the composites. More recently, there have been various efforts to amplify the positive effects on the environment by replacing the conventional polymers by bio-derived renewable polymers.

Poly(lactic acid) (PLA) is one of the most commonly investigated renewable synthetic thermoplastics. Natural fibre reinforced PLA composites were characterized and were proved to have competitive mechanical properties. It has many excellent assets including its biodegradability. However it lacks long term durability required in certain applications. Cellulose acetate, polyethylene terephthalate and polyamide are also available options these days as renewable plastics.

A more recent commercial alternative to renewable thermoplastics was unveiled by Braskem SA, which has commercialized polyethylene produced from ethylene that is made from ethanol derived from sugar cane. Polyethylene produced from this method is from renewable resources. This is valuable since it is an effective way to capture carbon dioxide. This alternative gives another opportunity to utilize the renewable thermoplastics into composites. The molecular, chemical and physical properties of this renewable polyethylene

are the same as the polyethylene made from petrochemical ethylene. However, the availability is limited to few grades currently.

There is a wide variety of natural fibre that can be applied for the composites. Recently, wheat straw, hemp, kenaf, flax oat hull and banana leaf are all under intensive investigation. Our research group has recently developed polypropylene filled with wheat straw fibre suitable for injection molding and application in interior automotive parts.

The objectives of this study were to employ renewable high density polyethylene (HDPE) into composites using wheat straw and flax fibre to extend the range of properties of the HDPE while keeping the amount of renewable content to nearly 100%. The chemical resistance of these materials has not been reported before and it was investigated here by measuring and comparing the properties before and after accelerated chemical ageing.

## **1.2 Thesis Layout**

This thesis is composed of 6 chapters. The layout is presented in Figure 1.1.

The first chapter has motivation and objectives of the overall study with the layout and the experimental plans. The second chapter reviews some literature about materials, processing and testing techniques. The next chapter lists material used along with the preparation and testing procedures. Chapter 4 and 5 provides experimental results and the discussions. Finally the last the chapter concludes the study and recommends some future works.

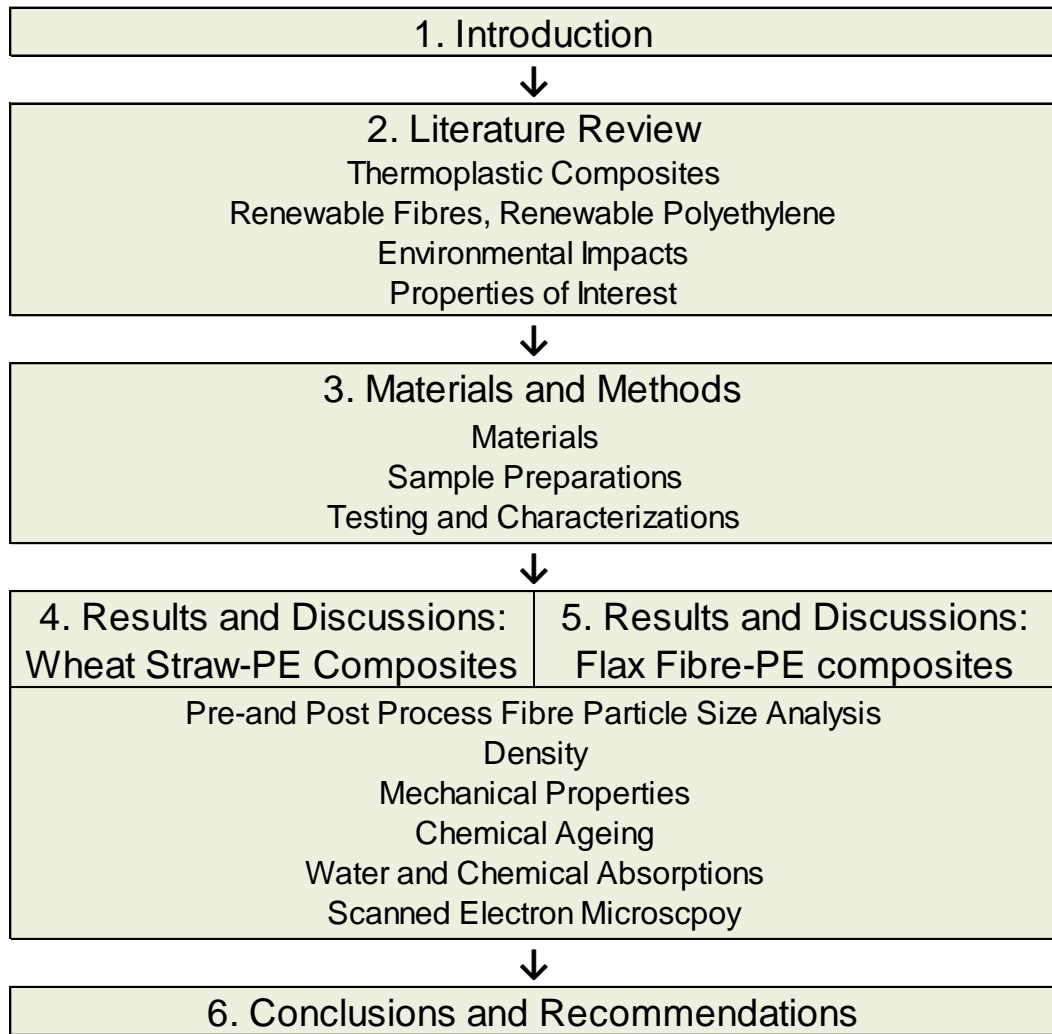


**Figure 1.1 Thesis Layout with contents**

### 1.3 Experimental Plan

Figure 1.2 summarizes the experimental plans with materials, processing and characterization procedure.

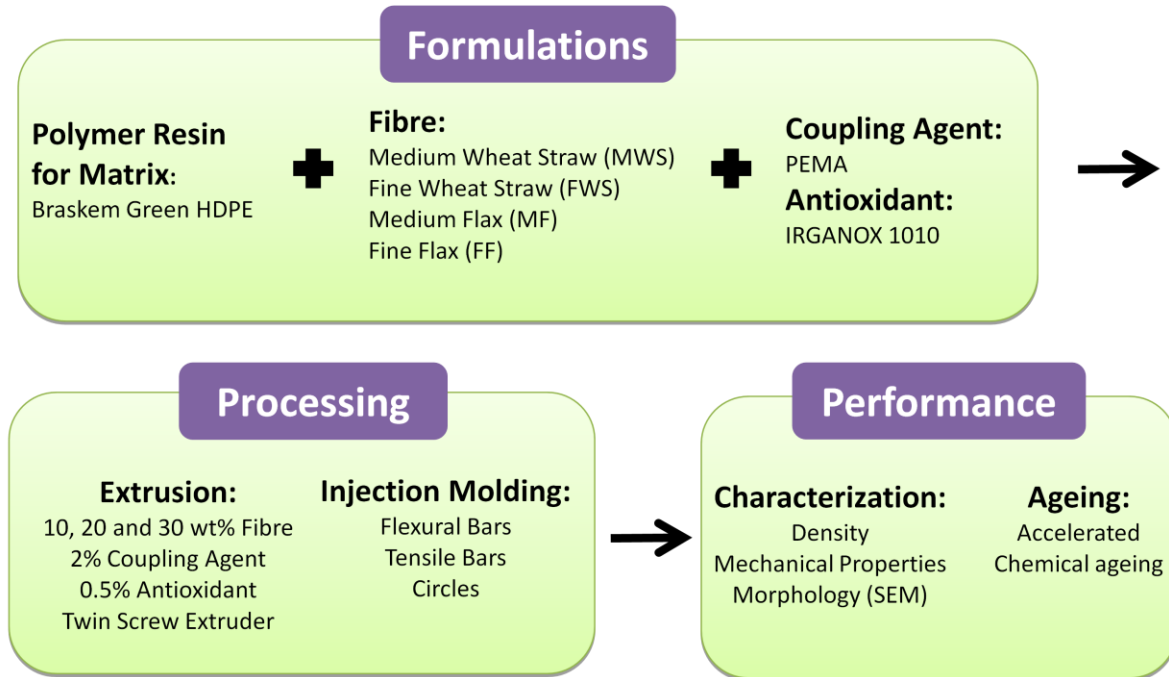


Figure 1.2 Experimental Plan

## Chapter 2

### Literature Review

#### 2.1 Thermoplastic Composites

Plastic materials can be categorized into two different groups: thermosets and thermoplastics. Thermosets are irreversibly cured that once the hardening process is completed, they cannot be reshaped. On the other hand, thermoplastics are easily reshaped number of times with high temperature. (Fried 2003) Because of this advantage, thermoplastics are applied in many areas via various processing techniques. However, as the society always demands materials with better performance in specific applications, thermoplastics are utilized into the form of composites.

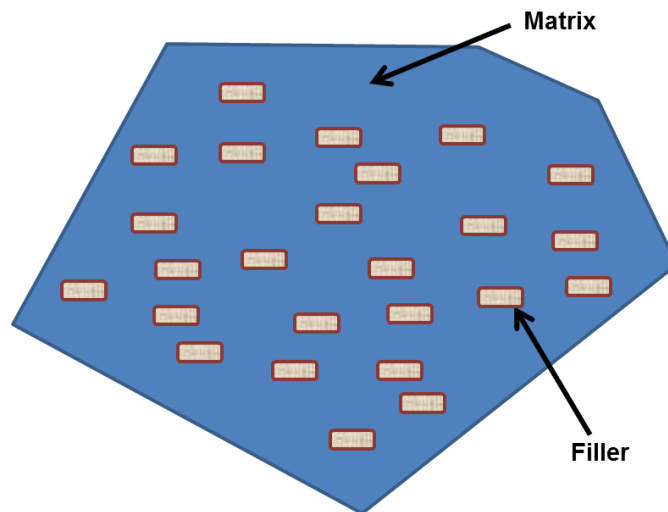


**Figure 2.1 Schematics of Thermoplastic Composite**

The ultimate purpose of composite material is to improve the properties by combining two or more different materials together. The idea of composite is applied in not only plastics but

also metals and ceramics. As seen in Figure 2.1, thermoplastic composites are combined with matrix and dispersed filler. Matrix is the thermoplastics material and the filler (or dispersed phase) can be varied depending on the purpose and applications. It can be further categorized into renewable and non-renewable material for the matrix, and organic and inorganic for the filler. (Zini 2011) Figure 2.2 shows some of the examples in different groups of material. Utilizing renewable thermoplastics and organic fillers is the products of more recent developments. These materials will be further discussed in the later sections.

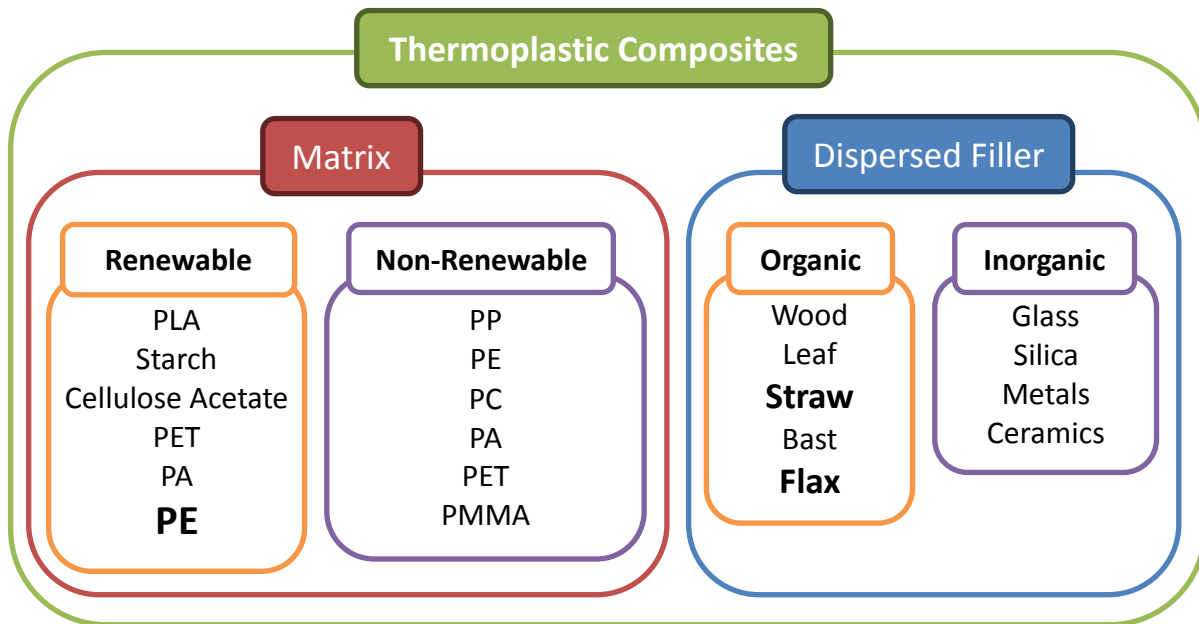
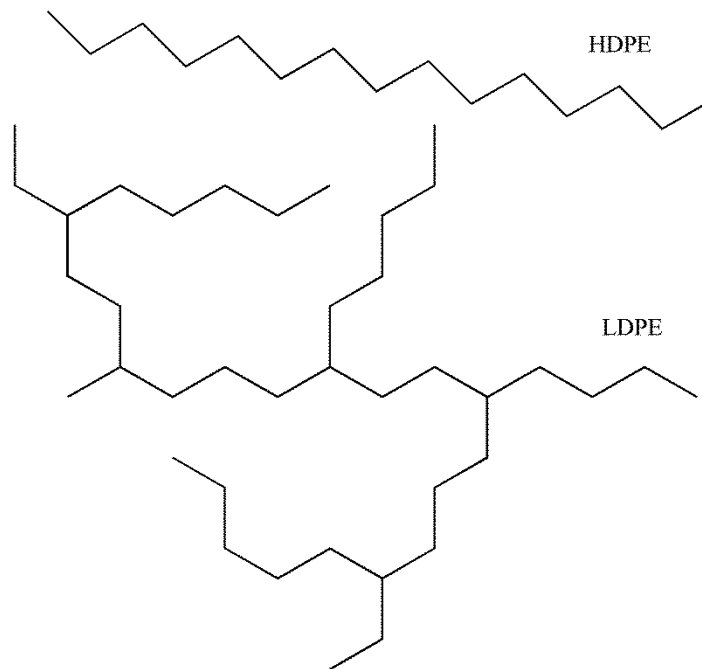


Figure 2.2 Types of matrix and dispersed filler materials for thermoplastic composites

## 2.2 Renewable Polyethylene

A commodity plastic, polyethylene (PE) is the most widely used plastic in the world. It is under the category of thermoplastic which can be easily processed and re-processed using high temperature. The chemical formulae only contain carbon and hydrogen atoms. PE can be further categorized into different groups based on their density. High density polyethylene (HDPE) has a density range between 0.940 and 0.965 g/cm<sup>3</sup>, low density polyethylene (LDPE) has a range between 0.915 and 0.942 g/cm<sup>3</sup>, and there are other subcategories such as linear low density polyethylene (LLDPE). (Hernandez 2004) The difference in density is determined by their degree of crystallinity which is determined by the amount of side chains

(degree of branching in the chemical structure chemical structures). HDPE has long linear chains with minimum amount of side chains whereas LDPE contains a higher amount of side chains off the main chain than HDPE (Figure 2.3). Due to its long chains with little branching, HDPE shows higher crystallinity than LDPE and, therefore, has higher density. Because of this, HDPE tends to have better chemical resistance and higher opacity than LDPE. Main applications for HDPE include household chemical containers, shampoo bottles, cosmetic containers, pharmaceutical bottles and other packaging applications. LDPE, on the other hand, shows other desirable properties including clarity, and flexibility; main applications are containers, shopping bags, agricultural films and stretch-wraps.



**Figure 2.3 Schematics of high density polyethylene (top) and low density polyethylene (bottom)**

The traditional way of manufacturing PE is based on non-renewable sources using ethylene feedstock-petrochemicals. Though it has been a luxury to human being to have this material over a century and used every day, it is based on non-renewable resources. According to the government of India's Central Institute of Plastics Engineering and Technology, the global demand of PE will grow from 80 M ton in 2012 to 120 M ton in 2020. This is a very rapid increase and is problematic if the petrochemical derived PE is used continuously. Additionally, in many markets the consumers have requested materials that are

environmentally friendly and have reduced CO<sub>2</sub> footprint. Therefore, the major driving force for renewable thermoplastics is based on consumer demand.

A more environment friendly alternative was recently commercialized by a chemical company in Brazil (Braskem SA). Instead of collecting resources from petrochemical, they harvested sugar cane and manufactured PE from it. Ethanol extracted from sugarcane becomes the source of the monomer, ethylene. Then the ethylene is polymerized to produce PE (Figure 2.4). (Morschbacker 2009)

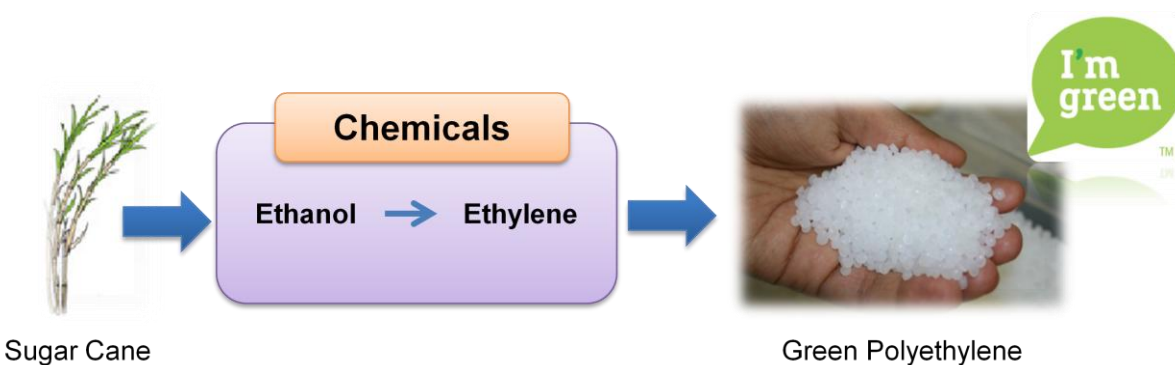


**Figure 2.4 Process of manufacturing renewable polyethylene from sugar cane**

The sugar cane production accounts about 7.8 hectares and only about 1% of this land is used specifically for ethanol production. Therefore it hardly competes against the food sources. Also, this method is a very sustainable way of manufacturing. It has significantly lower greenhouse gas emissions with nearly 100% made from renewable materials. This PE's bio-based carbon content analysis report can be found in the Appendix section. The production captures about 2.5 kg of CO<sub>2</sub> per 1kg of PE resin produced. (Braskem 2009)





**Figure 2.5 The belly pan of a hybrid-electric experimental vehicle will be made from renewable PE**

The PE produced via this environment friendly method is no different from the one derived from petrochemicals. Although there are limited numbers of grades present today, their properties are as excellent as the counterpart. Braskem produces HDPE, LDPE and LLDPE for specific applications. More recently, some companies including Proctor and Gamble started mass production of their consumer product using this renewable PE. A group of students from the University of Waterloo participating in a hybrid-electric vehicle competition mounted the belly pan made from this material as well (Figure 2.5).

### **2.3 Renewable Fibre**

Reinforcing polymers using glass fibre in commodity plastics are very attractive due to high mechanical properties with low cost (Witten 2010). These glass fibre reinforced plastics applied in various applications including transportation industries such as automotive and aeronautics. However, the major downside of this material is associated with the high density (approx.  $2.5 \text{ g/m}^3$ ). This significantly increases the weight of the material considering commodity plastics have densities around  $1 \text{ g/m}^3$ . Considering the transportation of this

material, it is the opposite of what today's environmental expectations since it requires more energy.

**Table 2.1 Applications of glass-fibre plastic composites in Europe in 2010 (Witten 2010)**

Applications	Percentage
Construction	36%
Transportation	34%
Electronic	14%
Sports & Leisure	14%
Others	2%

Natural fibre reinforced plastics are reported to be used as early as 1900's. Natural fibres became good alternatives to heavy non-renewable fillers such as glass fibres. They have much lower specific gravity than glass. Sometimes these fibres are byproducts of agricultural industry and do not compete with food production. When put into composites with thermoplastic matrix to replace glass fibre, they boast low weight, low cost and high properties. There already are many studies to understand their properties and processing techniques since late 20<sup>th</sup> century. Some of physical properties are listed in Table 2.2.

**Table 2.2 Physical properties of glass and some plant fibres (Zini 2011)**

Fiber	Density (g/cm <sup>3</sup> )	Elongation (%)	Young's Modulus (GPa)	Tensile Strength (MPa)
Glass	2.5	2.5	70	2000-3500
Flax	1.5	1.2-3.2	27-80	345-1500
Cotton	1.5-1.6	3.0-10	5.5-12.6	287-800
Jute	1.3-1.5	1.5-1.8	10.0-55.0	393-800
Hemp	1.5	1.6	70	550-900
Sisal	1.3-1.5	2.0-2.5	9.4-28	511-635

In North America, crops such as wheat, soy, corn and flax are very abundant, whereas in East Asia, rice in the number one crop grown and harvested. Even the same species have different genotypes around the world. Because of this, plastic composite materials containing these fibres vary depending on the availability as well.

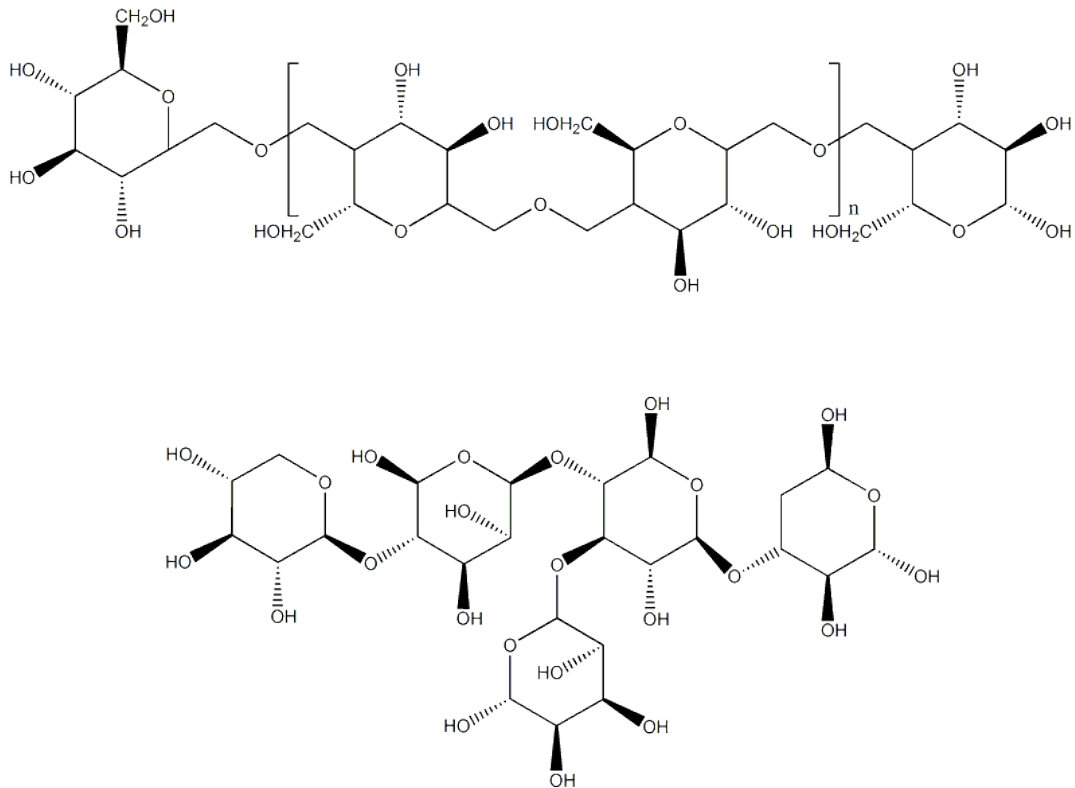


**Figure 2.6 Chemical structure of cellulose (top) and hemicellulose (bottom)**

The three main chemical structures of plant fibres are cellulose, hemicellulose and lignin. The concentration of these constituent plays major roles for the mechanical and chemical properties of end products. The cellulose content is crucial for good strength, stiffness and stability, whereas hemicellulose also contributes to structural stability. Other components include small compounds such as wax and pectin. (Mohanty 2005) Figure 2.6 shows structures of cellulose and hemicellulose. Though lignin also plays a role in structural support, it may cause potential problem when fibres are mixed with plastic. This is because lignin has a low thermal stability temperature and can contribute to thermal degradation when processing thermoplastic composites.

### 2.3.1 Wheat Straw

Wheat straw is one of the most abundant crops harvested in Canada. Grain takes about 30% and the straw takes about 70% by weight of the plant. Grain is the desired product and used as food. Straw is the byproduct and is utilized in areas including animal beddings, mushroom

composting, and sometimes burned as biofuel. Millions of tones of this byproduct residue are produced in the industries. Uses of wheat are well categorized in Figure 2.7. Recently, wheat straw became one of plant fibres that are popular as filler materials in plastic composites. High contents of cellulose (35-40%) and hemicellulose (45-55%) in the fibre make wheat straw a good reinforcing material for the polymer matrix. (McKean 1997) There have been numerous studies and publications utilizing wheat straw as dispersed phase in the composite materials during the last couple of decades. (Helbert 1996, Hornsby 1997, Panthapulakkal 2006) Many of them have demonstrated the benefits of using this fibre.

As briefly mentioned in the introduction chapter, a recent exciting development of wheat straw-polypropylene composites from our research group have been utilized as an automotive interior part. 2010 Ford Flex contains a trim bin that was manufactured using this material (Figure 2.8). It was a great step forward showing the wheat straw-plastic composites have competitive features that the material can replace other traditional plastics.

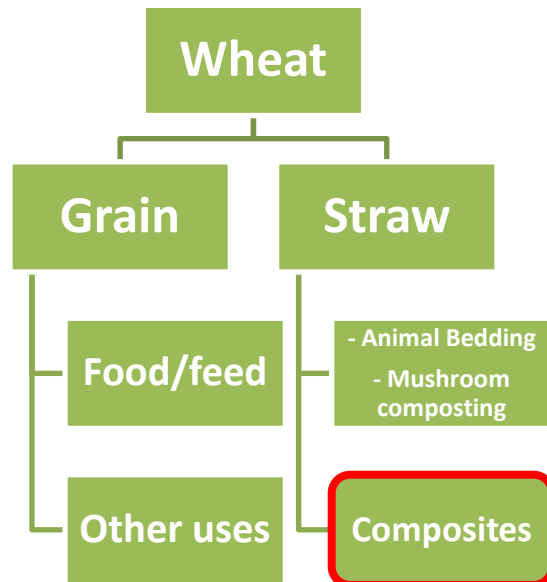


Figure 2.7 Uses of wheat



Figure 2.8 Wheat straw-polymer composite as interior part material in Ford Flex 2010

### 2.3.2 Flax Fibre

Flax is a blue-flowered plant grown in cool and northern climate. Flax has taken a crucial role in Canadian agricultural economy. Canada is the leader in world flax production. Annually, over 0.5 million ton of flax products are produced in Alberta, Saskatchewan, and Manitoba. It is one of five major Canadian crops and is exported to Europe, the US, Japan and South Korea. (Flax Council of Canada 2012) Over 90% of flax products produced in Canada is exported. The primary commercial product is the oilseed. According to Ministry of Agriculture and Agri-Food Canada, Over 400 kha of area was seeded and 1.36 ton/ha of yield was recorded in 2012 (Table 2.3) (Ministry of Agriculture and Agri-Food Canada 2012).

Farming flax always has problems with the byproducts. The stem fibres take a long time to decompose and this makes it difficult to spread onto the soil after harvest. Because flax fibres wrap themselves and sit in the soil they become potential obstacles to wheels and shovels.

Traditionally they were burned directly, but these days, they are collected and chopped effectively first and then spread back in the field. They are also used as animal bedding and burning sources. Another commercial use is to make specialty papers such as cigarette paper and bible book paper.

**Table 2.3 Flax production statistics in year 2010-2012 (Ministry of Agriculture and Agri-Food Canada 2012)**

Year	2010-2011	2011-2012	2012-2013
Area Seeded (kha)	374	281	425
Area Harvested (kha)	353	273	403
Yield (t/ha)	1.2	1.35	1.36
Production (kt)	423	368	547
Exports (kt)	404	410	525

Recently, flax processors turn their interest to the filler for plastic composites. Flax plastic composites are reported to be used to make interior automotive parts. One of the advantages of flax is that is a relatively tall plant, thus contains less contaminants. Also, the fibre content can vary from 8 to 40% by weight. (Flax Council of Canada 2012) This means the useful fibre tonnage could be up to 250,000 ton annually.

Elaborating more on potential applications, there are numerous opportunities for the uses of flax fibre. By simply burning the bales, it becomes a good fuel sources. Local commercial users in the agricultural or mining industry can utilize this burning source. Also, it can be used in pulping industry as pulp sweeteners. During the paper recycling process, flax fibre can be added to maintain the original strength as every recycling process reduce the mechanical properties of paper (Gutierrez 2003).

Flax has been utilized in other industries as a plastic reinforcing material for weight reduction, low cost and positive environmental impact. There have been numerous studies conducted and published utilizing this fibre into plastic composites. Many of them showed the competitiveness of the material that can be utilized in various types of applications. (Oksman 2003, Baley 2002, Cantero 2003) Studies show the long flax fibres can have benefits of producing equivalent stiffness-to weight ratio compared to glass fibres. However, the long fibres are particularly difficult to process with plastic and the processing temperature

is limited because they thermally degrade after a long exposure to high temperature (Bravo 2011).

## 2.4 Additives

### 2.4.1 Antioxidant

Most plastic processing involves high temperature and pressure environment. Oxidation reaction can easily happen in this environment resulting degradation of polymers. Oxidation reactions produce free radicals that cause damage to the polymeric chains. The physical appearance and the mechanical performance of the final product can be affected by the oxidation reaction. (Murphy 1996) An effective way to avoid this thermal degradation via oxidation of the material is to use antioxidant.

Common antioxidant species used in polyolefin (PE, PP, etc.) processing are sterically hindered phenolic substances (Figure 2.9). They prevent the oxidation during the high temperature processing by preventing the formation of free radicals. (Pritchard 1998)

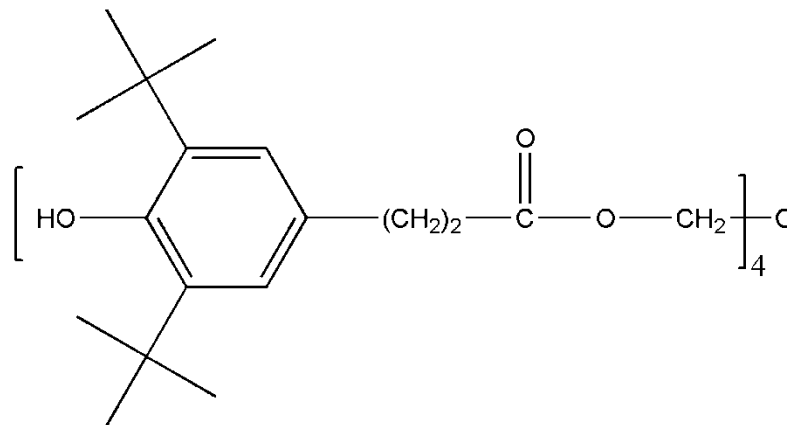


Figure 2.9 Sterically hindered phenolic antioxidant IRGANOX 1010 (Ciba)

### 2.4.2 Coupling Agent

Plant fibres tend to have hydrophilic in nature whereas some polymers including PE and PP are hydrophobic. When combining the two substances into composites, it is quite challenging due to the difference. There is a need for bridging materials that can hold both hydrophilic

and hydrophobic phases. A material that has both hydrophobic and hydrophilic ends that can interact with fibres and the polymer will do the job.

Often coupling agent is used as additives while processing the plant fibre-polymer composites. For example, polyethylene grafted maleic anhydride has a long PE chain covalently attached to hydrophilic maleic anhydride end (Figure 2.10). This amphiphilic structure enhances the adhesion between the two different phases. (Karian 2003)

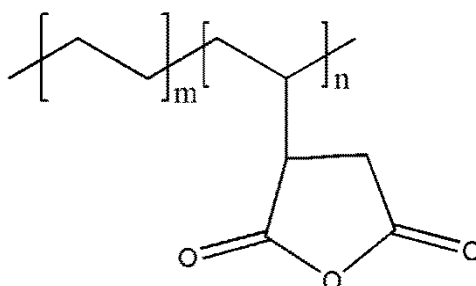


**Figure 2.10 Polyethylene grafted maleic anhydride**

There have been studies showing the improvements in mechanical properties of composites when the right amount of coupling agents were used. (Cui 2010, Fatoni, 2012, Liu 2003) The optimization step is necessary to maximize the advantage of using the substances.

## **2.5 Environmental Impact of Renewable Composite Materials**

Employing both matrix and reinforcing materials from renewable sources, the environmental benefit of replacing the traditional material is quite significant. A visualization and comparison to traditional polymer materials have been done in this section. There were three factors considered: energy requirement, CO<sub>2</sub> emissions and approximate cost. The energy requirement is measured in mega joule (MJ) per kilogram of material produced. The CO<sub>2</sub> emission has the unit of kg of CO<sub>2</sub> emitted per kg of material produced. Finally, the approximate cost is compared in US dollars per kg of material.

The energy requirement for the renewable PE (Green PE) is 57 MJ/kg. (Braskem 2009) This is significantly lower compared to traditional PE production, 83 MJ/kg. Petrochemical



driven materials including polystyrene (88 MJ/kg), polyethylene terephthalate (83 MJ/kg) and polypropylene (77 MJ/kg) have significantly high energy requirements. (Vink 2003)

As highlighted in earlier sections, the Green PE captures CO<sub>2</sub>. It captures 2.5 kg of CO<sub>2</sub> per kg of resin produced. That is, it has a negative CO<sub>2</sub> footprint. (-2.5 kg CO<sub>2</sub>/kg material). (Braskem, 2009) Again this environment friendly material is advantageous over traditionally manufactured PE emitting 2.1 kg of CO<sub>2</sub> per kg of resin produced. Polystyrene, polyethylene terephthalate, and polypropylene produce 2.75, 3.3, and 2 kg of CO<sub>2</sub> per kg of resin produced respectively. (Vink 2003)

With approximate costs of these materials and employing wheat straw as the reinforcing material in the composites (ICIS Pricing 2012), visual comparison was done in Figure 2.11. The price of wheat straw was provided from industrial partner. The size of circle represents the energy requirement for production. It is clearly seen that Green PE has smaller size than LDPE and PET. Its size gets further reduced when wheat straw content increases in the composites. In terms of CO<sub>2</sub> emissions, the Green PE and its composites are located on the left half (carbon capturing) of the graph whereas LDPE and PET are located on the right side (carbon emitting). It is also expected to see the reduction in cost when the WS content increases in the composite.

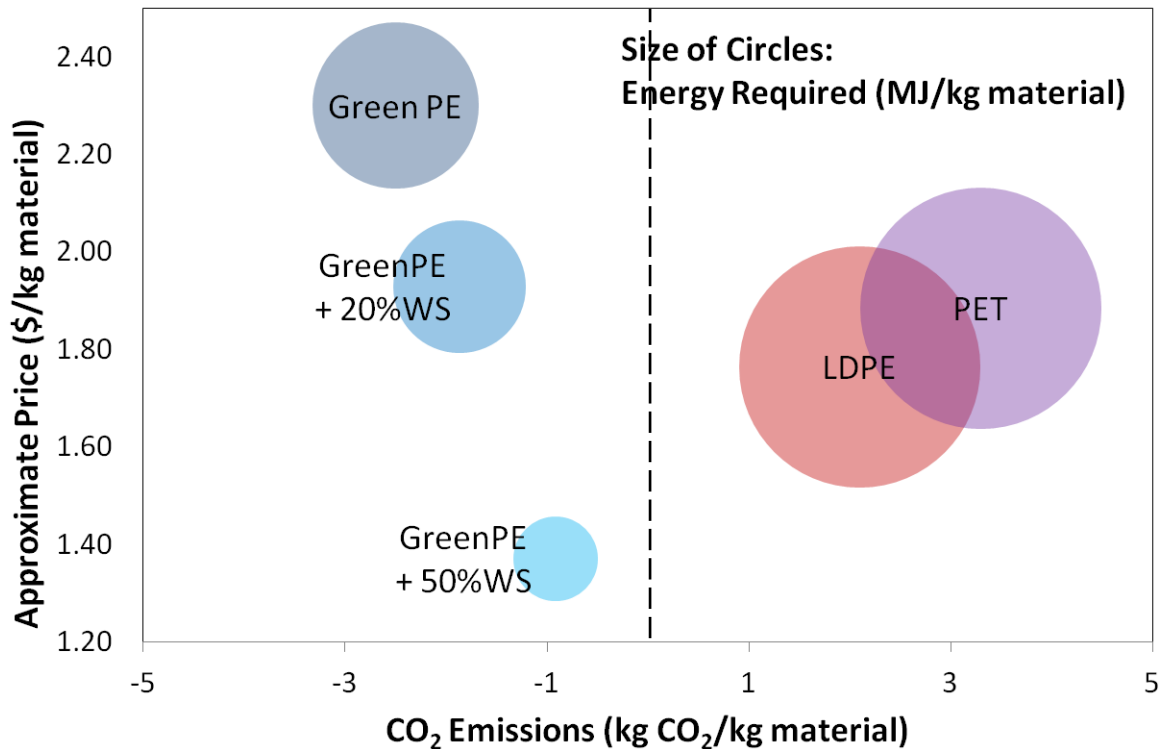


**Figure 2.11 Energy requirement, CO<sub>2</sub> emissions and approximate prices to produce 1kg of petrochemical derived low density polyethylene, polyethylene terephthalate, renewable Green polyethylene and its wheat straw composites**

## 2.6 Properties of Interest

Characterization of composite materials can be done via both quantitative and qualitative investigations. There are standardized methods such as American Society for Testing and Materials (ASTM) standards available to follow. Repeated trials are necessary to report the data and to analyze.

Not only the material itself but also the processing environments and technique can influence the properties. Even with the same material, if one was injection molded and the other was hot pressed, they certainly show different physical properties. If one was processed at high temperature and the other was processed at low temperature, again, they will exhibit differences.

Information about the properties of interest is covered in this section. Fibre particle size, density, strength, modulus, impact behaviour, chemical ageing behaviour and chemical resistance are all included.

### **2.6.1 Pre- and Post-Process Fibre Particle Size**

Before producing composites, the morphology of the reinforcing materials is to be analyzed. Colour, length, width and the aspect ratio are properties of interest. However, the reinforcing material tends to change these properties once it goes through a series of high temperature and pressure processing steps. (Reddy 2010) During extrusion process, large amount of stress can be applied to the particles and may end up breaking into smaller pieces. Therefore, it is necessary to analyze the reinforcing particles after the processing as well. It gives not only the better understanding of the composites but also the information about how much damage the processing has done to the particles.

Aspect ratio of a particle can be defined as the ratio between the length and the width. A sphere will have an aspect ratio of 1 whereas long string will have a very high aspect ratio. Although the orientation of the particles in the matrix can vary the result, generally speaking, high aspect ratio yields higher stiffness and strength of composites (Le Moigne 2011, Puglia 2008). Hence, it is a crucial procedure to do the size analysis and obtain the aspect ratio.

It is difficult to do study on the small fibre particles with simple visual inspection (naked eyes). Often, they are observed using optical microscope or sometimes electron microscope for micrometer or smaller (nanometer). The images can be processed by available software and the aspect ratio is easily calculated.

### **2.6.2 Density**

Density measurement of material is one of the most elementary but significant steps of characterization. Materials with fine physical properties with low cost are desired and traditionally, many reinforcing materials have been utilized to achieve this goal. For example, glass fibre reinforced plastics have been suitable for the needs. However, if there are lighter and low density alternatives available, transporting these materials will consume less energy.

For the automotive applications, lighter parts will reduce the weight of the vehicle and therefore improvement in fuel efficiency is expected. Both manufacturer and the end user can benefit from low density material.

There is a standardized test measuring plastic material's density and specific gravity (ASTM D792). This method is suitable for testing in both water and liquids other than water. For some polymer and polymer composites, their specific gravity is less than one at room temperature and therefore they float in water. Hence, liquids that have a lower density than water such as ethanol are used to measure these polymers. The dry mass and the apparent mass upon immersion of samples are used to calculate the specific gravity.

Density of some commodity polymers, glass, water and ethanol are listed in Table 2.4 (Hernandez 2004, Clemons 2010).

**Table 2.4 Density of commodity polymers, glass, water and ethanol at room temperature**

Material	Density (kg/m <sup>3</sup> )
Low Density Polyethylene	915-942
High Density Polyethylene	940-965
Polypropylene	855-946
Polyethylene Terephthalate	1300-1400
Polyamide (Nylon 6,6)	1150
Polycarbonate	1200-1220
Glass	2490
Water	1000
Ethanol	789

### 2.6.3 Flexural Properties

Commonly used flexural testing methods, three point and four point bending tests measure the force required to bend a beam of plastic. Both ASTM D790 and ISO 178 are three point bending tests for flexural properties. Flexural strength measures the ability to resist against flexural deformation (bending). The modulus gives the ratio between the strength and the strain. A schematic image of the three point test is shown in Figure 2.12 (a). The load cell attached takes the measurement and sends both displacement and force data to the computer attached. Then the following formulae calculate flexural strength, strain and the modulus:

$$\sigma_f = \frac{3PL}{2bd^2}; \quad \varepsilon_f = \frac{6Dd}{L^2}; \quad E_B = \frac{\sigma}{\varepsilon_f}$$

where:

$\sigma_f$  = strength or stress in the outer surface at midpoint, MPa

P = load at given point, N

L = support span, mm

b = width of beam tested, mm

d = depth of beam tested, mm

$\varepsilon_f$  = strain in the outer surface, mm/mm

D = maximum deflection on the centre of the beam, mm

$E_B$  = modulus of elasticity in bending, MPa

Rigid fillers for the plastic composites commonly increase the stiffness. However, they may have negative effects on the strain to failure. The strength of the material also can be reduced when there is not enough interfacial interaction between the fillers and the matrix. (Haupt & Wetzel, 2005) (Leong, Abu Bakar, Mohd. Ishak, Ariffin, & Pukanszky, 2004) If the stress is not sufficiently transferred from one phase to the other, the reduction in mechanical properties may occur.

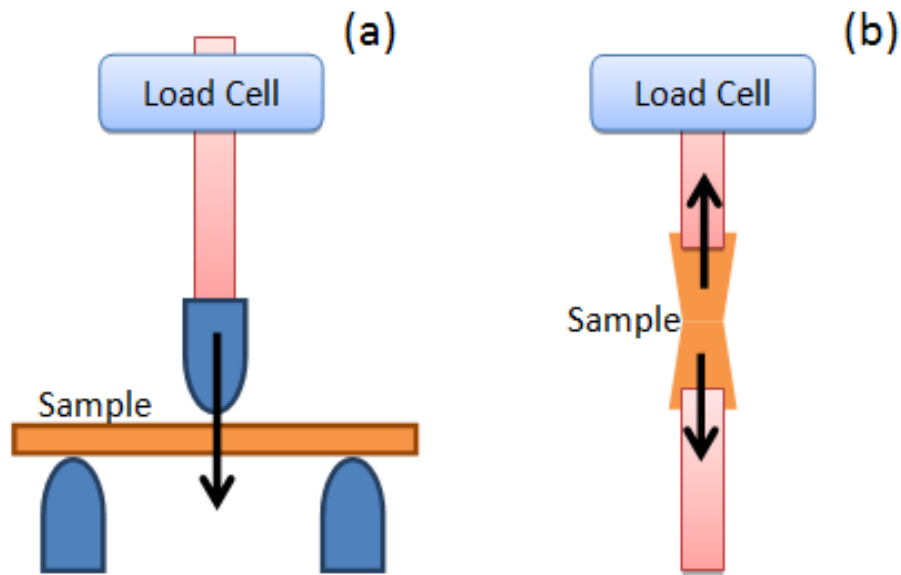


Figure 2.12 (a) Three-point flexural test; (b) tensile test

#### 2.6.4 Tensile Properties

Figure 2.12 (b) shows a schematic image of a tensile test. The specimen undergoes deformations and the load cell attached transports the stress data to the computer. This procedure can provide tensile strength, modulus and elongation at break. Typically, a specimen undergoes elastic deformation which is a reversible one. Once, it reaches the yield strength (elastic limit), the visco-elastic deformation takes place. Visco-elastic (plastic) deformation is a permanent one that the material loses elasticity. Eventually, the failure occurs. Brittle materials tend to have no noticeable changes while the sample elongates prior to the failure (Black 2011).

A stress-strain curve helps to visualize the phenomenon during the test. Tensile strength can be calculated by dividing the maximum load by the average cross-sectional areas. The percent elongation at break is obtained by dividing the length of extension by the original gauge length and multiplying by 100%. ASTM D1708 describes a standard method for tensile properties of plastics by use of microtensile specimens.

### **2.6.5 Impact Properties**

Impact is a very important aspect when characterizing materials. Impact tests are conducted in numerous ways that each of them has different advantages.

IZOD impact test uses a pendulum, which specimen is held in a cantilevered beam in IZOD. A notch is made prior to the test and the pendulum hits the top half of the notched specimen. The test shows impact strength which is the amount of energy that the specimen withstands and absorbs before the fracture. The value is reported in J/m. ASTM D256 well describes standard methods for the IZOD pendulum impact resistance of plastics.

Another useful type of standardized method is the Gardner impact test. It determines the relative ranking of materials according to the amount of energy required to crack or break a flat specimens. A weight falls in a vertical tube and hit the striker resting on top of a specimen. Repeated trials are to be conducted and the mean failure energy is reported. Figure 2.13 illustrates tool components of Gardner impact test. ASTM D5420 describes the standard methods of Gardner impact test.

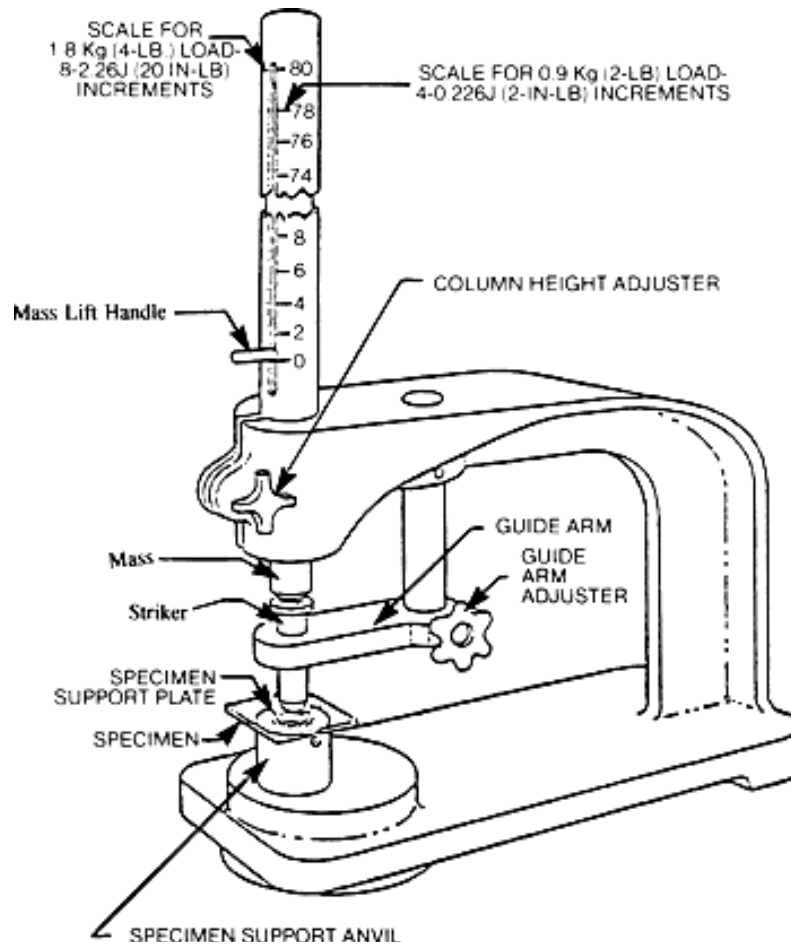


**Figure 2.13 Illustration of Gardner impact test**

### **2.6.6 Chemical Ageing and Absorption**

Ageing of plastic materials can occur due to many reasons. High or low temperature, ultraviolet radiation, biological (microbial) factors and chemical wearing are all common cause of plastic ageing. (Hamid 2000) Packaging applications such as liquid storage tanks, household chemical containers and automotive applications such as windshield washer fluid tanks are all in direct contact with different chemicals. It is crucial to determine the effect of these chemicals on the properties of the plastic materials.

Plant fibre-plastic composites are especially sensitive to water due to the fibre's hydrophilic environment. The osmosis takes place that the moisture gets absorbed into the



matrix via the fibres. When in contact with not only water but also low and high pH, and organic contents, detrimental effects on the material's performance may be expected.

There is a list of standard reagents that can be used in ageing process in ASTM D543. This list includes inorganic and organic acids, alkalis, alcohol, and industrial detergent. The mechanical property tests following the immersion in these reagents along with monitoring the weight changes of specimens will assist to understand the ageing behavior.

### **2.6.7 Scanning Electron Microscopy**

Scanning electron microscopy (SEM) is a powerful tool to investigate the morphology of materials. It yields a very high resolution of images by utilizing a beam of electron traveling to the surface of the samples. Depending on the microscope, SEM has an ability to see nano-size structures.

Nevertheless, there is a disadvantage of using electron beam over visual wave length (optical microscopy). The surface of the material has to be conductive so that electrons can travel easily. A lot of plastic composites are non-conductive materials. Therefore, without any pre-treatment, it is impossible to visualize under the SEM. To overcome this disadvantage, the samples are coated with a thin layer of either carbon or gold. (Echlin 2009)

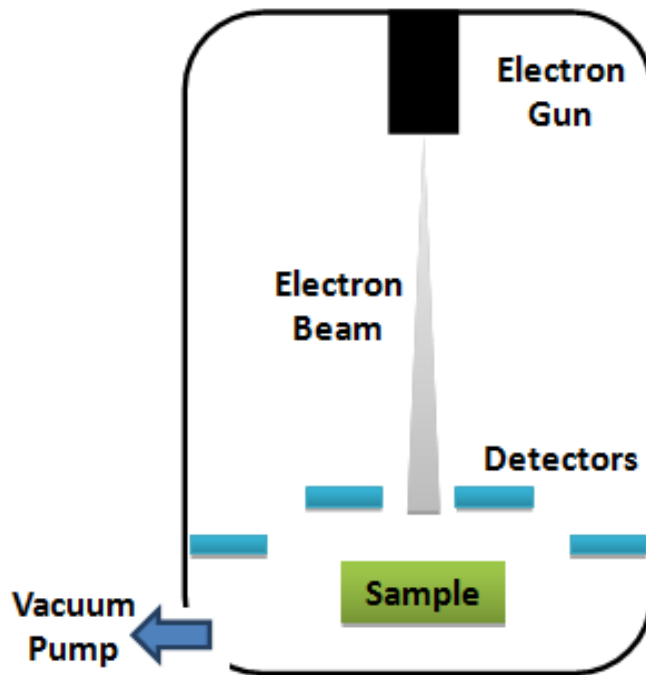


**Figure 2.14 Simple schematic image of scanned electron microscope (SEM)**

A simplified schematic image illustrating the mechanism of SEM is illustrated in Figure 2.14. The electron gun shoots electron beam towards the sample with a known voltage. Once the electron reaches the surface of the sample, they interact with the surface and scatter. Different detectors are mounted and detect the specific scattering of electrons. (Amelinckx 2008)

There are a few valuable morphological properties that can be obtained when studying the composites via SEM. The roughness of the surface, amount of fibres present on the surface, distribution of fibres in the matrix, fracture mechanisms and interaction between different phases are all important characteristics to investigate under the SEM. Furthermore, chemically aged samples can be compared with the pre-treated ones.

## Chapter 3

### Materials and Methods

#### 3.1 Materials

Extrusion grade (MFI = 0.33 g/10min at 190°C, 5kg, ASTM D1238) high density polyethylene [SGM9450F] (Braskem, Brazil) in white pellet form was used as the matrix material. Differential Scanning Calorimetry (DSC) and the Fourier Transform Infrared Spectroscopy (FTIR) measurement of this polyethylene resin are shown in Figure 3.1 and Figure 3.2 respectively. This polymer is a new grade offered by Braskem being made by renewable carbon. Ethanol extracted from sugar cane was the source of ethylene, and the ethylene went through polymerization to manufacture polyethylene.

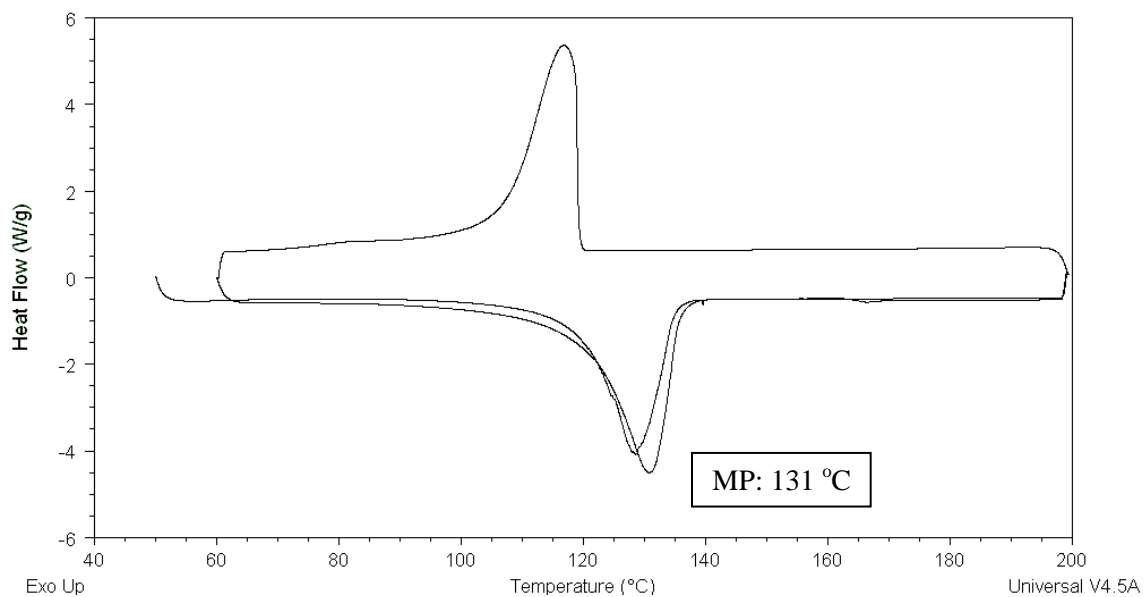


**Figure 3.1 Differential Scanning Calorimetry (DSC) graphics of pure renewable polyethylene resin used in this study**

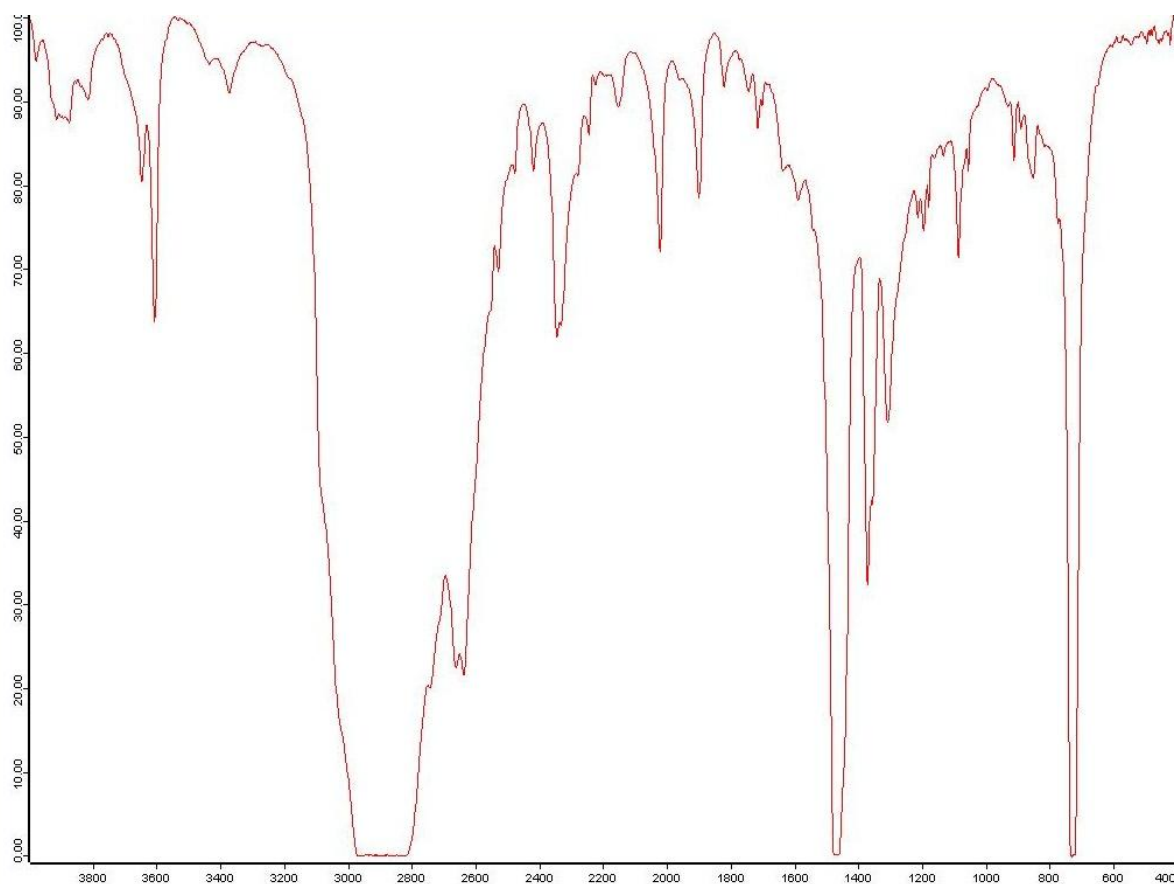


**Figure 3.2 Fourier Transform Infrared spectroscopy of Braskem resin used in this study**

Wheat straw was harvested from the regions in Ontario, Canada and obtained through a distributor (OMTEC, Canada). There were two different sizes of wheat straw used. Fine grade wheat straw went through a sieve that has a size of 0.5 mm and the medium grade with the sieve size between 0.5 and 1.3 mm. Two different kinds of flax fibre were used as well. FlaxFill™ and FlaxFlour™ from SWM International were used. The flax was harvested from Manitoba and Saskatchewan, Canada, and North Dakota, USA. Antioxidant Irganox 1010 (BASF) and the Licocene polyethylene grafted maleic anhydride (PEMA) 4221 fine grain (Clariant) were used as additives.

Chemical reagents include hydrochloric acid (Fisher Scientific), glacial acetic acid (Fisher Scientific), sodium hydroxide (Caledon Laboratory Chemicals, Canada), ethyl alcohol (VWR), IGEPAL CO-630 (Sigma-Aldrich) and deionized water. The chemical reagents were diluted in deionized water and their concentrations are shown in Table 3.1.

**Table 3.1 Concentrations of Diluted Chemical Reagents**

Chemical Reagent	Concentration (wt-%)
Hydrochloric Acid	10
Acetic Acid	5
Sodium Hydroxide	10
Ethyl Alcohol	50
IGEPAL	10

### 3.2 Sample Preparations

Both wheat straw composites and flax composites had six different formulations prepared to study the effects of fibre size and concentrations. Table 3.2 and Table 3.3 summarize the formulations of each component in the composites. Polyethylene (PE) was prepared and tested as a reference. 10, 20 and 30 wt-% fine (PE-fws10, PE-fws20, PE-fws30) and 10 and 20 wt-% medium (PE-mws10, PE-mws20) size wheat straw composites were prepared. Formulations with 10, 20 and 30% fine (PE-ff10, PE-ff20, PE-ff30) and 10 and 20 wt-% medium (PE-mf10, PE-mf20, PE-mf30) size flax fibre composites were prepared as well. Antioxidant was added at 0.5 wt-% to all formulations and coupling agent was added 2 wt-% to formulations containing straw or flax.

**Table 3.2 Samples prepared with different wheat straw sizes and concentrations, and different polymer concentrations**

Labels	Wheat Straw		HDPE	Antioxidant	Coupling Agent
	Type (f/m)	Concentration (wt-%)	Concentration (wt-%)	Concentration (wt-%)	Concentration (wt-%)
PE	-	0	97.5	0.5	2
PE-fws10	fine	10	87.5	0.5	2
PE-fws20	fine	20	77.5	0.5	2
PE-fws30	fine	30	67.5	0.5	2
PE-mws10	medium	10	87.5	0.5	2
PE-mws20	medium	20	77.5	0.5	2

**Table 3.3 Samples prepared with different flax fibre sizes and concentrations, and different polymer concentrations**

Labels	Flax Fibre		HDPE	Antioxidant	Coupling Agent
	Type (f/m)	Concentration (wt-%)	Concentration (wt-%)	Concentration (wt-%)	Concentration (wt-%)
PE	-	0	97.5	0.5	2
PE-ff10	fine	10	87.5	0.5	2
PE-ff20	fine	20	77.5	0.5	2
PE-ff30	fine	30	67.5	0.5	2
PE-mf10	medium	10	87.5	0.5	2
PE-mf20	medium	20	77.5	0.5	2
PE-mf30	medium	30	67.5	0.5	2

The mixtures were first compounded in a co-rotating twin screw extruder (Haake MiniLab Micro-compounder, Thermo Electron Corporation). The mixtures were loaded into the extruder barrel using the hopper. Instead of pushing in the mixtures manually, about 3 kg of weights were used to give pressure evenly and continuously when loaded. This process forces the feed in the extruder. The melting temperature of HDPE used was 131 °C (Differential Scanning Calorimetry measurement – Figure 3.1), therefore, the processing temperature needed to be higher than 131 °C. After numerous trials, the suitable temperature for the extruder was at 165 °C and the rotating speed was 150 rpm.

Then the compounded material was air-cooled and hand pelletized into an average size of 1.0 cm in length. The pellets were then injection molded (Injection Molding Apparatus, Ray-Ran). There were two temperature control panels on the injection molder; one was the barrel and the other was the tool temperature control panels. They control the barrel and the mold temperatures respectively. The barrel temperature was at 190 °C and the tool temperature was set at 115 °C. Pressure of 100 psi with 15 seconds of injection periods was applied. As shown in Figure 3.3, there were three different geometric specimens: plain rectangular bars, dumbbell shapes and circular specimens. The plain bar shaped specimens were used for flexural and impact strength tests (ASTM D790 and ASTM D256), the dumbbell-shaped specimens were used for tensile tests (ASTM D1708), and the circular specimens were for the Gardner impact tests (ASTM D5420).



**Figure 3.3 Flexural (left, rectangular), Tensile (centre, dumbbell) and Gardner Impact (right, circular) Specimens for Characterizations and Testing**

In order to remove the thermal history of the injection molded specimens, annealing procedure was followed. They were put into an oven and the temperature was raised to 120 °C. They were annealed for 15 minutes and cooled down at 10 °C/min rate. The final step prior to testing and characterizations, they were placed into a conditioning chamber with a temperature,  $23 \pm 1$  °C and humidity  $50 \pm 5$  % for 48 hours.

Typically 100 g of pre-processed material yielded 20 flexural and 20 tensile bars, or 25 circles for Gardner's impact test in the end.

### **3.3 Characterization**

#### **3.3.1 Pre- and Post-Processing Fibre Particle Size Analysis**

The analysis on fibre was done prior to processing. Using a stereo microscope (Leica MZ6), images of fibres were taken. The measurements were made using ImageJ, a java-based image processing software. The software gave information including length and width of each fibre particle. The aspect ratio was calculated using the ratio between the length and the width. The length and the aspect ratio of each type of fibre was reported and compared.

In order to collect and investigate the fibres after processing, a Soxhlet extractor was used. Some standards were used as a guide (ASTM C613/C613M). No. 4 ashless filterpaper in a

cone shape was inserted into the soxlet with about 1 to 2 g of processed samples. Xylene was used as a solvent. As a heating source, an oil bath with a temperature range between 205 to 220 °C was used. The extraction process lasted for 24 hours after the first reflux taking place. Finally, the fibres in the filter paper cone was rinsed with fresh boiling xylene and dried in the oven at 50 °C for 10 minutes. The same particle size analysis was done as described earlier.

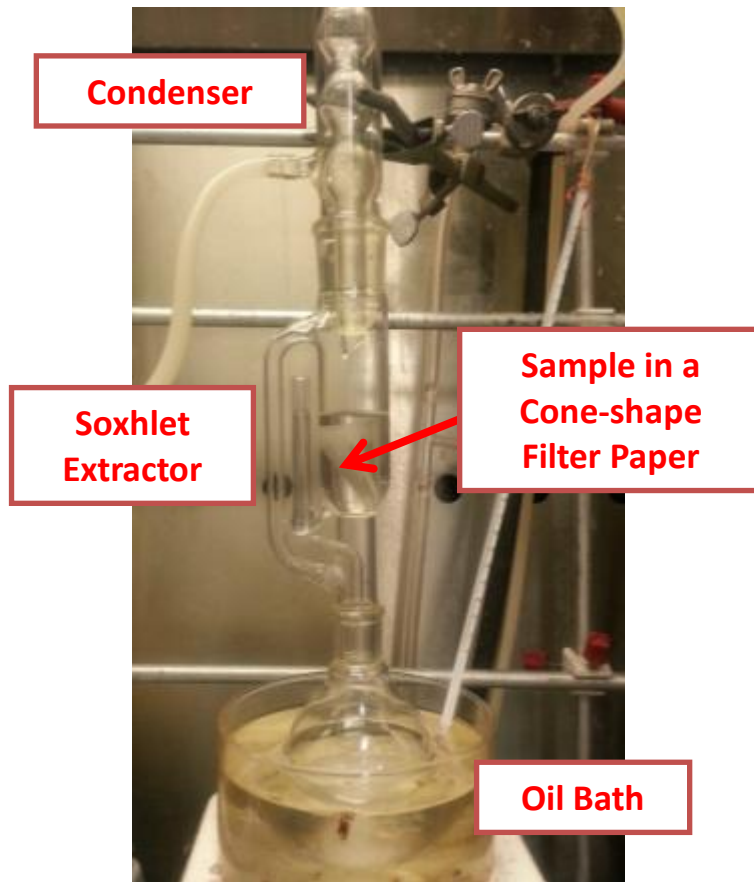


**Figure 3.4 Collecting fibres after processing using a Soxhlet extractor system**

### **3.3.2 Density**

The density of each sample was obtained via the standard method outlined in ASTM D792 at 23°C. Since the density of water is higher than polyethylene and the composites produced, ethanol was used as immersion liquid. Five flexural bars were prepared and cut in half prior to obtaining their dry weights using a Mettler Toledo analytical balance (AB 304-S). Then



the samples were suspended and completely immersed in the ethanol and their weights were measured once again. Finally, the density of ethanol was obtained using a 25 mL pycnometer. As the standard outlines, the specific gravity of the samples were calculated using the following equation:

$$\text{sp gr } 23/23^{\circ}\text{C} = (a*d)/(a-b)$$

where:

sp gr 23/23°C = Specific gravity at 23°C

a = Apparent mass of dry specimen

b = Apparent mass of specimen completely immersed

d = Specific gravity of ethanol

Then, the density was calculated as following:

$$D^{23^{\circ}\text{C}}, \text{ kg/m}^3 = \text{sp gr } 23/23^{\circ}\text{C} * 997.5$$

where:

$D^{23^{\circ}\text{C}}, \text{ kg/m}^3$  = Density of sample at 23°C

### 3.3.3 Mechanical Properties

For the studies of effects of fibre concentration and their sizes, tensile strength and elongation at break data were obtained via tensile tests (ASTM D1708). Q Series Mechanical Test Machine (Test Resources Inc.) was used for testing. A dumbbell shaped bar was placed between the upper and lower grips. The distance between the grips was  $22 \pm 0.5$  mm after placing the bar. Tensile force was applied to pull the bar at a rate of 1.3 mm/min. Six replicate tests were carried out for each sample and their averages with standard deviations were reported. Tensile strength and the percentage elongation at break were calculated via the following equations:

$$\text{Tensile Strength} = \frac{\textit{Maximum Force}}{\textit{Unit Cross – Sectional Area}}$$

$$\% \text{ Elongation at Break} = \frac{\text{final gage length} - \text{original gage length}}{\text{original gage length}} \times 100\%$$

Flexural strength and modulus were found via flexural test (ASTM D790). The same testing machine as the tensile test was used utilizing the 3-point bending system. Six replicate tests were conducted for each sample and their averages with standard deviations were reported. The values were calculated using the equations outlined in Chapter 2.

Impact strength was examined via IZOD impact test (ASTM D256). Test method A of the standard was used. A depth of 2.5 mm notch was creased before the test was conducted. The specimen was mounted vertically on a Monitor Impact Tester (Testing Machine Inc.) and hit by a 5 ft-lb swinging pendulum type hammer at 90°. The result was reported in joules per metre. Six replicate tests were done, and their averages with standard deviations were reported.

Another type of impact analysis was done via Gardner impact test (ASTM D5420) to obtain the impact failure energy. An 8 lb weight was dropped through a guide tube and impacted a striker resting on top of a supported circular specimen. The procedure determined the energy that caused 50% of the specimens tested to fail (mean failure energy). A failure was defined as complete cracking through the specimen. The weight was dropped from a height and if the sample fails, the drop height was reduced by a half an inch. If the sample did not fail then the height was increased by a half an inch. Repeating this procedure more than 20 times, the average failure height was calculated as the ASTM standard indicates.

### **3.3.4 Chemical Ageing and Chemical Absorptions**

The accelerated chemical ageing was carried out with a) 10% hydrochloric acid (HCl), b) 5% acetic acid (HAc), c) 10% sodium hydroxide (NaOH), d) 50% ethyl alcohol (EtOH), and e) 10% IGEPAL solutions prepared in water IGEPAL. The effect of ageing in water was evaluated using deionized water. These reagents and concentrations were selected from the list of suggested standards found in ASTM D543, Standard Practices for Evaluating the Resistance of Plastics to Chemical Reagents. The weights of all testing samples were measured before emerging them into the solutions prepared. The ageing was carried out by

placing the samples in the solutions for 7, 14 and 30 days at room temperature ( $23 \pm 1$  °C). After removing from the solutions, they were rinsed using deionized water, dried, and the weight measurements were taken again. They were placed back to the conditioning chamber for 48 hours prior to mechanical tests. After 30 days, the weights were measured every month up to one year for wheat straw composites and up to 6 months for the flax fibre composites. The weight change was calculated using the following equation:

Weight Change =

$$(\text{Original Dry weight} - \text{Dry Weight after Absorption}) / (\text{Original Dry weight})$$

### **3.3.5 Scanned Electron Microscopy**

For the morphological studies, the scanning electron microscopic (SEM) images were collected using Leo 1550 Gemini SEM. Since the composite materials studied were not conductive, they were gold coated with a thickness of 10 nm. Initially, an Extra High Tension (EHT) value of 10 kV was used to capture the images. However, after a certain time, while taking the images, melting of polymer matrix was observed. Since the discovery, 5 kV of EHT was used instead of 10 kV.

Two different surfaces of composite materials were studied (Figure 3.5). The first surface was the fractured surface from IZOD impact test. For this surface, Secondary Electron 2 (SE2) detection signal was used. The second surface investigated was the smooth surface of flexural bars and InLens detection signal was used.

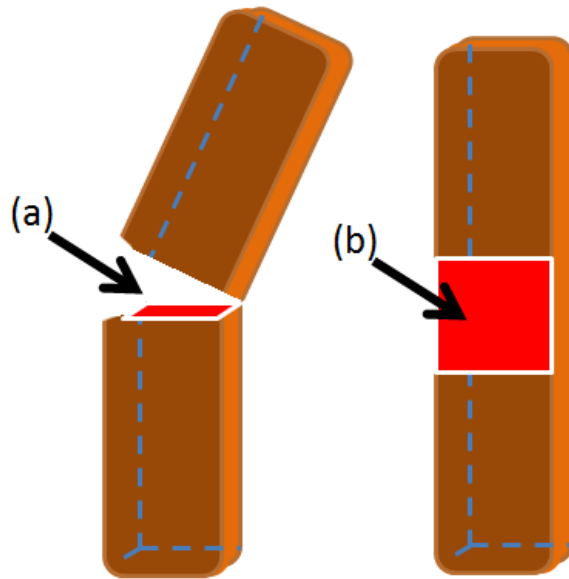


**Figure 3.5 Surfaces investigated under SEM. (a) Fractured surface from IZOD impact test; (b) Regular smooth surface of flexural bar**

## Chapter 4

### Results and Discussions: Wheat Straw-Renewable Polyethylene Composites

#### 4.1 Fibre Particle Size Analysis

Two grades of wheat straws were examined by a series of particle size analyses. Figure 4.1 shows the length of wheat straw particles for both fine and medium grades. The medium grade had an average of 1.08 mm in length with the standard deviation of 0.45mm. The fine wheat straw had 0.65 mm in average length with the standard deviation of 0.36mm. The aspect ratio of wheat straw (ratio between length and width of each particle) was calculated and it is shown in Figure 4.2. The medium wheat straw (MWS) particles had the aspect ratio and its standard deviation of 4.53 and 3.01 respectively. On the other hand, the fine wheat straw (FWS) had aspect ratio of 3.67 and standard deviation of 2.33.

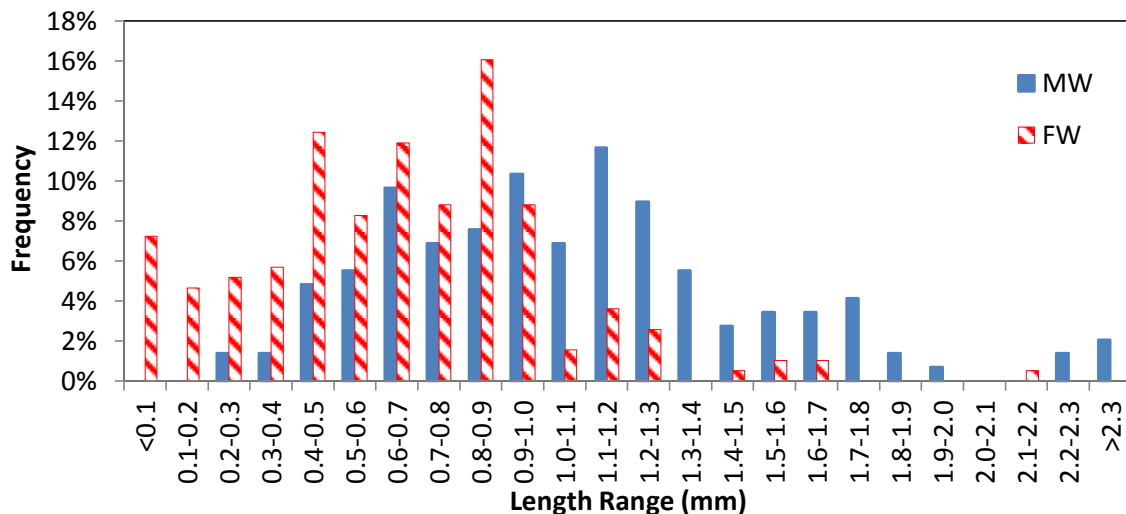


**Figure 4.1 Length in mm of medium wheat straw (MW) and fine wheat straw (FW) particles before processing**

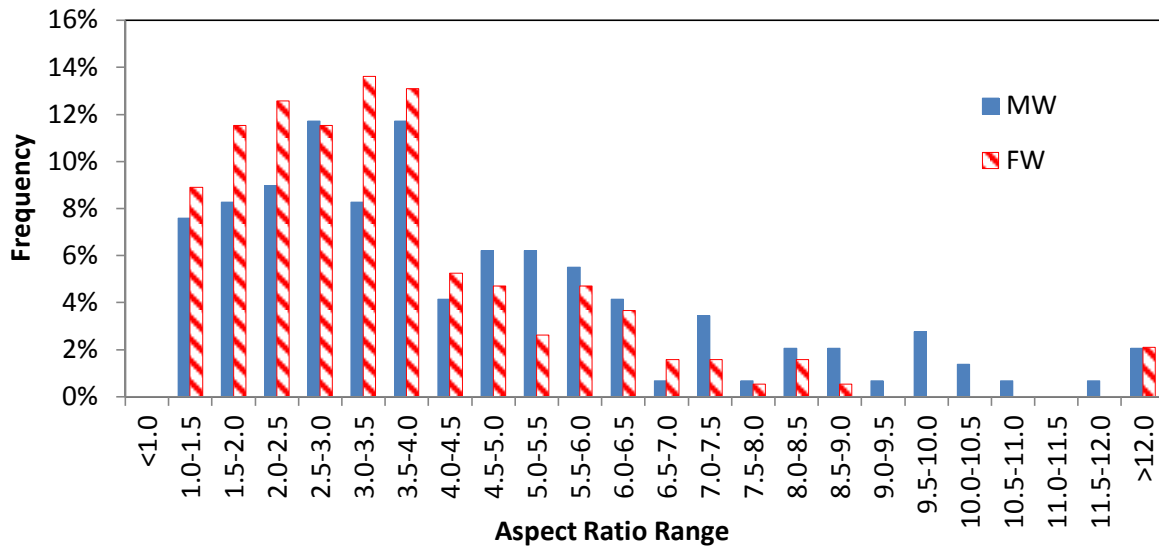


**Figure 4.2 Aspect ratio of medium wheat straw (MW) and fine wheat straw (FW) particles before processing**

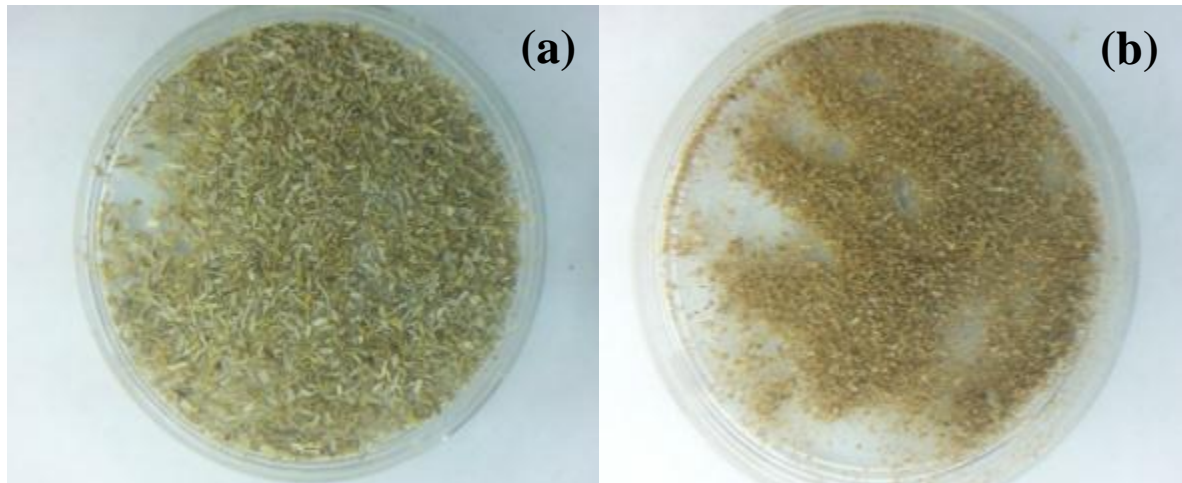


**Figure 4.3 Medium Size Wheat Straw (a) before and (b) after processing**

The particle size changes when the composites are prepared. To evaluate the change in the particle size, the polyethylene and the straw particles were separated using the Soxhlet extraction system. Figure 4.3 compares the fibre before processing and after processing (extrusion and molding). The first observation was the colour change. Definitely, the colour

became darker after processing. Before processing, there was a variety of colours seen from the population; some were white and some showed yellow or yellowish brown. However, after a series of high temperature processing, the colour of the majority of particles became brown. Another observation was the fibre size. Even with simple inspection from naked eyes, it was easy to see the reduction in size. In order to understand this phenomenon better, another particle size analysis was done.

The average lengths of post-processed particle size were 0.49 and 0.42 mm for medium and fine WS respectively. These are significant changes from the original value. MWS particles were reduced by 55% and the FWS particles were reduced by 35%. Both populations showed major reductions in length. Using the new length and the width information, new aspect ratios were calculated. The post-processed MWS and FWS's aspect ratios were 2.68 and 2.63. These are also significant reduction from the original values. These are 41 % and 28 % drops from the pre-process aspect ratios. This means the morphology of particles were changed from rod-like to more sphere-like shape. The high temperature and the shear from the process have influenced the transformation. Figure 4.4 clearly represent the changes. The range distribution comparisons of before and after processing data are found in the Appendix section.

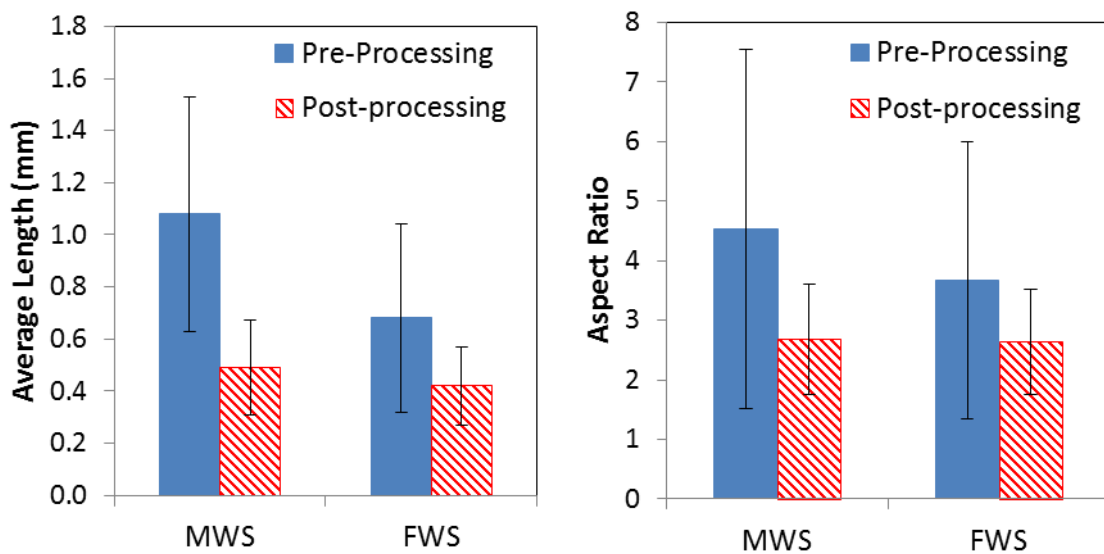


**Figure 4.4 Average length and aspect ratio comparisons of pre- and post-processed wheat straw particles**

## 4.2 Density

The densities of WS composites were measured and they are shown in the Figure 4.5 along with the pure polyethylene sample. As expected, the density of PE was within the typical range of high density polyethylene. Both MWS and FWS composites showed almost linear increase as the fibre contents went up.

The change in density was expected because the density of wheat straw is higher than the density of polyethylene. However, when compared to other composites with inorganic fillers, this is a very minor growth. Sharma has reported the increase in density of talc-polypropylene (PP) composite was much higher when compared WS-PP composites. (Sharma 2012)

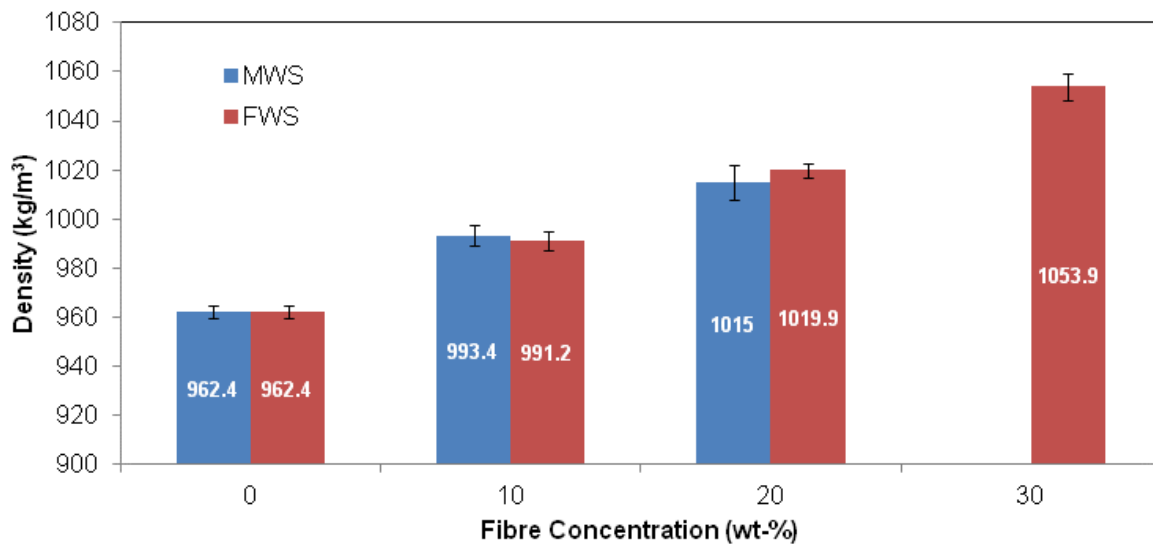


Figure 4.5 Density of pure polyethylene and WS composites

## 4.3 Mechanical Properties

### 4.3.1 Effects of Fibre Size

The formulations shown in Table 3.2 went through a series of mechanical tests and the results are shown in Table 4.1. The comparisons of PE-fws10 to PE-mws10, and PE-fws20 to PE-mws20 were done to study the effects of fibre size in the composites.



**Table 4.1 Tensile strength, elongation at break, flexural strength and modulus, IZOD impact strength, and Gardner impact failure energy of pure PE and WS composites**

Sample	Tensile Strength (MPa)	Elongation at Break (%)	Flexural Strength (MPa)	Flexural Modulus (MPa)	IZOD Impact Strength (J/m)	Gardner Impact Failure Energy (J)
PE	52.46 (0.77)*	33.32 (1.94)	26.20 (1.51)	627.30 (49.32)	471.59 (17.03)	14.31 (0.52)
PE-fws10	53.05 (1.97)	26.64 (1.20)	32.03 (1.37)	723.29 (34.12)	117.63 (7.38)	8.89 (0.23)
PE-fws20	51.38 (1.31)	23.86 (1.07)	38.13 (1.24)	881.75 (48.12)	80.23 (6.70)	6.51 (0.08)
PE-fws30	46.59 (2.13)	18.02 (0.67)	39.09 (3.45)	978.21 (68.52)	62.52 (8.75)	5.40 (0.13)
PE-mws10	52.11 (2.32)	25.21 (1.45)	31.79 (2.18)	708.79 (55.90)	128.78 (8.24)	9.08 (0.23)
PE-mws20	52.09 (1.69)	23.97 (1.80)	38.99 (1.55)	900.21 (30.40)	95.12 (7.15)	7.14 (0.12)

\* The values inside the brackets are the standard deviations of repeated trials.

Figure 4.6 is a comparison of 20 wt-% fibre composites (PE-fws20 and PE-mws20) that helps to visualize the difference in the two. Tensile strength, elongation at break, flexural strength and flexural modulus showed no significant changes when the fibre size increased from fine to medium. However, it was clear to see an improvement in both impact properties (IZOD and Gardner) when fibre size and the aspect ratio increased. At 10 wt-% fibre content, IZOD impact strength increased from 117.63 to 128.78 J/m (9.5% increase). Though it was a small increase, Gardner impact failure energy improved as well (2.1%). This effect was amplified when the fibre contents were doubled. At 20% fibre content (PE-fws20 and PE-mws20), IZOD impact strength and Gardner impact failure energy increased by 18.6% and 9.7% respectively.

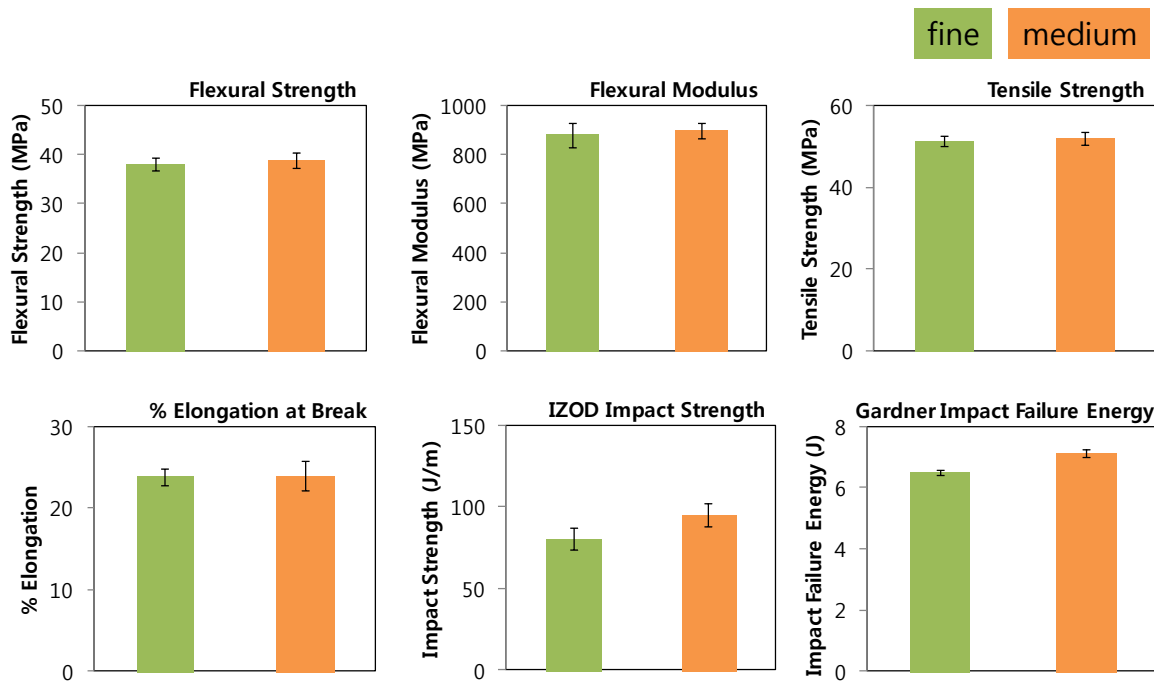


**Figure 4.6 Flexural strength, flexural modulus, tensile strength, percentage elongation at break, IZOD impact strength and Gardner impact failure energy of PE-fws20 and PE-mws20**

Although there were improvements in some mechanical properties when larger size WS with better aspect ratio was implemented, it is difficult to conclude that medium WS has a strong advantage over fine WS. As it was seen in the previous section that both post-processed WS had not a lot of difference in size and aspect ratio regardless of pre-processed conditions. In order to sort the fibres according to their sizes, there has to be another separation process. It is well known that separation process of materials takes majority of energy requirement in overall manufacturing process. It is an obvious decision to reduce as many steps as possible if the result is not affected. Therefore, it can be concluded that there is no significant need for separating fine and medium grades for this purpose of manufacturing PE composites.

#### 4.3.2 Effects of Fibre Concentration

The fibre contents ranged between 0 and 30% in the samples, PE (0 wt-%), PE-fws10 (10 wt-%), PE-fws20 (20 wt-%) and PE-fws30 (30 wt-%). In order to examine the effects of filler concentration, the performance of these samples were compared. These values are also found

in Table 4.1. Figure 4.7 below compares 0, 10, 20 and 30 wt-% fibre composites (fine grade) that helps to visualize the trend and differences.

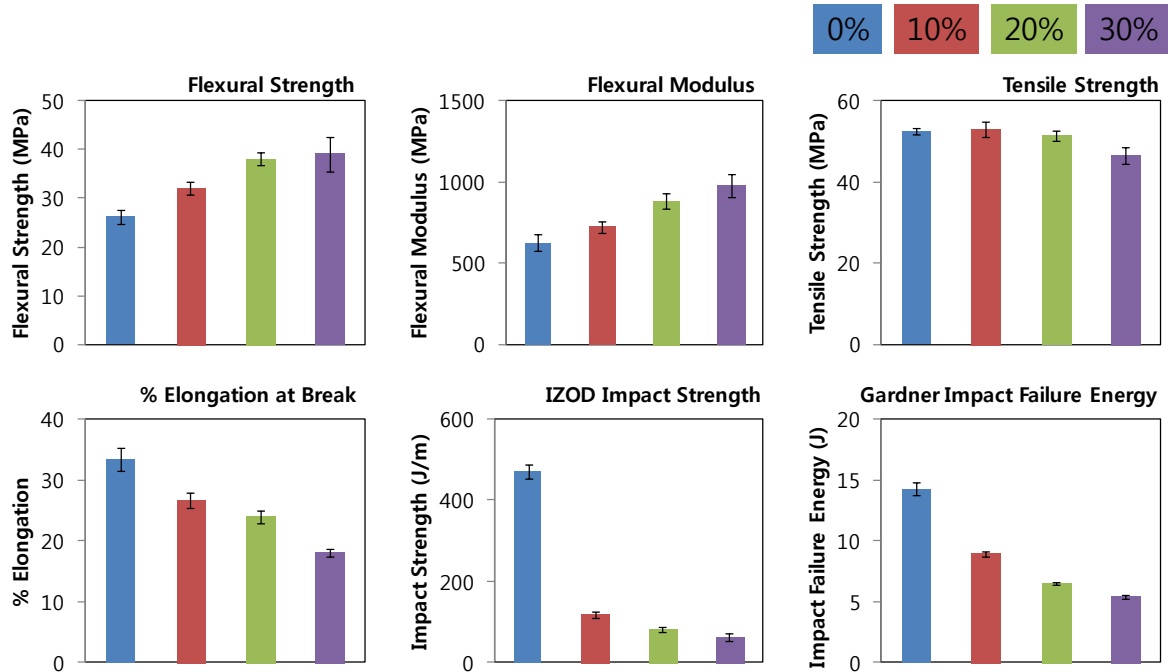


**Figure 4.7 Flexural strength, flexural modulus, tensile strength, percentage elongation at break, IZOD impact strength and Gardner impact failure energy of PE, PE-fws10, PE-fws20 and PE-fws30**

There were evident improvements in some properties whereas some decreased quite significantly as the fibre concentration increased. Flexural strength and modulus increased by 49.2 and 55.9% respectively as the fibre content increased from 0 to 30 wt-% (PE to PE-fws30). It is an obvious result to see the increase in these properties when WS content increased. Rigid particles such as WS improve the stiffness of composites. However, tensile properties appeared to show noticeable decline. Tensile strength dropped from 52.46 to 46.59 MPa (11.9 % decrease) and the elongation at break was reduced from 33.32 to 18.02 % (45.9 % decrease).

As many other previous studies had confirmed, impact properties had the most significant decrease. IZOD impact strength and Gardner impact failure energy were reduced by 86.1 and 62.2 % respectively. Although both these properties are from impact tests, the amounts of decrease are significantly different. This is because of the mechanism of the tests. IZOD

impact test is done on the samples which already have notches. This test gives better parameters for the propagation of cracks than Gardner impact tests. On the other hand, samples for Gardner impact tests do not have a notch or cut prior to the test. Therefore, the failure energy in this test is a combination of energy required first to initiate and then to propagate the cracks.

#### **4.4 Chemical Aging**

Both pure PE and composites containing 10 wt-% of straw (PE-fws10) were put into chemical aging experiment. Table 4.2 summarizes the result obtained after 30 days of exposure to various chemical.

As expected, PE did not show any evident changes in all their properties monitored. The retention of the property is calculated as the ratio of the value of a given property at a given time (after ageing) to the value of the property before ageing. The retention of the properties was very high for all five mechanical properties. Unlike the pure PE samples, the PE-fws10 showed less retention in some of the properties. The reductions in tensile properties were especially noticeable. Though it was within the range of error, exposure to sodium hydroxide solution had the most significant effects both quantitatively and qualitatively. Tensile strength and elongation at break were reduced to 49.43 MPa and 22.92 % respectively (Table 4.2). Prior to the exposure, they were 53.05 MPa and 26.64 % as they are found in Table 4.1.

Qualitatively, leaching behaviour was observed from samples in sodium hydroxide solution. Fibres located on the surface of the sample bars leached out and turned the solution into yellow. A closer look at this phenomenon is discussed in the later section.

The diffusion of the chemical solution took place through the fibres. When considering the surface area to volume ratio, the smaller tensile bars (dog-bone shape) were higher than the flexural bars (plain rectangular bar). Therefore there were more fibres exposed to the surface of the tensile bars per volume. This was why the tensile properties were more sensitive to the chemical exposure compared to flexural and impact.

Property retention versus time graphs are shown in Figure 4.8. For all five graphs, property retentions for samples exposed to chemicals were not so far away from the ones exposed to water along the time line. Though significant leaching was observed in the NaOH solution, in terms of properties, they were not significantly different from the samples in water.

**Table 4.2 Tensile strength, elongation at break, flexural strength, modulus and IZOD impact strength of pure PE and PE-fws10 composite samples after 30 days of exposure to various chemical reagents**

Reagent	Sample	Tensile Strength (MPa)	Elongation at Break (%)	Flexural Strength (MPa)	Flexural Modulus (MPa)	IZOD Impact Strength (J/m)
Hydrochloric Acid	PE	52.73 (1.74)	31.48 (2.71)	26.33 (0.90)	661.89 (51.34)	468.90 (12.56)
	PE-fws10	50.64 (2.14)	23.11 (1.32)	32.28 (1.32)	726.12 (24.31)	119.23 (9.34)
Acetic Acid	PE	52.41 (0.96)	33.42 (2.45)	25.42 (0.83)	634.01 (49.29)	465.16 (21.70)
	PE-fws10	49.75 (2.11)	23.02 (0.89)	31.43 (1.52)	714.59 (27.91)	116.5 (5.17)
Sodium Hydroxide	PE	53.02 (1.31)	33.5 (2.01)	25.94 (0.67)	623.99 (32.74)	469.78 (15.12)
	PE-fws10	49.43 (1.94)	22.92 (1.62)	31.63 (1.58)	711.82 (26.55)	120.34 (7.59)
Ethyl Alcohol	PE	52.09 (1.12)	33.88 (1.71)	25.72 (0.74)	643.91 (48.42)	456.36 (23.15)
	PE-fws10	50.12 (1.72)	23.32 (1.31)	32.25 (1.43)	716.41 (24.03)	119.16 (6.48)
IGEPAL	PE	52.15 (1.08)	33.07 (1.91)	25.98 (0.70)	654.78 (42.31)	473.42 (16.96)
	PE-fws10	50.18 (1.62)	22.92 (1.72)	32.22 (1.29)	722.9 (23.50)	117.11 (7.56)
Water	PE	52.41 (2.03)	33.45 (2.12)	25.11 (0.95)	632.7 (46.24)	471.23 (19.88)
	PE-fws10	50.24 (2.01)	23.18 (1.44)	32.32 (1.33)	723.58 (24.31)	117.69 (7.80)

\* The values inside the brackets are the standard deviations of repeated trials.

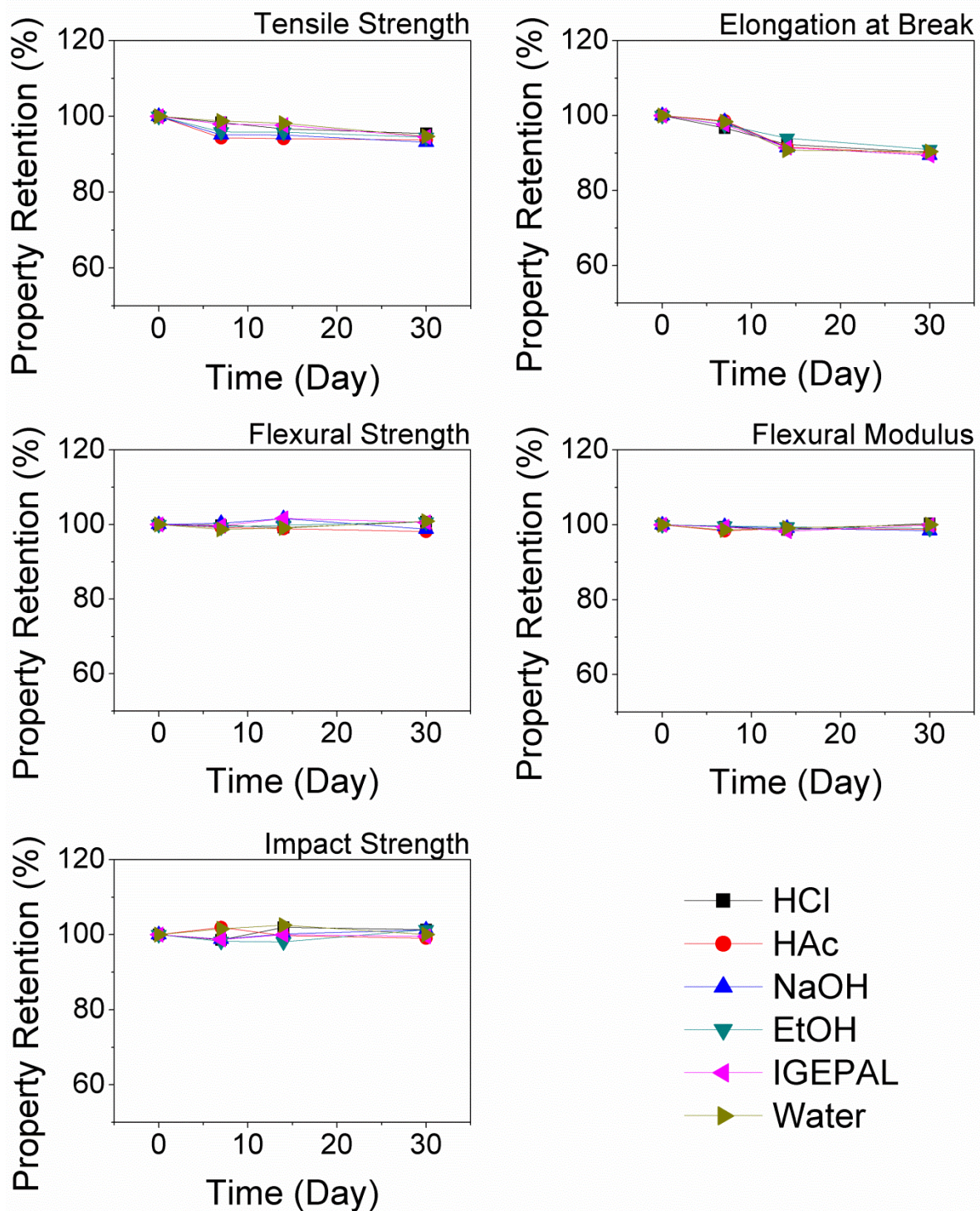


**Figure 4.8** Property retention in tensile strength, elongation at break, flexural strength, flexural modulus and IZOD impact strength of PE-fws10 at 0, 7, 14 and 30 days of exposure to chemical reagents



## 4.5 Water and Chemical Absorptions

The weight difference was also monitored in order to obtain the amount of absorption that has taken place throughout 30 day period (Figure 4.9). The non-WS samples had very small weight gains. All six samples had less than 0.1 % weight gain even after 30 days of chemical exposure. The WS composite on the other hand, as expected, had sharper weight gains. Almost 0.5 % weight gains were observed throughout the 10% WS composite samples. This phenomenon was simply because there was faster diffusion took place when fibres were present on the surface of samples. For the 20% WS composites, the weight gains were up to 0.8% except the exposure to NaOH solution. The leaching behaviour was more evident in NaOH solution that cavities were created on the surface, which resulted higher flux.

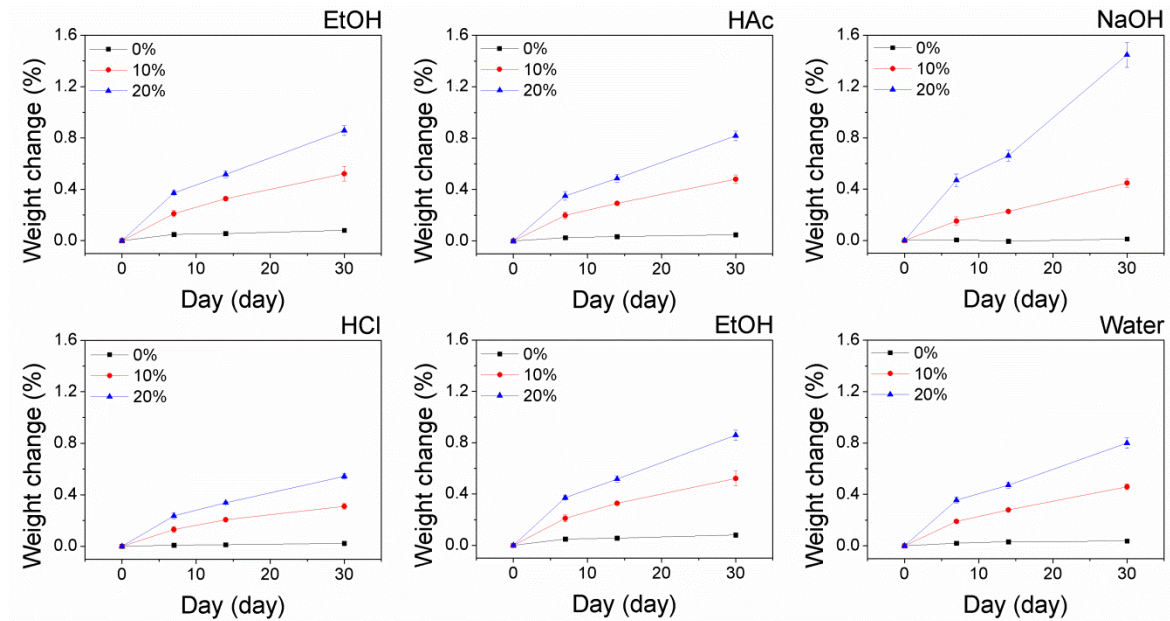


Figure 4.9 Weight change comparison of composites with PE, PE-10fws and PE-20fws. Exposure to HCl, HAc, NaOH, EtOH, IGEPAL, and Water for 0, 7, 14 and 30 days

## 4.6 Scanned Electron Microscopy

### 4.6.1 Cut Surface from IZOD Impact Test

The cut samples obtained from IZOD impact test were compared under scanned electron microscope (SEM) and they are shown in Figure 4.10 (a) and (b). The cut surface of PE-fws10 (Figure 4.10 (b)) shows a well distributed fibre present in the sample. As previous

studies with WS-PP composites have shown already (Sharma 2012, Güttler 2009), in the presence of coupling agent, the fibres had decent bonding with the PE matrix here as well. Since the coupling agent, polyethylene grafted maleic anhydride, has both hydrophilic and hydrophobic ends, it helped the bonding between hydrophilic fibres and hydrophobic PE matrix. Very few fibres were pulled out from the matrix and instead, a lot of broken and chopped out fibres were present on the fractured surface.

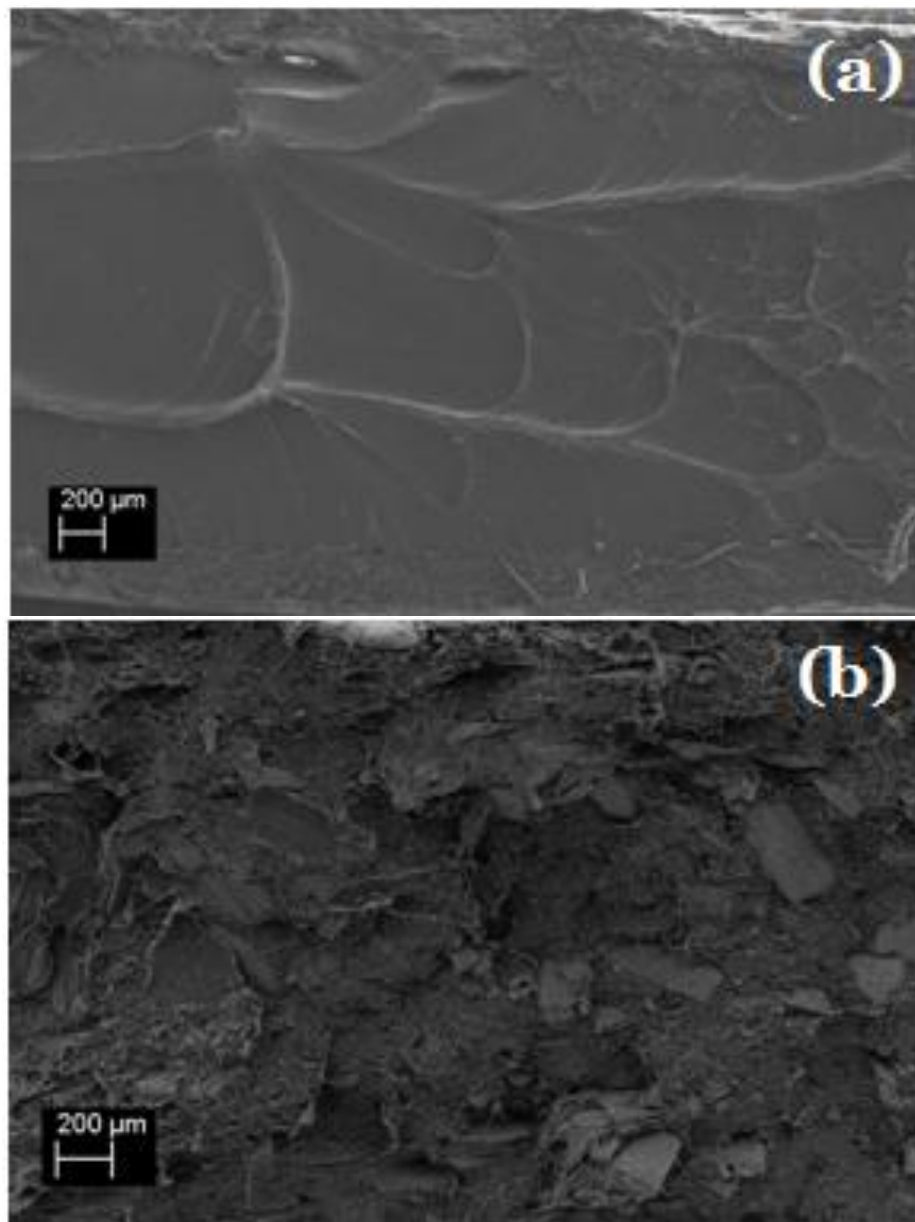


**Figure 4.10 SEM image of cut surface of (a) pure PE and (b) PE-fws10 composite**



#### **4.6.2 Chemically Aged Surface**

When exposed to the chemical agents, leaching of the fibres, especially in NaOH solution was observed. This turned the colour of the solution into yellow. In order to analyze the damage on the surface, SEM images of the surfaces were taken before and after the ageing. Figure 4.11 (a) and (b) compare the surface of WS composite before and after the exposure to NaOH solution. As expected, the damage on NaOH treated sample was more evident. The fibre exposed to the basic environment had leached out leaving rough surface.

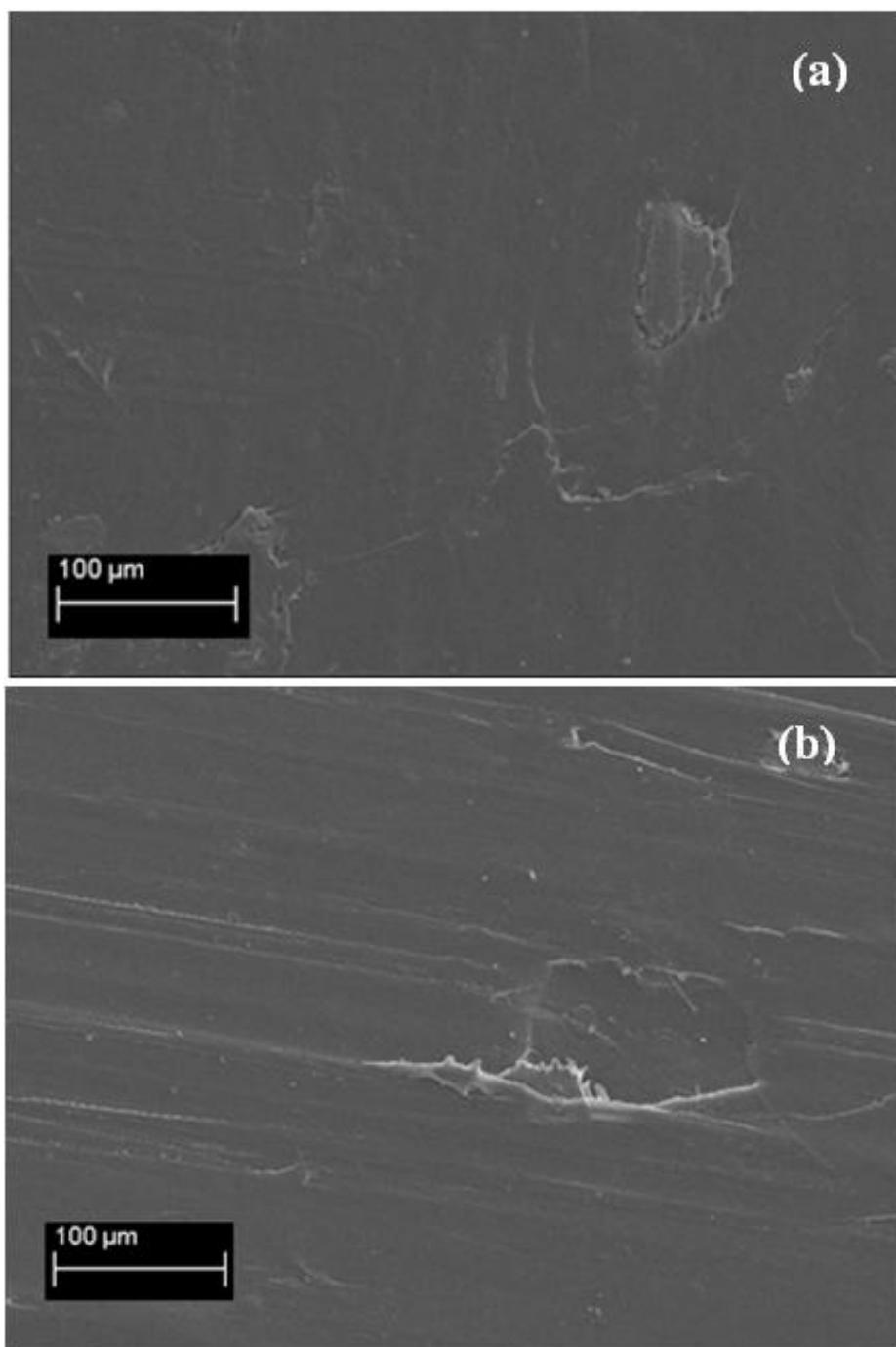


**Figure 4.11** Surface of (a) untreated and (b) NaOH treated PE-fws10 composite

## Chapter 5

### Results and Discussions: Flax Fibre-Renewable Polyethylene Composites

#### 5.1 Pre- and Post-Processing Fibre Particle Size Analysis

When received, both types of flax fibres were analyzed before put into the composites. Particle size analysis was done to measure their major axis (length) and minor axis (width) sizes, and to obtain the aspect ratio. Figure 5.1 shows the distribution of length of the particles. In order to obtain this data, there were more than 200 particles analyzed under the optical microscope for each population. Although majority were in between 0.5 to 2.5 mm, the medium flax (MF) fibres had a very broad range that some were larger than 4.0 mm. On the other hand, fine flax (FF) fibres were much shorter in length that there was almost no particle larger than 1.0 mm. The average length of MF was 1.88 mm with the standard deviation of 1.08 mm. The average length of FF was 0.23 mm with the standard deviation of 0.22 mm.

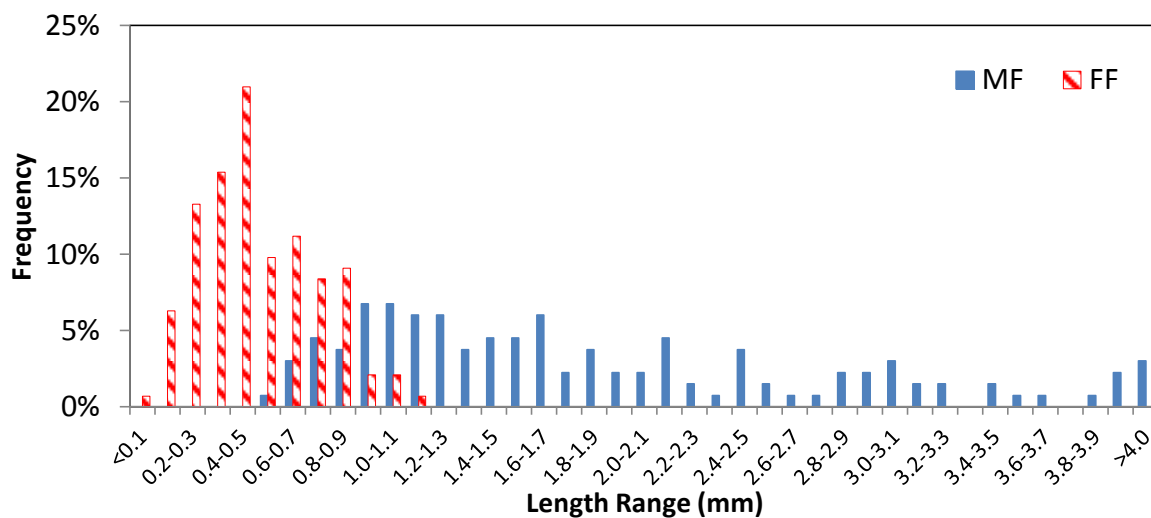


**Figure 5.1** Length in mm of medium flax (MF) and fine flax (FF) fibre particles before processing

The two populations were very different in aspect ratio as well. Figure 5.2 compares their distributions. MF had a very broad distribution where a significant portion of the fibre showed a large aspect ratio. The average aspect ratio of MF was 4.52 with the standard deviation of 2.35. However, the majority of FF particles were in round shape and their average aspect ratio was 2.93 with the standard deviation of 2.36.

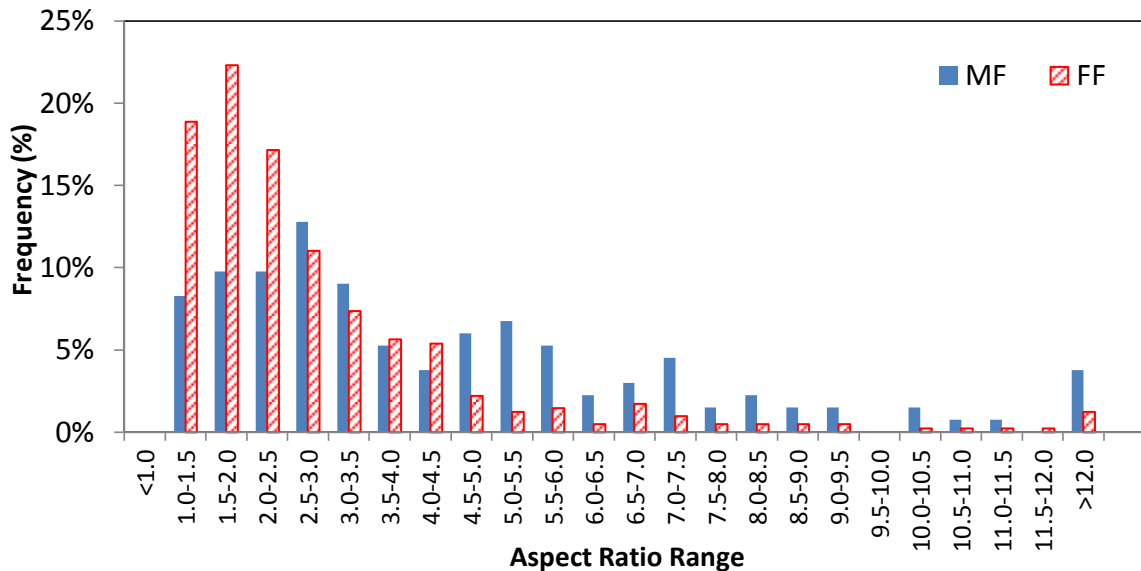


**Figure 5.2 Aspect ratio of medium flax (MF) and fine flax (FF) particles before processing**

After the mixture of fibres and the polymer were extruded and injection molded, the fibres were re-collected using the boiling xylene and the Soxhlet extractor. The same particle size analysis was conducted again. Figure 5.3 shows good comparisons of pre- and post-processed particles. The range distribution comparisons of before and after processing data are found in the Appendix section. As expected, the particle size was reduced significantly. Post-processed MF's average length was 0.51 mm and that of FF was 0.22 mm. Particularly, MF showed 73% reduction in length where FF did not show any significant changes. Similar pattern was observed in aspect ratio that MF had 48% reduction whereas FF only had 30% reduction.

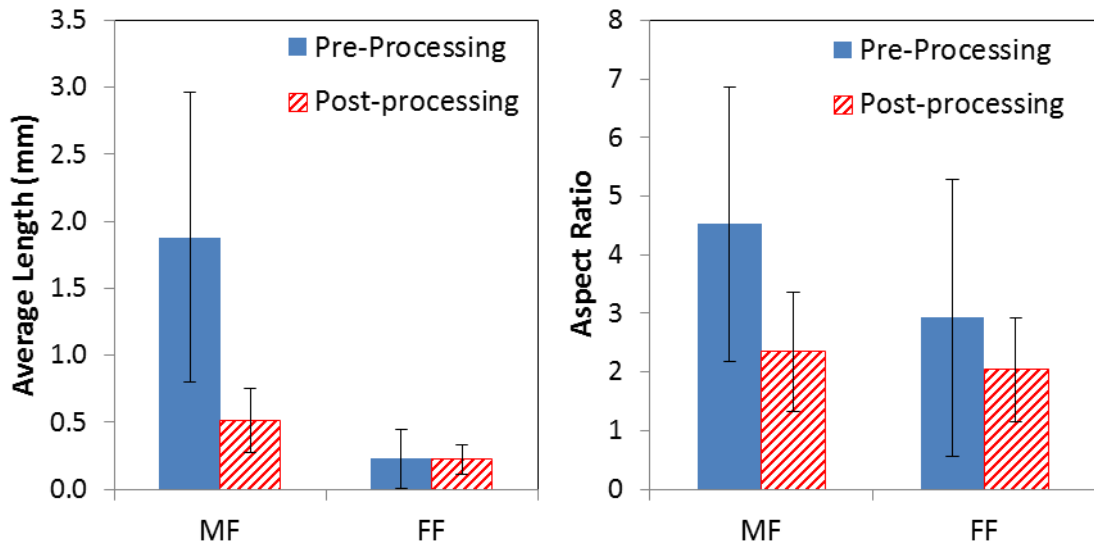


**Figure 5.3 Average length and aspect ratio comparisons of pre- and post-processed flax fibre particles**

From this study, notable results were obtained. Recalling data from the WS study, the average length of post-processed MWS and FWS were 0.49 and 0.42 mm. Considering these with the MF result (0.51 mm), it seemed regardless of the particle size before processing, they all ended up in the similar size after a series of processing (Table 5.1). The original average length of FF was much smaller (0.23 mm) compared to other three populations. Every composite sample was processed under the same condition (extrusion and molding temperature, extrusion rpm, and injection pressure). The stress applied continuously broke down the particles in the extruder until they reached the critical size which was small enough that a greater force was needed to further reduce them.

**Table 5.1 Average length and aspect ratio of post-processed fibres**

	MWS	FWS	MF	FF
Average Length (mm)	0.49 (0.18)	0.42 (0.15)	0.51 (0.24)	0.22 (0.11)
Average Aspect Ratio	2.68 (0.93)	2.63 (0.88)	2.34 (1.02)	2.04 (0.89)

\* The values inside the brackets are the standard deviations of repeated trials.

## 5.2 Density

The densities of flax composites were calculated from the results obtained and they are shown in Figure 5.4 along with the pure polyethylene sample. Same as WS composites, both MF and FF composites showed almost linear increase as the fibre contents went up.

Again, this flax-PE composite can be a possible alternative to the inorganic filler composites because of their low density.

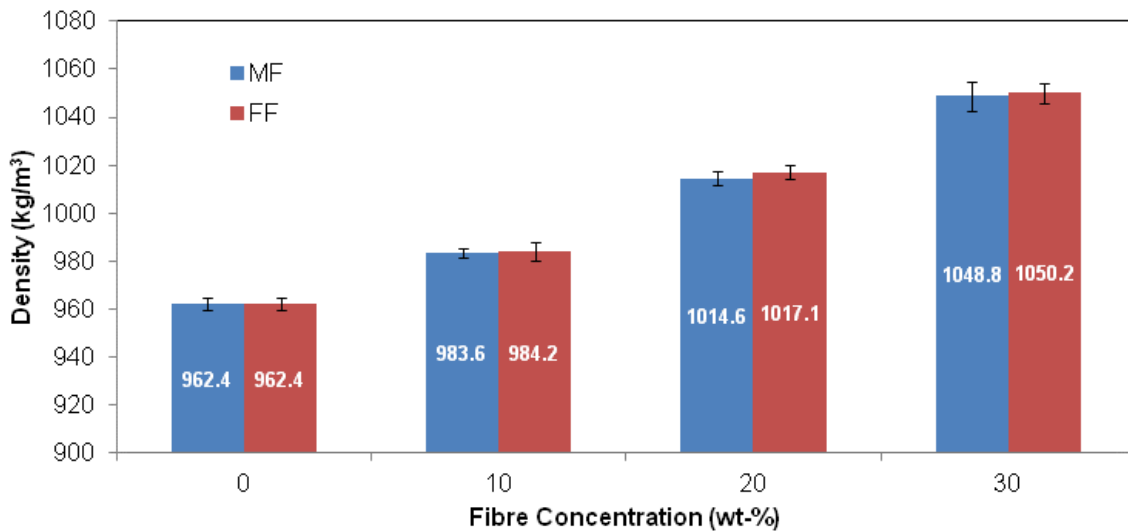


Figure 5.4 Density of pure polyethylene and flax fibre composites

## 5.3 Mechanical Properties

A series of mechanical tests were done to characterize the flax-PE composites prepared. As it was outlined in the materials and method chapter, two different sizes of flax fibres were put into the composites with the concentrations of 10, 20 and 30 wt-%. A summary of mechanical properties can be found in Table 5.2.

**Table 5.2 Tensile strength, elongation at break, flexural strength and modulus, IZOD impact strength, and Gardner impact failure energy of flax composites**

Sample	Tensile Strength (MPa)	Elongation at Break (%)	Flexural Strength (MPa)	Flexural Modulus (MPa)	IZOD Impact Strength (J/m)	Gardner Impact Failure Energy (J)
PE-ff10	47.67 (1.47)*	28.26 (0.77)	27.55 (0.31)	701.07 (28.61)	100.37 (8.25)	10.18 (0.14)
PE-ff20	44.92 (1.43)	25.41 (1.08)	30.9 (0.90)	912.9 (21.30)	70.78 (3.16)	7.20 (0.27)
PE-ff30	43.85 (1.24)	22.29 (1.18)	32.55 (0.46)	1178.5 (36.89)	56.25 (5.29)	5.81 (0.33)
PE-mf10	49.37 (1.15)	27.01 (1.16)	30.79 (0.29)	991.42 (52.10)	134.27 (13.87)	10.54 (0.26)
PE-mf20	46.93 (1.28)	23.02 (0.75)	31.84 (2.23)	1066.4 (60.46)	90.44 (5.78)	7.62 (0.07)
PE-mf30	42.56 (1.48)	19.72 (0.32)	33.37 (2.10)	1204.4 (106.68)	67.76 (10.89)	6.01 (0.31)

\* The values inside the brackets are the standard deviations of repeated trials.

### 5.3.1 Effects of Fibre Size

Tensile strength, elongation at break and flexural strength showed no significant changes when the flax fibre size increased from fine to medium (Figure 5.5). However, there was a strong evidence of improvement in flexural modulus and the both impact properties (IZOD and Gardner) when fibre size and the aspect ratio increased. At 10 wt-% fibre content, IZOD impact strength increased from 107.37 to 134.27 J/m (33.8% increase). At 20 and 30 wt-%, it increased by 27.8 and 20.5% respectively. The Gardner impact failure energy was increased by 3.5, 5.8 and 3.4% at 10, 20 and 30 wt-% fibre content.

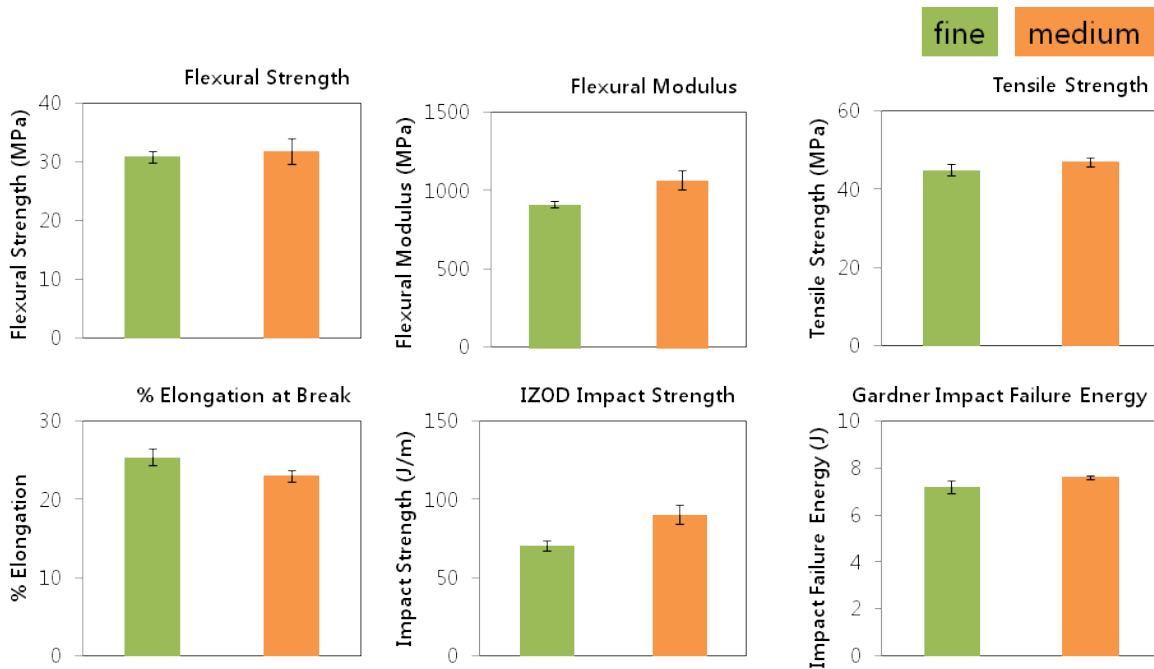


**Figure 5.5 Flexural strength, flexural modulus, tensile strength, percentage elongation at break, IZOD impact strength and Gardner impact failure energy of PE-ff20 and PE-mf20**

In the previous chapter, a conclusion was made that PE-mws and PE-fws had no significant difference when comparing their mechanical properties. On the contrary, PE-mf and PE-ff differ significantly. It was inevitable to see the gap between these two grades because their pre- and post-processed particle size analysis revealed the variance as mentioned previously. Unlike WS fibres, the flax fibres differed in their lengths and aspect ratios even after processing. The aspect ratios of filler particles in the composite greatly affect the properties of the final product. It was proven in numerous previous studies that the reinforcement effect of the fibres gets amplified as the aspect ratio increases.

### 5.3.2 Effects of Fibre Concentration

The fibre contents ranged between 0 and 30% in the samples. In order to examine the effects of filler concentration, the mechanical performance of these samples were compared. These values are also found in Table 5.2.

Similar patterns were observed in the flax reinforced composites as it was observed for the wheat straw (Figure 5.6). Some properties have improved while some did not as the fibre



content increased up to 30 wt-%. Flexural strength and modulus increased by 24.2 and 87.9% respectively as the fine flax (FF) content increased from 0 to 30 wt-% (from PE to PE-ff30). For the MF composites (from PE to PE-ff30), they increased by 27.4 and 92.0%, respectively. Again, it was quite obvious to see this result that increase in flax fibre content yielded significant increase in flexural properties. Rigid particles such as flax fibre improve the stiffness of composites. Tensile properties, on the other hand, declined when the fibre concentration increased. FF composites' tensile strength dropped from 52.46 to 43.85 MPa (-16.4%) and the elongation at break was reduced from 33.32 to 22.29 % elongation (-33.1%). For the MF composites they dropped to 42.56 MPa (-18.9%) and 19.72% elongation (-40.8%).

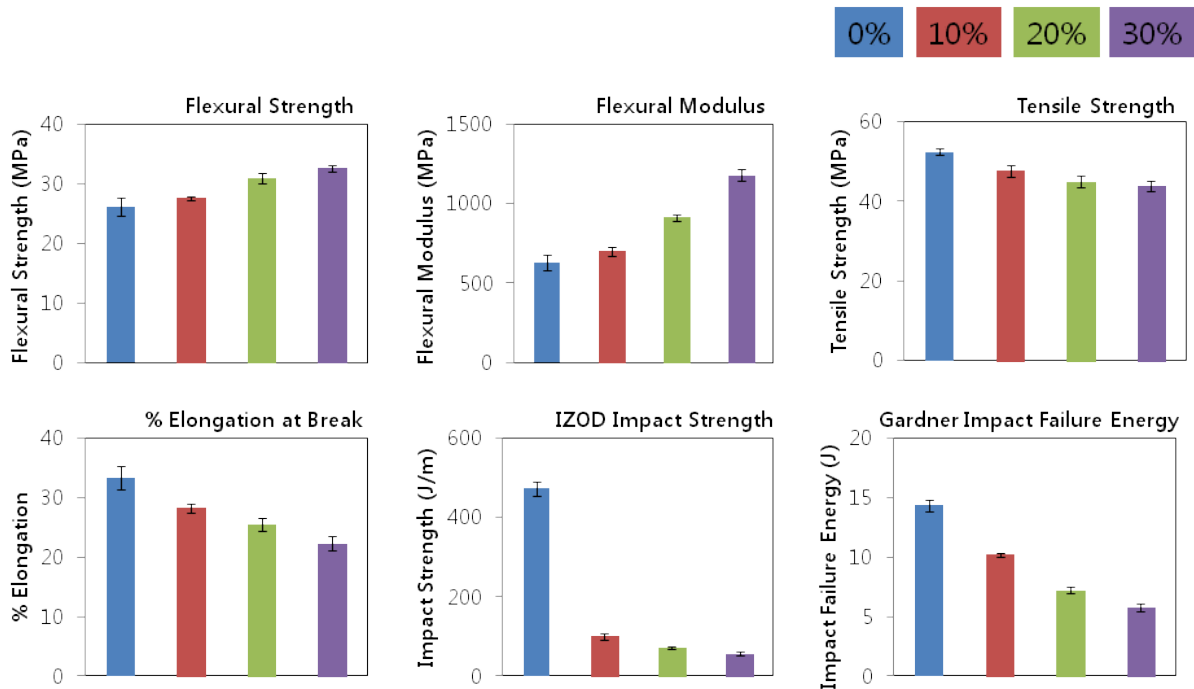


**Figure 5.6 Flexural strength, flexural modulus, tensile strength, percentage elongation at break, IZOD impact strength and Gardner impact failure energy of PE, PE-ff10, PE-ff20 and PE-ff30**

It was already mentioned about the difference in the two impact tests (IZOD and Gardner) conducted in the previous section. Using the MF, the IZOD impact strength and the Gardner impact failure energy were reduced by 88.0 and 59.4%. Almost the same amount of decrease was observed in FF composites that 85.6% reduction in the IZOD impact strength and 58.0% reduction in the Gardner impact failure energy were recorded.

## 5.4 Chemical Ageing

Flax fibre composites (PE-ff10, -ff20, -ff30, -mf10, -mf20, and -mf30) were put into chemical ageing experiment. Table 5.3 summarizes the result obtained from PE-ff10 after 30 days of exposure to various chemical.

Unlike the pure PE samples (Table 4.2), the PE-ff10 showed less retention in some of the properties. The reductions in tensile properties were especially noticeable. Though it was within the range of error, exposure to sodium hydroxide solution had the most significant effects both quantitatively and qualitatively. Tensile strength and elongation at break were reduced to 43.92 MPa and 24.98 % respectively. Prior to the exposure, they were 47.67 MPa and 28.26 % as they are found in Table 5.2. Flexural modulus and strength, and IZOD impact strength did not show any significant changes after the ageing.

**Table 5.3 Tensile strength, elongation at break, flexural strength, modulus and IZOD impact strength of 10% fine flax composite (PE-ff10) samples after 30 days of exposure to various chemical reagents**

Reagent	Sample	Tensile Strength (MPa)	Elongation at Break (%)	Flexural Strength (MPa)	Flexural Modulus (MPa)	IZOD Impact Strength (J/m)
-	PE-ff10	47.67 (1.47)*	28.26 (0.77)	27.55 (0.31)	701.07 (28.61)	100.37 (8.25)
Hydrochloric Acid	PE-ff10	45.94 (1.95)	26.12 (0.80)	27.23 (0.18)	720.84 (23.86)	100.58 (9.50)
Acetic Acid	PE-ff10	45.14 (1.50)	26.30 (0.80)	27.68 (1.58)	680.83 (23.82)	100.58 (9.57)
Sodium Hydroxide	PE-ff10	43.92 (1.35)	24.98 (1.06)	27.47 (0.05)	721.40 (26.34)	101.51 (7.10)
Ethyl Alcohol	PE-ff10	43.10 (1.05)	25.04 (1.03)	27.50 (0.52)	706.76 (23.08)	103.69 (9.43)
IGEPAL	PE-ff10	46.33 (1.57)	24.83 (0.83)	27.21 (0.66)	693.35 (28.95)	96.89 (7.99)
Water	PE-ff10	44.95 (1.53)	25.48 (0.82)	27.64 (0.47)	701.20 (26.77)	100.63 (9.37)

\* The values inside the brackets are the standard deviations of repeated trials.

Again, same as the WS study, leaching behaviour was observed from samples in sodium hydroxide solution. Fibres located on the surface of the sample bars leached out and changed

the colour of the solution into dark yellow. This is further discussed in the later sections with weight changes and scanned electron microscopic images.

The diffusion of the chemical solution took place through the fibres. When considering the surface area to volume ratio, the smaller tensile bars were much higher than the flexural bars. Therefore there were more fibres exposed to the surface of the tensile bars per volume. This was why the tensile properties were more sensitive to the chemical exposure compared to flexural and impact.

Property retention versus time graphs are shown in Figure 5.7. It is comprehensible to see the decrease in tensile strength and the elongation at break. Although the impact strengths fluctuate, they were within the minor error range.

The entire PE-ff10, PE-ff20 and PE-ff30 chemical exposure data is shown in Table 5.4 and PE-mf10, PE-mf20 and PE-mf30 data is represented in Table 5.5. Similar patterns were observed in all these different composites. There were minor decreases in tensile properties while others did not show any significant changes. When the fibre content increased, the percentage property retention decreased. For example, PE-mf10's tensile strength dropped from 48.87 to 43.32 MPa (-11.4%), and PE-mf30 dropped from 42.56 to 33.39 MPa (-21.5%) when exposed to sodium hydroxide for 30 days. It is an expected result that there certainly were more fibres exposed to the surface when the fibre content went up to 30% in the composites.

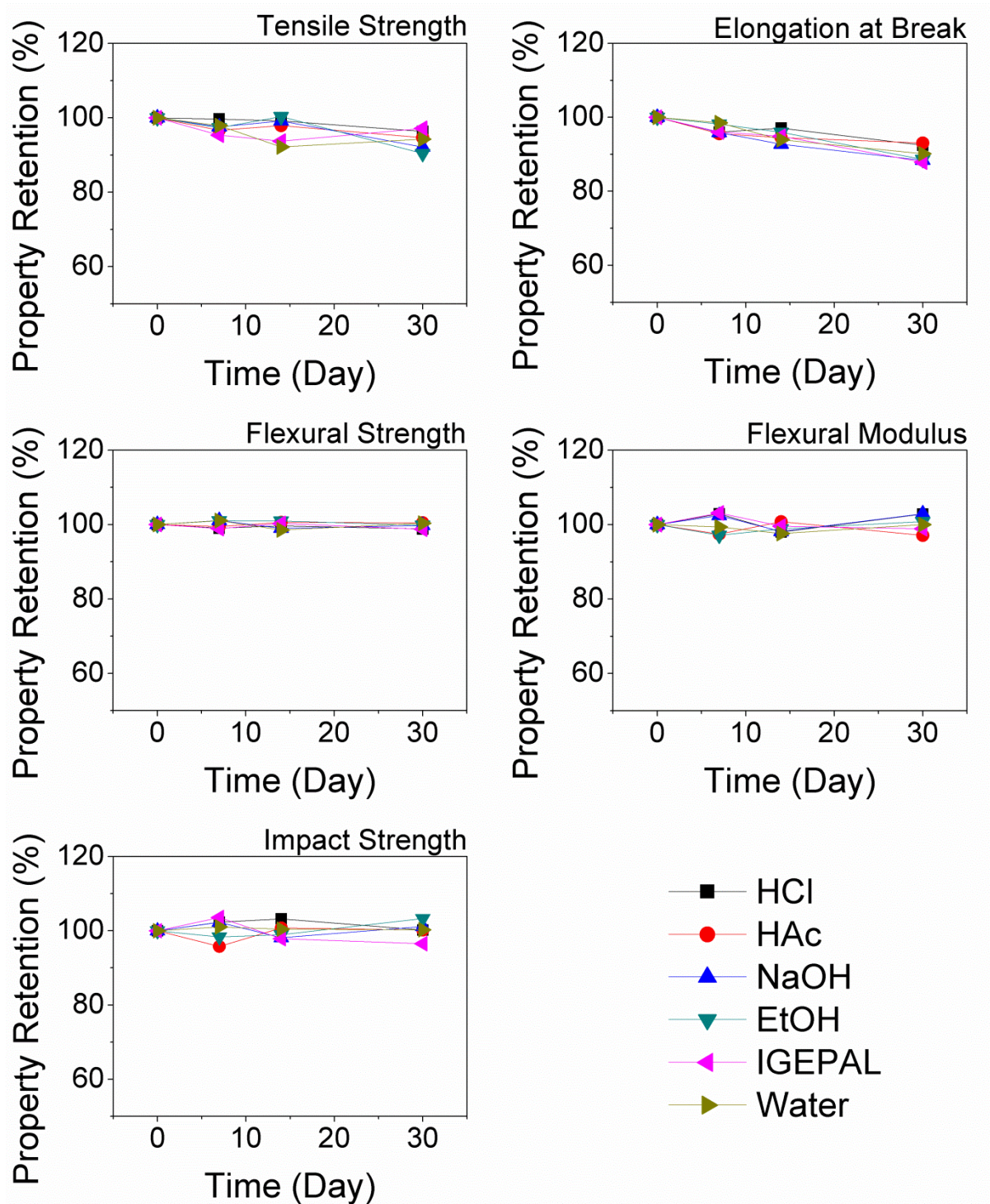


**Figure 5.7** Property retention in tensile strength, elongation at break, flexural strength, flexural modulus and IZOD impact strength of PE-ff10 at 0, 7, 14 and 30 days of exposure to chemical reagents

**Table 5.4 Tensile strength, elongation at break, flexural strength, modulus and IZOD impact strength of 10, 20 and 30% fine flax composite samples after 7, 14 and 30 days of exposure to various chemical reagents**

Reagent (time)	Sample	Tensile Strength (MPa)	Elongation at Break (%)	Flexural Strength (MPa)	Flexural Modulus (MPa)	IZOD Impact Strength (J/m)
-	PE-ff10	47.67	28.26	27.55	701.07	100.37
HCl (7 days)	PE-ff10	47.50	27.13	27.29	721.17	102.70
HCl (14 days)	PE-ff10	47.28	27.43	27.45	687.04	103.59
HCl (30 days)	PE-ff10	45.94	26.12	27.23	720.84	100.58
HAc (7 days)	PE-ff10	46.07	27.00	27.40	683.05	96.12
HAc (14 days)	PE-ff10	46.67	26.71	27.71	706.46	101.15
HAc (30 days)	PE-ff10	45.14	26.30	27.68	680.83	100.58
NaOH (7 days)	PE-ff10	46.51	27.10	27.85	718.08	102.67
NaOH (14 days)	PE-ff10	47.27	26.20	27.28	688.00	98.51
NaOH (30 days)	PE-ff10	43.92	24.98	27.47	721.40	101.51
EtOH (7 days)	PE-ff10	46.41	27.74	27.83	681.00	98.71
EtOH (14 days)	PE-ff10	47.83	27.12	27.81	693.18	99.31
EtOH (30 days)	PE-ff10	43.10	25.04	27.50	706.76	103.69
IGEPAL (7 days)	PE-ff10	45.46	27.14	27.26	722.84	103.95
IGEPAL (14 days)	PE-ff10	44.68	26.82	27.63	697.95	98.22
IGEPAL (30 days)	PE-ff10	46.33	24.83	27.21	693.35	96.89
Water (7 days)	PE-ff10	46.67	27.84	27.84	696.59	101.42
Water (14 days)	PE-ff10	43.94	26.55	27.15	684.29	100.82
Water (30 days)	PE-ff10	44.95	25.48	27.64	701.20	100.63
-	PE-ff20	44.92	25.41	30.9	912.9	70.78
HCl (7 days)	PE-ff20	43.37	24.43	31.44	916.30	69.64
HCl (14 days)	PE-ff20	41.24	24.40	31.02	898.33	71.26
HCl (30 days)	PE-ff20	41.05	22.34	29.84	908.24	68.40
HAc (7 days)	PE-ff20	42.74	24.17	31.38	901.02	68.68
HAc (14 days)	PE-ff20	43.35	24.26	30.14	910.26	72.40
HAc (30 days)	PE-ff20	42.74	21.85	30.92	919.79	72.49
NaOH (7 days)	PE-ff20	43.45	24.20	30.52	918.89	72.80
NaOH (14 days)	PE-ff20	42.64	23.85	30.21	918.53	66.91
NaOH (30 days)	PE-ff20	40.09	22.66	32.18	900.56	67.70
EtOH (7 days)	PE-ff20	42.08	24.17	30.09	914.46	71.00
EtOH (14 days)	PE-ff20	41.86	22.49	30.73	929.56	66.61

EtOH (30 days)	PE-ff20	42.10	22.27	29.87	900.10	68.90
IGEPAL (7 days)	PE-ff20	43.02	23.84	30.93	907.43	72.20
IGEPAL (14 days)	PE-ff20	42.77	23.37	31.37	924.40	67.55
IGEPAL (30 days)	PE-ff20	40.46	22.02	30.63	928.36	68.73
Water (7 days)	PE-ff20	43.10	24.38	30.49	903.76	71.52
Water (14 days)	PE-ff20	40.23	23.39	31.16	923.31	69.75
Water (30 days)	PE-ff20	41.54	23.20	31.04	922.63	71.30
<hr/>						
-	PE-ff30	43.85	22.29	32.55	1178.47	56.25
HCl (7 days)	PE-ff30	41.08	20.38	33.00	1151.99	55.25
HCl (14 days)	PE-ff30	38.99	20.53	32.61	1172.76	53.29
HCl (30 days)	PE-ff30	38.15	18.54	32.93	1197.76	58.63
HAc (7 days)	PE-ff30	40.46	19.89	32.66	1150.63	54.38
HAc (14 days)	PE-ff30	38.88	20.59	31.91	1192.49	56.00
HAc (30 days)	PE-ff30	39.39	19.42	31.86	1175.34	53.44
NaOH (7 days)	PE-ff30	39.94	19.73	32.22	1207.44	53.63
NaOH (14 days)	PE-ff30	39.30	20.44	32.40	1191.29	59.47
NaOH (30 days)	PE-ff30	37.39	16.70	32.82	1192.70	54.61
EtOH (7 days)	PE-ff30	39.06	20.39	32.43	1200.42	53.18
EtOH (14 days)	PE-ff30	39.18	20.33	31.87	1181.44	55.86
EtOH (30 days)	PE-ff30	38.80	19.36	33.20	1185.47	53.86
IGEPAL (7 days)	PE-ff30	38.86	19.72	32.55	1201.30	55.74
IGEPAL (14 days)	PE-ff30	41.24	18.89	32.13	1175.20	58.89
IGEPAL (30 days)	PE-ff30	37.37	17.84	32.93	1167.79	53.76
Water (7 days)	PE-ff30	40.89	21.09	32.23	1186.03	52.24
Water (14 days)	PE-ff30	38.46	18.97	33.23	1157.15	55.21
Water (30 days)	PE-ff30	39.60	20.06	32.36	1155.63	53.65

**Table 5.5 Tensile strength, elongation at break, flexural strength, modulus and IZOD impact strength of 10, 20 and 30% medium flax composite samples after 7, 14 and 30 days of exposure to various chemical reagents**

Reagent (time)	Sample	Tensile Strength (MPa)	Elongation at Break (%)	Flexural Strength (MPa)	Flexural Modulus (MPa)	IZOD Impact Strength (J/m)
-	PE-mf10	49.37	27.01	30.79	991.42	134.27
HCl (7 days)	PE-mf10	47.86	26.41	30.99	988.94	136.38
HCl (14 days)	PE-mf10	47.30	25.25	31.00	957.44	132.60
HCl (30 days)	PE-mf10	47.08	25.27	30.64	969.22	131.20
HAc (7 days)	PE-mf10	47.20	25.96	30.72	1028.80	128.74
HAc (14 days)	PE-mf10	47.68	25.58	31.07	1031.07	132.84
HAc (30 days)	PE-mf10	46.54	25.99	30.76	997.74	129.30
NaOH (7 days)	PE-mf10	48.87	26.38	30.73	963.41	137.32
NaOH (14 days)	PE-mf10	49.00	26.68	30.74	1032.46	127.78
NaOH (30 days)	PE-mf10	43.32	23.97	30.62	1013.29	132.66
EtOH (7 days)	PE-mf10	48.03	26.69	31.06	1029.07	132.91
EtOH (14 days)	PE-mf10	47.60	26.04	30.98	993.59	131.83
EtOH (30 days)	PE-mf10	45.66	23.52	30.41	1019.45	129.83
IGEPAL (7 days)	PE-mf10	48.75	26.45	30.96	1013.12	129.46
IGEPAL (14 days)	PE-mf10	48.81	26.24	31.19	982.23	135.65
IGEPAL (30 days)	PE-mf10	46.95	25.93	31.10	982.25	135.56
Water (7 days)	PE-mf10	48.61	26.93	30.72	981.43	128.16
Water (14 days)	PE-mf10	49.03	25.75	30.39	972.31	135.68
Water (30 days)	PE-mf10	46.59	23.59	30.61	1018.46	135.46
-	PE-mf20	46.93	23.02	31.84	1066.42	90.44
HCl (7 days)	PE-mf20	44.21	21.45	33.56	1035.71	90.93
HCl (14 days)	PE-mf20	42.93	21.28	31.97	1097.68	87.24
HCl (30 days)	PE-mf20	41.75	20.69	34.87	1102.64	91.00
HAc (7 days)	PE-mf20	43.13	21.37	34.00	1084.88	91.64
HAc (14 days)	PE-mf20	43.22	21.11	30.80	1025.60	85.88
HAc (30 days)	PE-mf20	43.39	20.58	29.74	1030.22	88.40
NaOH (7 days)	PE-mf20	44.19	21.32	30.17	1109.65	93.07
NaOH (14 days)	PE-mf20	44.18	21.62	32.53	1072.36	92.41
NaOH (30 days)	PE-mf20	42.30	18.82	28.63	1061.80	89.21
EtOH (7 days)	PE-mf20	43.01	22.01	33.34	1056.30	92.33
EtOH (14 days)	PE-mf20	42.35	21.45	31.18	1104.47	87.29

EtOH (30 days)	PE-mf20	42.08	19.55	29.21	1035.40	93.53
IGEPAL (7 days)	PE-mf20	43.50	21.45	33.74	1101.92	88.81
IGEPAL (14 days)	PE-mf20	42.43	20.90	32.28	1038.50	85.23
IGEPAL (30 days)	PE-mf20	43.51	20.08	34.22	1019.31	85.66
Water (7 days)	PE-mf20	44.87	22.34	30.09	1045.12	92.67
Water (14 days)	PE-mf20	41.94	20.80	34.09	1073.38	88.94
Water (30 days)	PE-mf20	43.34	20.77	30.37	1024.32	86.81
-	PE-mf30	42.56	19.72	33.37	1204.43	67.76
HCl (7 days)	PE-mf30	39.00	17.96	31.80	1148.92	64.77
HCl (14 days)	PE-mf30	38.41	17.35	33.74	1234.27	65.46
HCl (30 days)	PE-mf30	38.51	16.82	31.69	1209.24	70.41
HAc (7 days)	PE-mf30	37.46	18.04	31.40	1185.88	64.96
HAc (14 days)	PE-mf30	40.26	17.55	31.64	1124.84	63.85
HAc (30 days)	PE-mf30	36.97	17.08	35.12	1265.41	67.19
NaOH (7 days)	PE-mf30	38.82	18.13	33.65	1131.87	67.26
NaOH (14 days)	PE-mf30	40.06	17.69	36.09	1159.37	66.03
NaOH (30 days)	PE-mf30	33.39	16.07	34.49	1245.23	70.28
EtOH (7 days)	PE-mf30	39.74	17.93	35.42	1263.93	64.77
EtOH (14 days)	PE-mf30	39.59	17.64	34.02	1270.00	65.73
EtOH (30 days)	PE-mf30	36.46	17.20	33.97	1178.34	64.43
IGEPAL (7 days)	PE-mf30	38.45	17.88	34.27	1226.48	64.08
IGEPAL (14 days)	PE-mf30	37.76	17.47	36.17	1176.93	66.96
IGEPAL (30 days)	PE-mf30	36.84	16.74	33.91	1194.68	67.78
Water (7 days)	PE-mf30	37.64	18.01	34.81	1142.00	70.92
Water (14 days)	PE-mf30	39.99	17.71	36.35	1224.95	67.52
Water (30 days)	PE-mf30	36.68	17.07	35.20	1238.13	69.29

## 5.5 Water and Chemical Absorptions

Same as the WS composites, chemically exposed flax composites' weight difference was measured throughout the 30 day period and compared with the pure PE sample (Figure 5.8). Similar result was obtained that as the fibre content increased, higher flux was observed. Specimens exposed to NaOH, especially, had rapid increase in weight. The pure PE merely changed their weight in any of the six chemical exposures. The matrix polymer, HDPE, has very high crystalline content when compared to other thermoplastics (PP, LDPE, etc.). The mass transfer through the crystalline region is much slower than amorphous region. Fibres



exposed on the surface of specimens were mostly responsible for the high flux into the matrix of the composites. SEM images in the later sections show more fibres exposed to the surface as the concentration increases.

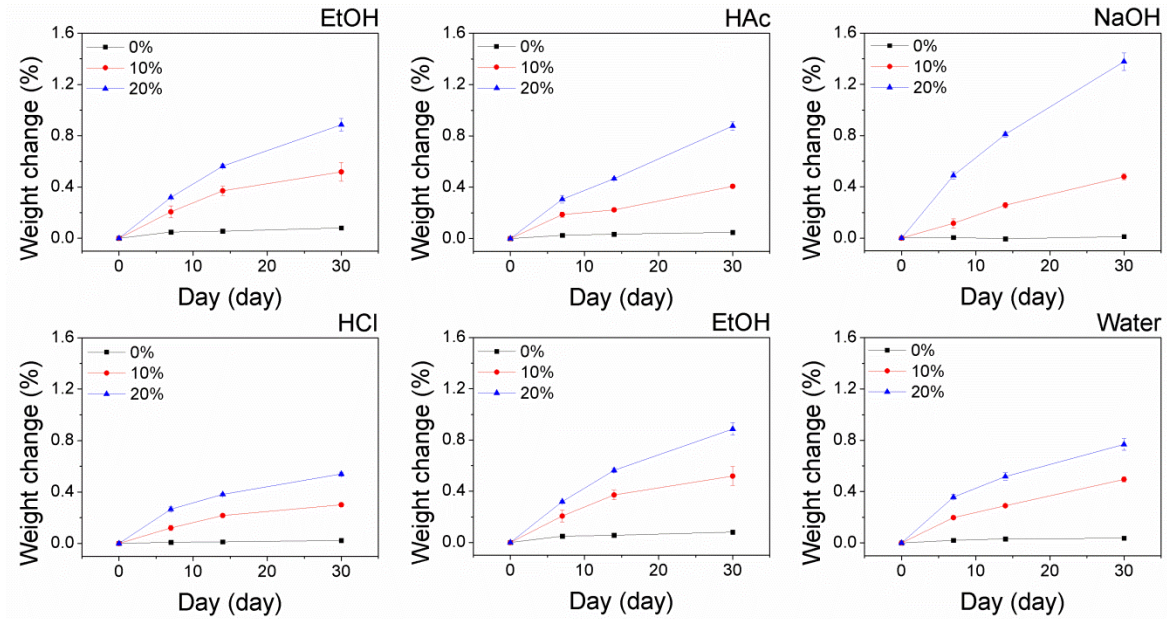


**Figure 5.8 Weight change comparison of composites with PE, PE-10ff and PE-20ff. Exposure to HCl, HAc, NaOH, EtOH, IGEPAL, and Water for 0, 7, 14 and 30 days**

## 5.6 Scanned Electron Microscopy

There were two different sections looked at under the scanned electron microscope. First was the cut surface from the IZOD impact test and the second section was the flat surface in the middle of flexural bars.

### 5.6.1 Cut Surface from IZOD Impact Test

After the IZOD impact test was done, the broken bars were collected and gold coated to investigate under the SEM. Figure 5.9, Figure 5.10 (a) and Figure 5.11 show the SEM image of fractured surface of PE-ff10, PE-ff20 and PE-ff30 respectively. It is easy to see the fibre content increased by comparing the three images.

Good dispersion of the reinforcing fibres was observed in all samples. The surface textures of fibres were well maintained even though the size and aspect ratio were reduced after processing.

In order to improve the mechanical properties of a composite material, it is crucial to have good interfacial bonding between different phases (reinforcing materials and matrix). Morphological study of the fractured surface can help understanding the interaction between the two phases. The obtained SEM images show a lot of chopped and sheared fibres. This is a good sign of bonding between the two phases. If there were weaker bonds present, the fibres would be pulled out during the fracture and leave empty spaces. Figure 5.10 (b) shows one of chopped fibre during the IZOD impact test. The hydrophilic natural fibres will not interact with hydrophobic polymer matrix unless there is a bridging material between the two. In this case, polyethylene grafted maleic anhydride (PEMA) was used. Since the PEMA has both hydrophilic and hydrophobic ends, it acts well for the interfacial bonding.

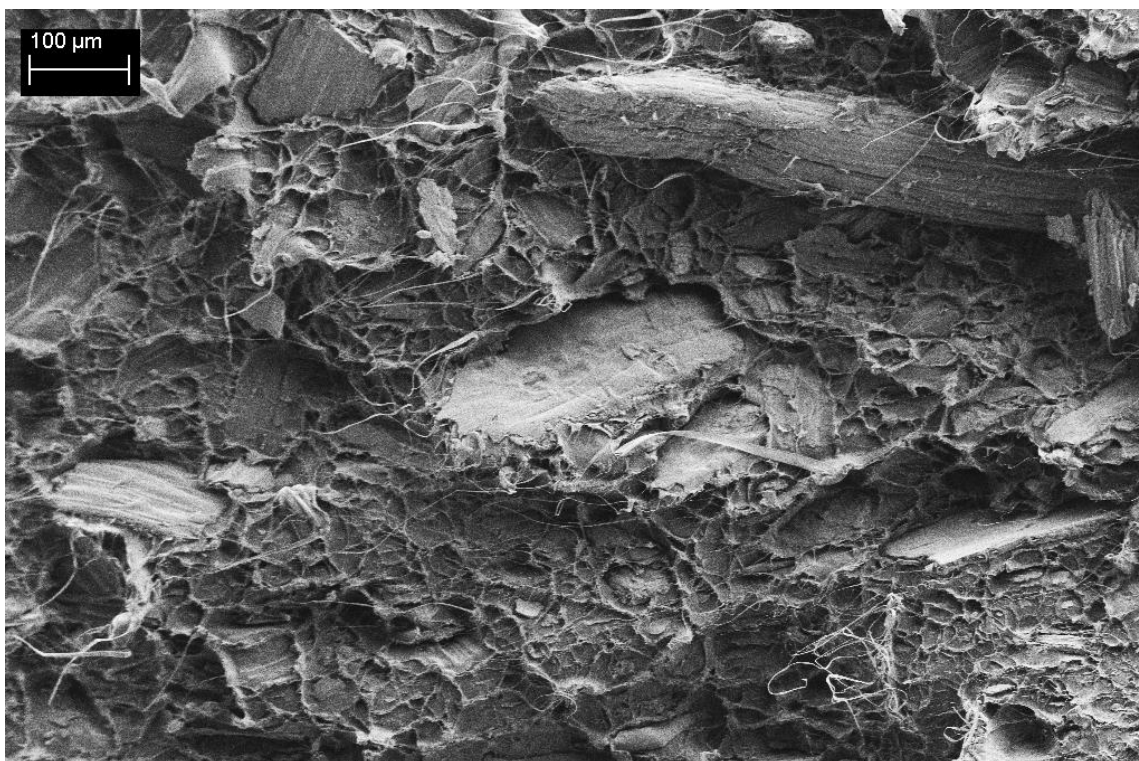


**Figure 5.9 SEM image (100x, 5kV) of the fractured surface of PE-ff10**

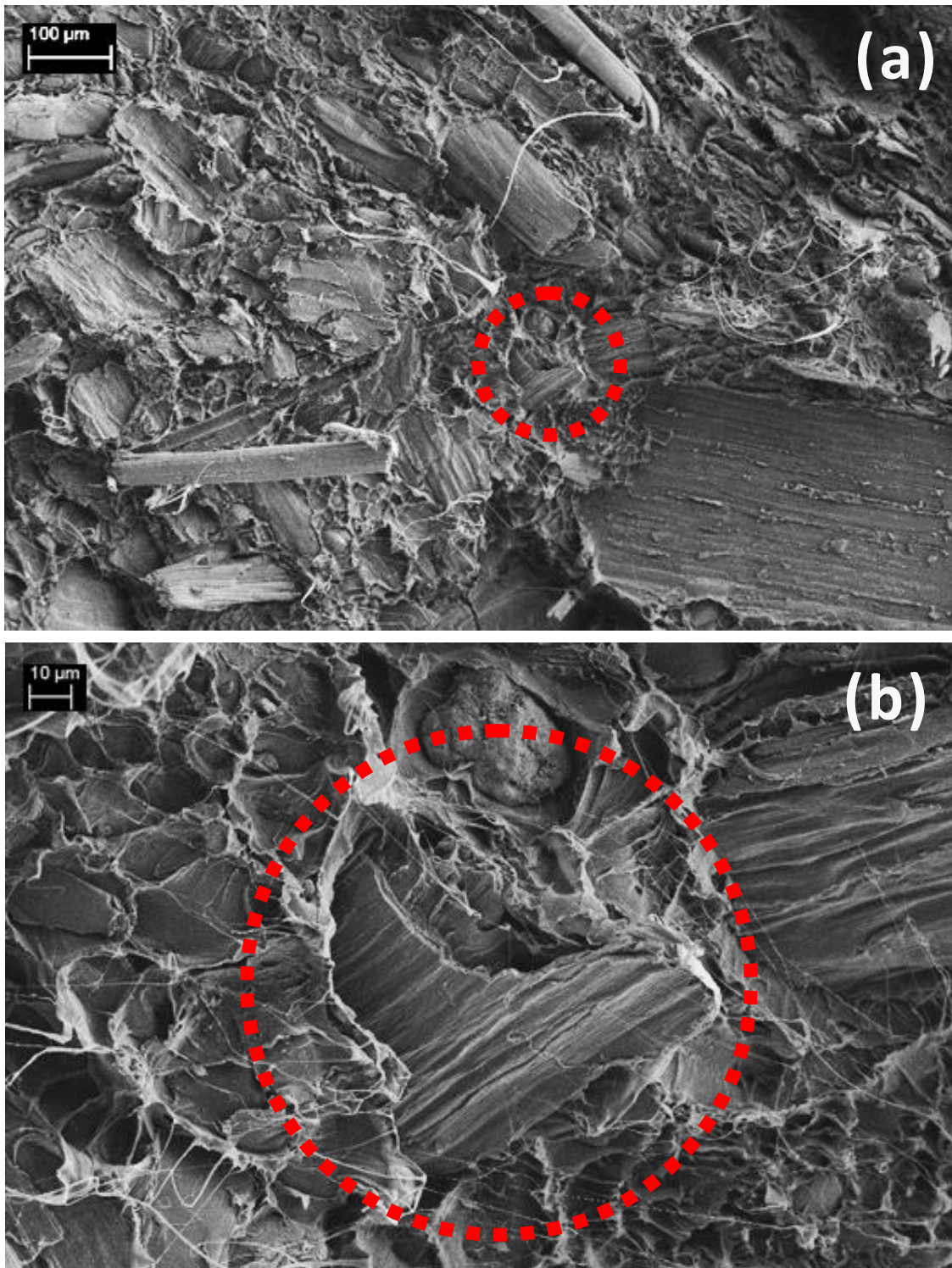
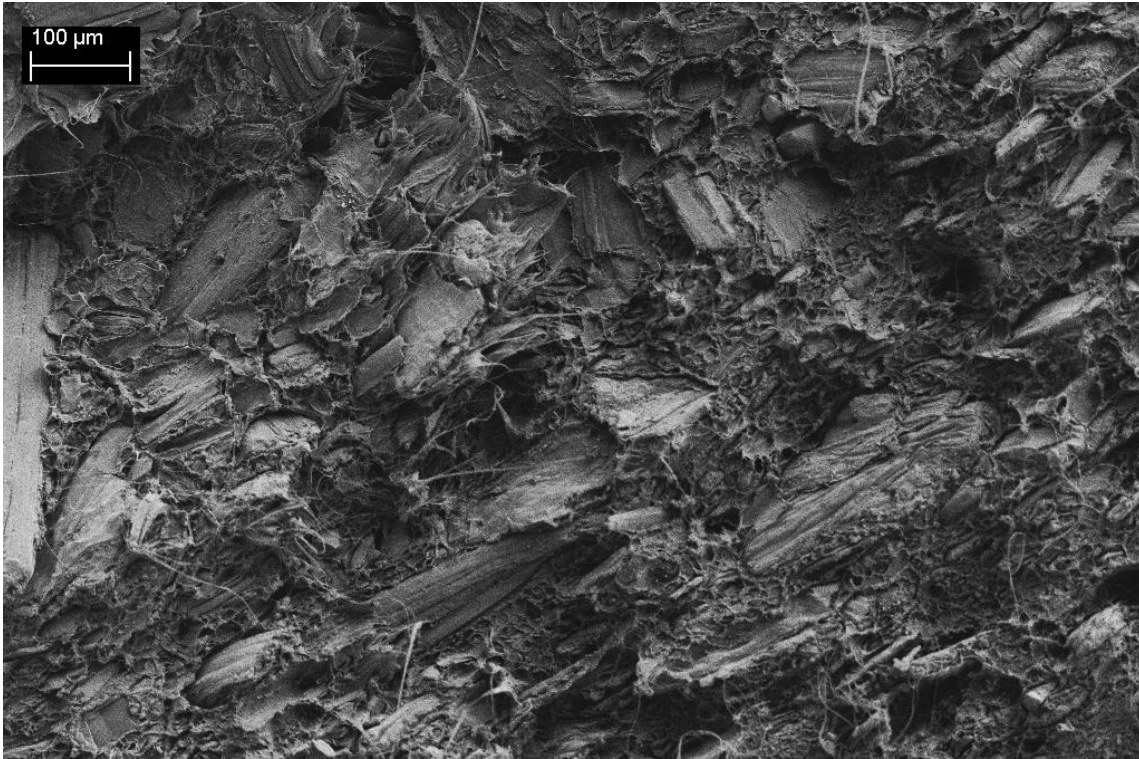


Figure 5.10 SEM images of the fractured surface of PE-ff20 at (a) 100x and 5kV, and (b) 500x, 5kV with broken fibre (in the red dotted circle)



**Figure 5.11 SEM image (100x, 5kV) of the fractured surface of PE-ff30**

One of the common problems in plastic processing includes voids. Voids are undesirable because they alter the properties of final products. It is difficult to detect them by naked eyes when they reside deep inside the matrix. Although the composites were processed in a careful manner, a few flexural bars contained small air bubbles in the end. Figure 5.12 is an SEM image of cut surface where the cavities were found. The diameter ranged approximately from 100 to 500  $\mu\text{m}$ . The injection molder used to prepare the bars did not have the extruder unit attached. It simply plunged the melted composites and quickly pushed them into the mold. Possibly, some air was trapped inside the injection barrel and went into the mold. There were a few plausible solutions that can be applied. Decreasing injection speed, increasing the injection pressure and injection-hold can be done to avoid the undesirable voids in the sample. Applying some of these techniques, less voids were observed in the end.



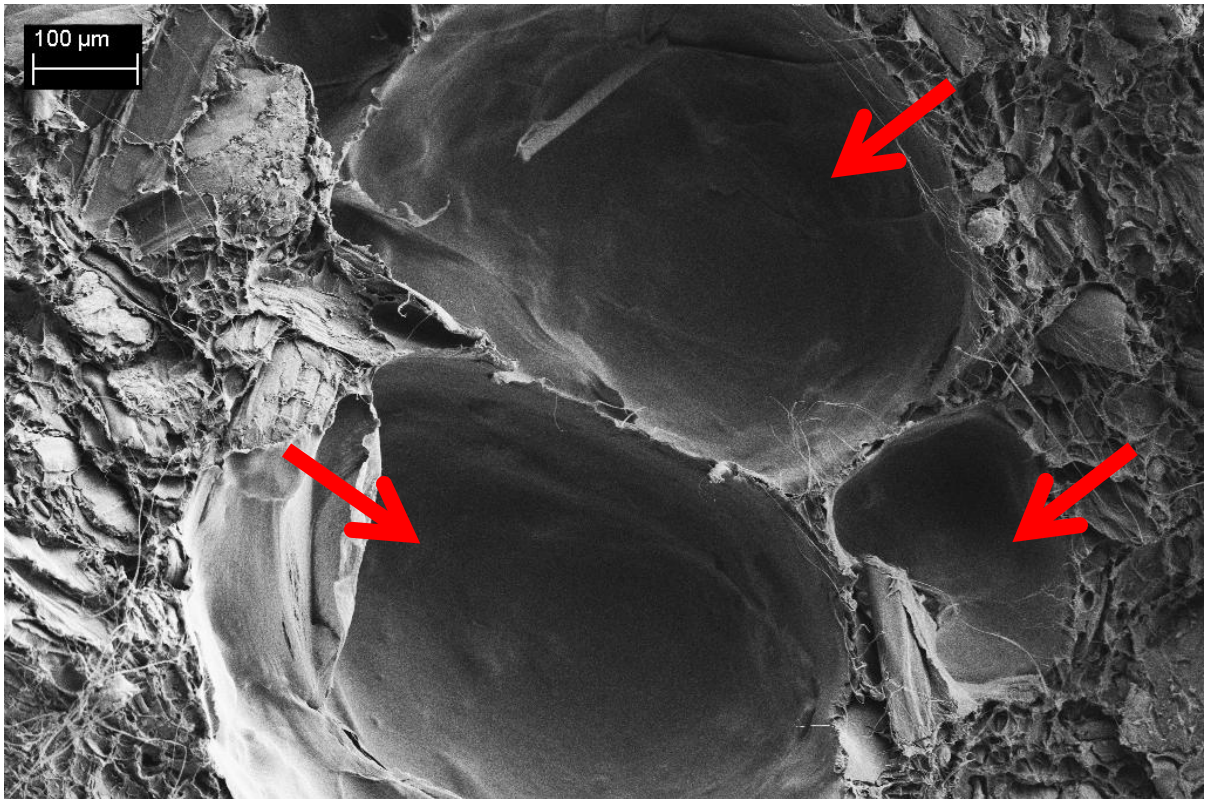


**Figure 5.12 SEM image (100x, 5kV) of fractured surface of PE-ff20 with air pockets**

### **5.6.2 Chemically Aged Surface**

In this section, the uncut surfaces of flexural bars were observed under the SEM. The amount of fibres exposed to the surface was compared between the low and high fibre content samples. Also, the effects of chemical ageing are highlighted by comparing images before and after the exposure.

Figure 5.13 and Figure 5.14 are SEM images (50x) of PE-ff10 and PE-ff30, respectively, before the ageing process. Although it was difficult to observe the difference between the two from naked eyes, PE-ff10 showed much smoother surface when compared to PE-ff30 under the SEM. Very few exposed fibres were seen on the surface of PE-ff10. However, PE-ff30 showed a lot of exposed fibres and display rough surface. This observation was crucial to understand the rate of water and chemical reagent absorptions. It is no surprise to see the higher flux in the PE-ff30 than PE-ff10 because there were a lot of “straws” present in PE-ff30. Capping the final product will be required to avoid or slow down the absorption.

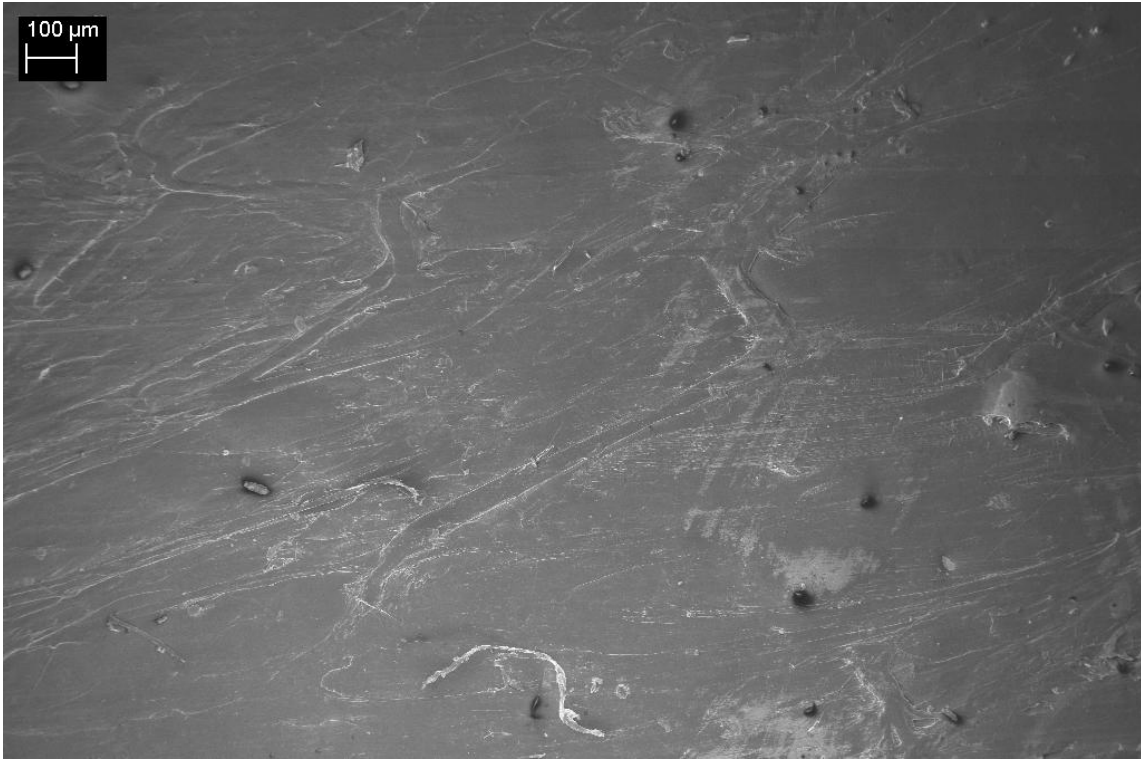


**Figure 5.13 SEM image (50x, 5kV) of the surface of PE-ff10**

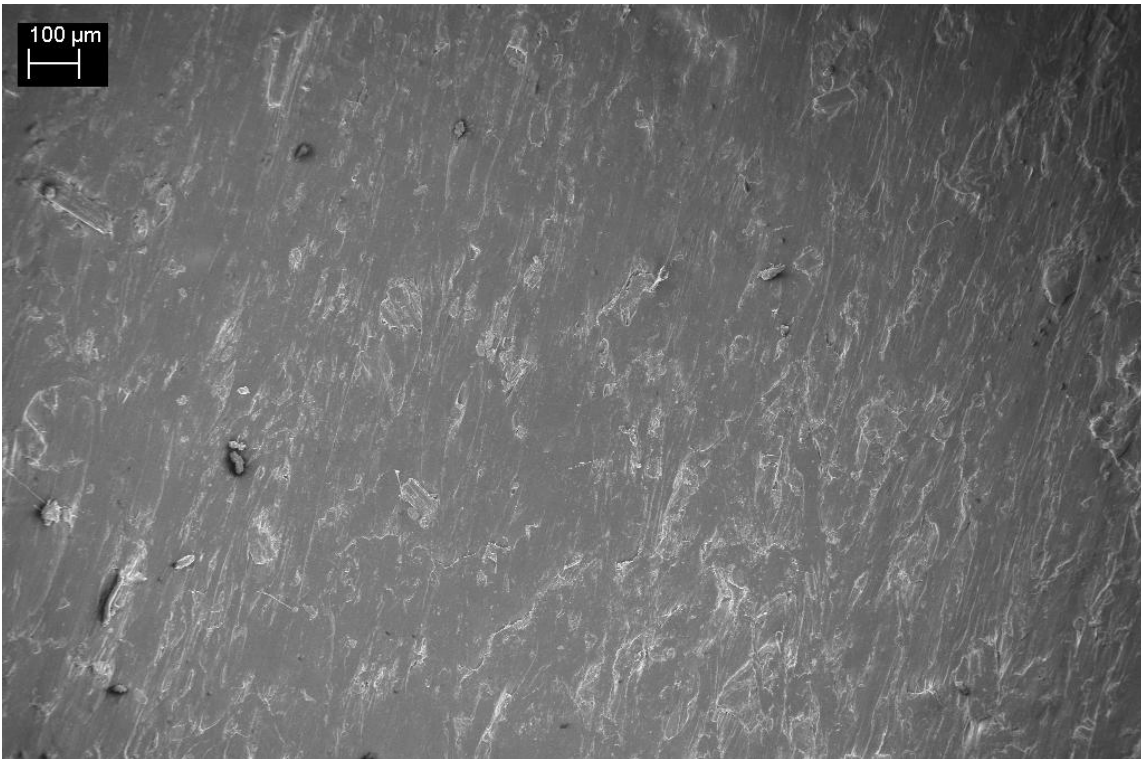


**Figure 5.14 SEM image (50x, 5kV) of the surface of PE-ff30**

Samples exposed to NaOH solution showed leaching behaviour. In order to clarify the amount of damage, SEM images of the aged surface were obtained. Figure 5.15 (a) shows the surface of PE-ff10 after 30 days of ageing in NaOH solution. No high magnification was necessary to see the apparent damages. The roughness significantly increased and there were small size cavities observed. The cavities are the spots where the fibres resided before the exposure. The low pH NaOH solution was detrimental to these fibres and left empty spaces. Figure 5.15 (b) is a higher magnification (500x) image of one of the cavities. Only the polymer matrix that was covering the fibre was left. The rest of the SEM images are found in the Appendix section.



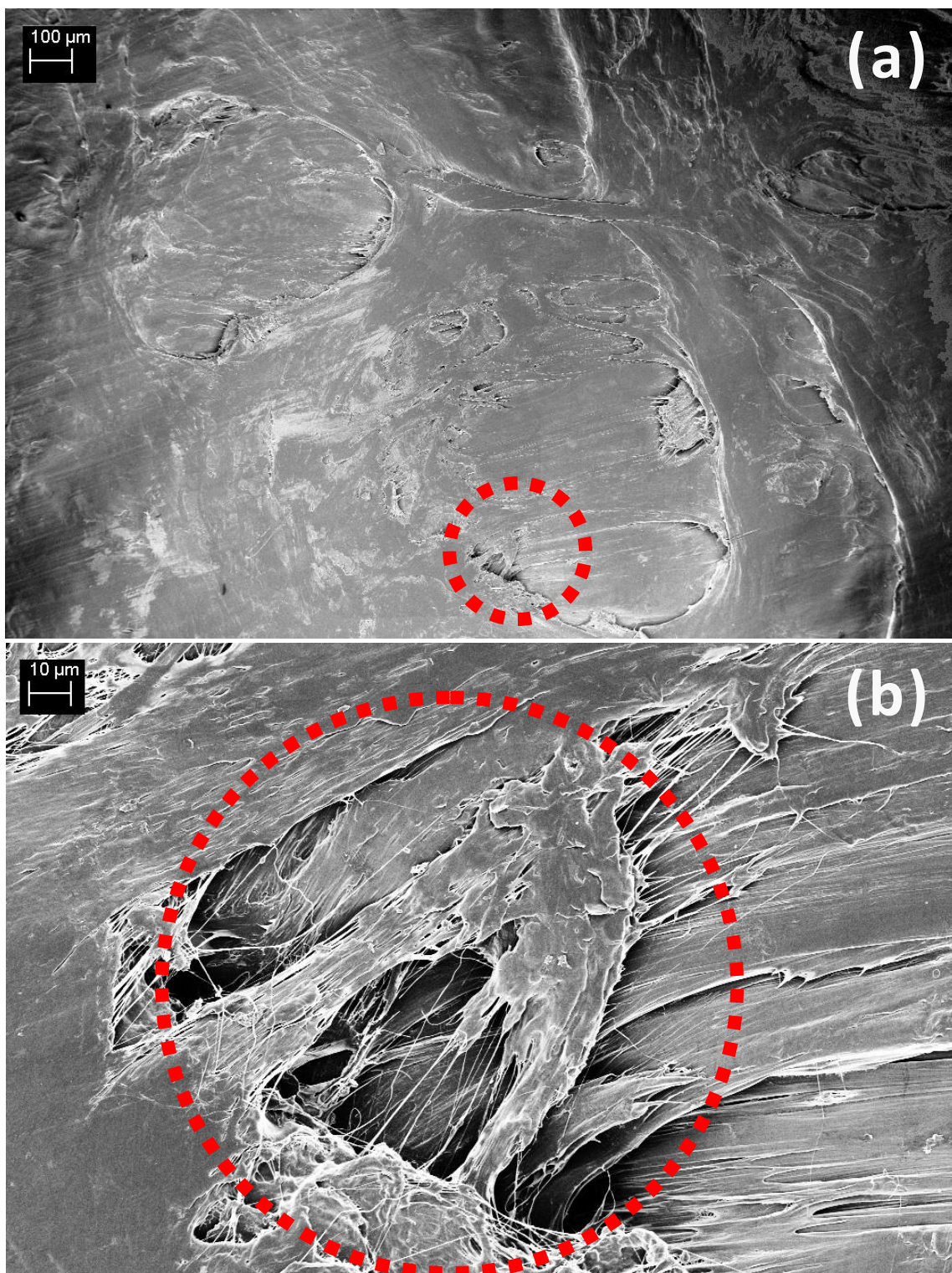


**Figure 5.15** SEM images of the surface of PE-ff10 aged in 10% NaOH solution for 30 days. (a) 50x and 5kV; (b) 500x and 5kV; Red circles highlight empty spaces where fibres leached out



## **Chapter 6**

### **Conclusion and Recommendation**

#### **6.1 Contributions and Summary**

Thermoplastic composites made with nearly 100 % of renewable feedstock were prepared. Two types of renewable fibre, wheat straw and flax fibres were used as the reinforcing material, and renewable high density polyethylene was employed as the matrix. The non-renewable content was limited to additives (antioxidant and coupling agent). Mechanical properties and chemical resistance of these composites were obtained. This is valuable information because there was no previous study systematically investigating these nearly 100 % renewable composites available in the literature.

Chapter 2 reviewed some background information along with relevant literatures. The key role of this chapter was to help readers to understand basic concepts of thermoplastic composites, renewable materials, mechanical properties and environmental aspects.

Chapter 3 described the materials and the methodology in detail. It contains the origin of renewable fibres and renewable thermoplastics used in the study. Preparation steps and characterization techniques were also covered in this chapter.

The results and discussions were presented in Chapter 4 and 5. Chapter 4 showed the mechanical properties and chemical resistance of wheat straw-renewable polyethylene composites. Chapter 5 had the study of flax-renewable polyethylene composites.

#### **6.2 Main Conclusions**

Wheat straw had two different grades in size. Each of them was compounded with high density polyethylene in a co-rotating twin screw extruder. The concentrations of fibres were varied from 0 to 30 wt-%. Then, injection molded samples were prepared for measurement of

properties: tensile, flexural, impact tests. The two grades of flax fibre composites were prepared in the same manner.

The effects of reinforcing fibre size were studied first. Both length and aspect ratio were considered. For both types of fibre composites, a general trend was observed. As the fibre size increased, there was no clear evidence of improvements in flexural (strength and modulus) and tensile (strength, percentage elongation at break) properties, whereas impact (IZOD impact strength, Gardner impact failure energy) properties showed some improvements. There was no substantial difference in size and aspect ratios in post-processed fibres that were actually residing in the matrix.

The effects of fibre concentration were investigated. There were remarkable improvements in flexural strength and modulus when the fibre content increased. However, minor decreases in tensile properties were observed. Furthermore, the impact properties were very sensitive to the concentration of fibres. As the fibre concentration went up, there were significant decreases in both IZOD impact strength and Gardner impact failure energy.

Chemical resistance of these composites was studied by exposing them in six different chemical solutions (hydrochloric acid, acetic acid, sodium hydroxide, ethyl alcohol, industrial detergent, water) for up to thirty days. The increase in weight and leaching behaviour was observed. Samples with greater fibre contents showed rapid increase in weight during chemical ageing. Because there were more fibres exposed on the surface after chemical ageing, it is likely that they contributed to improving the flux of liquids (used for chemical ageing) inside the sample. Among the physical properties, tensile properties were most susceptible to the chemical ageing. One possible reason could be due to the exposed surface area to volume ratio, which was the highest in tensile bars and therefore faster mass transfer taking place into the matrix per volume.

SEM analysis revealed the damage on the surface when exposed to the chemicals. The fibres on the surface had been leached out in the sodium hydroxide solution leaving empty spaces. The fractured surface was also monitored via SEM. Though it failed to show a clear

evidence of strong interfacial interactions between the fibre and the polymer, good dispersions were observed.

### **6.3 Recommendations**

Based on the studies conducted in this thesis, a few recommendations for the future study can be drawn.

Although the extruded and injection molded samples were successfully made in the end, it would have tremendous benefits if the viscoelastic behaviour of the composites were better understood. Dynamic mechanical thermal analysis (DMTA) can be done to evaluate the temperature dependent mechanical properties and viscoelastic behaviour of the composite material. This will improve not only the performance of the final product but also the processing environment. There has been a DMTA analysis done on wheat straw-polypropylene composites which provided significant information regarding their behaviour at a wide range of temperature. (Tajvidi 2012) A similar study is recommended to be conducted.

A long term chemical resistance tests are necessary too. Important information was gathered from 30-day exposure but since plausible applications utilizing these composite materials will require a lengthy life time, monitoring a long term ageing is required.

Ageing of plastic composite materials can occur in various ways. For wider uses, thermal and ultraviolet (UV) ageing should be considered as well. There have been previous studies done on the UV ageing of composite materials and a similar experiment can be performed. (Selden 2004) An accelerated weathering test can be advantageous to apply the composites in outdoor uses. A long term constant exposure to extreme temperatures will assist to characterizing and designing the material too.

## Bibliography

- Amelinckx, S., van Dyck, D., van Landuyt, J., & van Tendeloo, G. (2008). *Handbook of Microscopy Set: Applications in Materials Science, Solid-State Physics and Chemistry*. Wiley-VCH Verlag GmbH.
- ASTM International. (2010). ASTM D1708-10 Standard Test Method for Tensile Properties of Plastics by Use of Microtensile Specimens.
- ASTM International. (2010). ASTM D256-10 Standard Test Methods for Determining the IZOD Pendulum Impact Resistance of Plastics.
- ASTM International. (2010). ASTM D5420-10 Standard Test Method for Impact Resistance of Flat, Rigid Plastic Specimen by Means of a Striker Impacted by a Falling Weight (Gardner Impact).
- ASTM International. (2006). ASTM D543-06 Standard Practices for Evaluating the Resistance of Plastics to Chemical Reagents.
- ASTM International. (2010). ASTM D570-98 Standard Test Method for Water Absorption of Plastics.
- ASTM International. (2008). ASTM D618-08 Standard Practice for Conditioning Plastics for Testing.
- ASTM International. (2010). ASTM D790-10, Standard Test Methods for Flexural Properties of Unreinforced and Reinforced Plastics and Electrical Insulating Materials.
- ASTM International. (2008). ASTM D792-08 Standard Test Methods for Density and Specific Gravity (Relative Density) of Plastics by Displacement.
- Baley, C. (2002). Analysis of the flax fibres tensile behaviour and analysis of the tensile stiffness increase. *Composites - Part A: Applied Science and Manufacturing* , 33 (7), 939-948.
- Black, J., & Kohser, R. A. (2011). *DeGarmo's Materials and Processes in Manufacturing 11th Ed.* Wiley.
- Braskem. (2009). *Green Polyethylene Biopolymer, innovation transforming plastic into sustainability*. Braskem Catalog.
- Bravo, V., Mihai, M., McLeod, M. R., & Bureau, M. N. (2011). Direct Long Biofibre Thermoplastic Composites for Automotive, Aerospace and Transportation Industries. Troy, MI: Society of Plastic Engineer Automotive Composites Conference & Exhibition.
- Cantero, G., Arbelaiz, A., Llano-Ponte, R., & Mondragon, I. (2003). Effects of fibre treatment on wettability and mechanical behaviour of flax/polypropylene composites. *Composite Science and Technology* , 63 (9), 1247-1254.

- Clemons, C. M. (2010). Natural Fibers. In M. Xanthos, *Functional Fillers for Plastics 2nd Ed.* (pp. 195-206). Wiley-VCH Verlag GmbH & Co. KGaA.
- Cui, Y. H., Noruziaan, B., Cheung, M., & Lee, S. (2010). DSC analysis and mechanical properties of wood plastic composites. *Journal of Reinforced Plastics and Composites* , 29, 278-289.
- Echlin, P. (2009). *Handbook of Sample Preparation for Scanning Electron Microscopy and X-Ray Microanalysis*. Springer.
- Fatoni, R. (2012). Product Design of Wheat Straw Polypropylene Composite. *PhD Thesis* . University of Waterloo.
- Flax Council of Canada. (2012). Retrieved from Canada - A Flax Leader.
- Fried, J. (2003). *Polymer Science and Technology*. Prentice Hall.
- Gutierrez, A., & del Rio, J. C. (2003). Lipids from Flax Fibers and Their Fate in Alkaline Pulping. *Journal of Agricultural and Food Chemistry* , 51 (17), 4965-4971.
- Güttler, B. E. (2009). Soy–Polypropylene Biocomposites for Automotive Applications. *MASc Thesis* . University of Waterloo.
- Hamid, H. (2000). *Handbook of Polymer Degradation 2nd Ed.* CRC Press.
- Hauptert, F., & Wetzel, B. (2005). Reinforcement of Thermosetting Polymers by the Incorporation of Micro- and Nanoparticles. In *Polymer Composites* (pp. 45-62). Springer.
- Helbert, W., Cavaille, J. Y., & Dufresne, A. (1996). Thermoplastic nanocomposites filled with wheat straw cellulose whiskers. PartI: Processing and mechanical behavior. *Polymer Composites* , 17 (4), 604-611.
- Hernandez, R. J. (2004). Plastics in Packaging. In *Handbook of Plastics, Elastomers, and Composites* (pp. 627-692). McGraw-Hill.
- Hornsby, P. R., Hinrichsen, E., & Tarverdi, K. (1997). Preparation and properties of polypropylene composites reinforced with wheat and flax straw fibres: Part II Analysis of composite microstructure and mechanical properties. *Journal of Material Science* , 32 (4), 1009-1015.
- ICIS Pricing. (2012). *PET and Intermediates (USA)*. Reed Business Information Limited.
- ICIS Pricing. (2012). *Polyethylene (USA)*. Reed Business Information Limited.
- ISO. (2010). ISO 178:2010 Plastics - Determination of Flexural Properties.
- Karian, H. G. (2003). *Handbook of Polypropylene and Polypropylene Composites, Revised and Expanded*. CRC Press.

- Le Moigne, N., van den Oever, M., & Budtova, T. (2011). A statistical analysis of fibre size and shape distribution after compounding in composites reinforced by natural fibres. *Composites: Part A* , 42 (10), 1542-1550.
- Leong, Y. W., Abu Bakar, M. B., Mohd. Ishak, Z. A., Ariffin, A., & Pukanszky, B. (2004). Comparison of the Mechanical Properties and Interfacial Interactions Between Talc, Kaolin, and Calcium Carbonate Filled Polypropylene Composites. *Journal of Applied Polymer Science* , 91 (5), 3315-3326.
- Liu, W., Wang, Y. J., & Sun, Z. (2003). Effects of polyethylene-grafted maleic anhydride (PE-g-MA) on thermal properties, morphology, and tensile properties of low-density polyethylene (LDPE) and corn starch blends. *Journal of Applied Polymer Science* , 88 (13), 2904-2911.
- McKean, W. T., & Jacobs, R. S. (1997). *Wheat Straw as a Paper Fiber Source*. Clean Washington Center.
- Ministry of Agriculture and Agri-Food Canada. (2012). *Canada: Grains and Oilseeds Outlook*. Ministry of Agriculture and Agri-Food Canada.
- Mohanty, A. K., Misra, M., Drzal, L. T., Selke, S. E., Harte, B. R., & Hinrichsen, G. (2005). Natural Fibers, Biopolymers, and Biocomposites: An Introduction. In A. K. Mohanty, M. Misra, & L. T. Drzal, *Natural Fibers, Biopolymers, and Biocomposites* (pp. 1-36). Taylor and Francis.
- Morschbacker, A. (2009). Bio-Ethanol Based Ethylene. *Journal of Macromolecular Science* , 49 (2), 79-84.
- Murphy, J. (1996). *The additives for plastics handbook: antioxidants, antistatics, compatibilisers, conductive fillers, flame-retardants, pigments, plasticisers, reinforcements : classification, data, tables, descriptions, market trends, suppliers/brand names*. Elsevier Advanced Technology.
- Oksman, K., Skrifvars, M., & Selin, J. F. (2003). Natural fibres as reinforcement in polylactic acid (PLA) composites. *Composite Science and Technology* , 63 (9), 1317-1324.
- Panthapulakkal, S., Zereshkian, A., & Sain, M. (2006). Preparation and characterization of wheat straw fibers for reinforcing application in injection molded thermoplastic composites. *Bioresource Technology* , 97 (2), 265-272.
- Pritchard, G. (1998). *Plastic Additives: An A-Z Reference*. Springer.
- Puglia, D., Terenzi, A., Barbosa, S. E., & Kenny, J. M. (2008). Polypropylene-natural fibre composites. Analysis of fibre structure modification during compounding and its influence on the final properties. *Composite Interfaces* , 15 (2/3), 111-129.

- Reddy, R. C., Sardashti, P. A., & Simon, L. C. (2010). Preparation and characterization of polypropylene–wheat straw–clay composites. *Composites Science and Technology* , 70 (12), 1674-1680.
- Selden, R., Nystrom, B., & Langstrom, R. (2004). UV aging of poly(propylene)/wood-fiber composites. *Polymer Composites* , 25 (5), 543-553.
- Sharma, A. M. (2012). Mechanical Behaviour, Water Absorption and Morphology of Wheat Straw, Talc, Mica and Wollastonite filled Polypropylene Composites. *MASc Thesis* . University of Waterloo.
- Tajvidi, M., Sharma, A. M., & Simon, L. C. (2012). Viscoelastic Properties of Wheat Straw Fiber/Talc/Polypropylene Composites for Automotive Applications. *SPE Automotive Composites Conference and Exhibition*. Troy, MI.
- Vink, E. T., Rabago, K. R., Glassner, D. A., & Gruber, P. R. (2003). Applications of life cycle assessment to NatureWorks polylactide (PLA) production. *Polymer Degradation and Stability* , 80, 403-419.
- Witten, E. (2010). *Composites Market: Market Developments, Challenges, and Chances*. Germany: AVK Federation of Reinforced Plastics.
- Zini, E., & Scandola, M. (2011). Green Composites: An Overview. *Polymer Composites* , 32 (12), 1905-1915.

# Appendix

## Particle Size Analysis

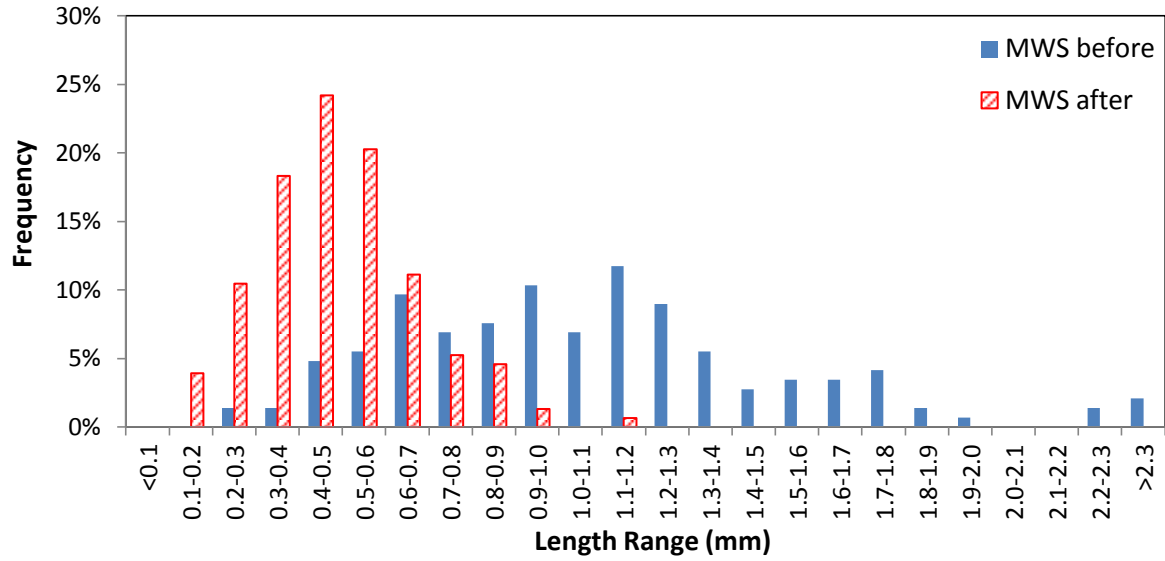


Figure A. 1 Length in mm of medium wheat straw (MWS) particles before and after processing

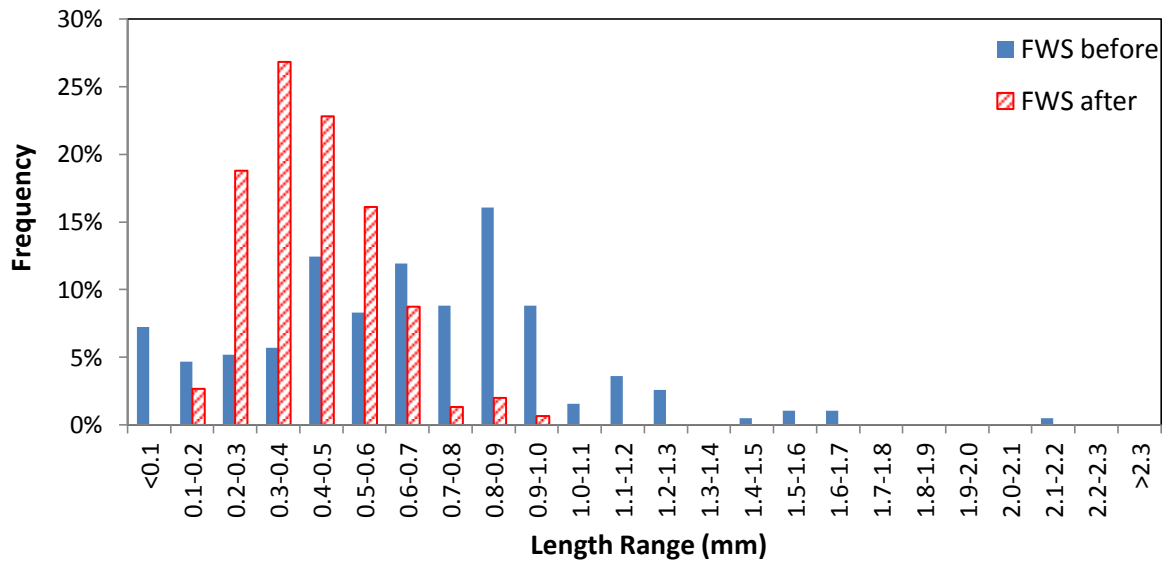


Figure A. 2 Length in mm of fine wheat straw (FWS) particles before and after processing



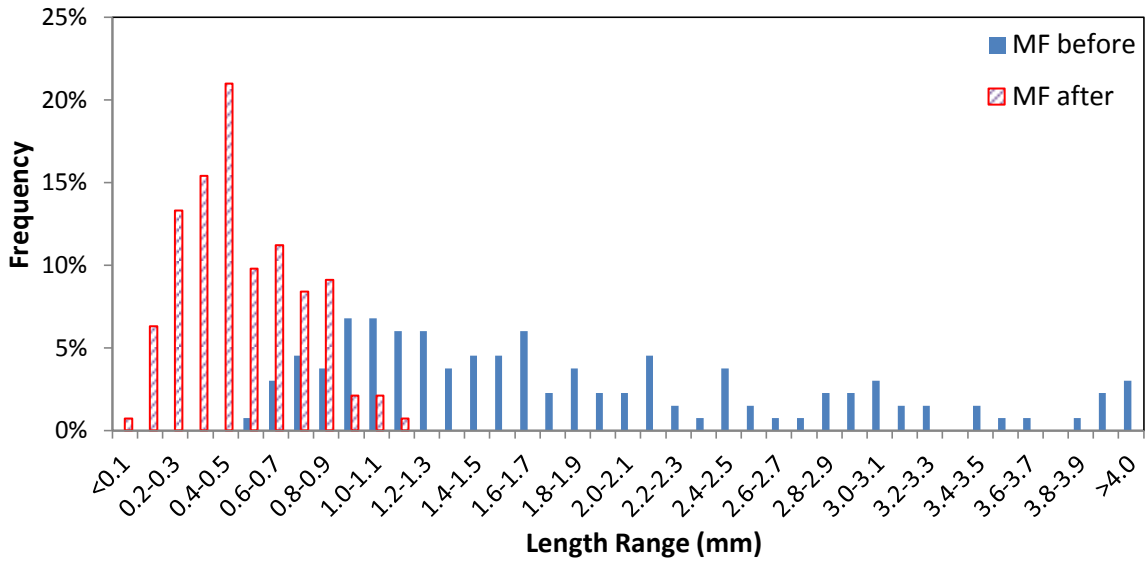


Figure A. 3 Length in mm of medium flax (MF) particles before and after processing

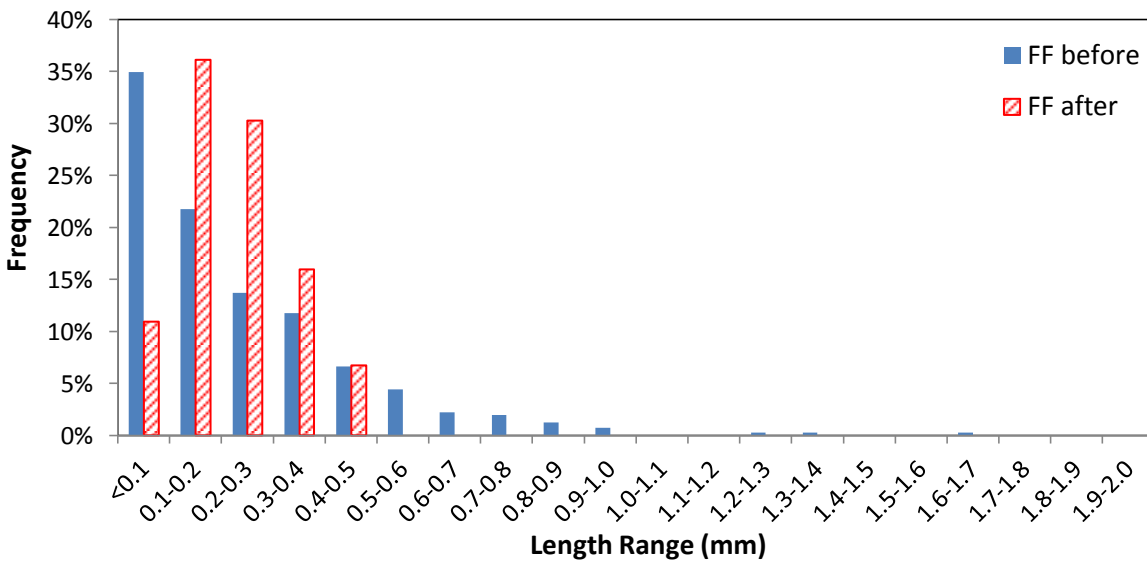
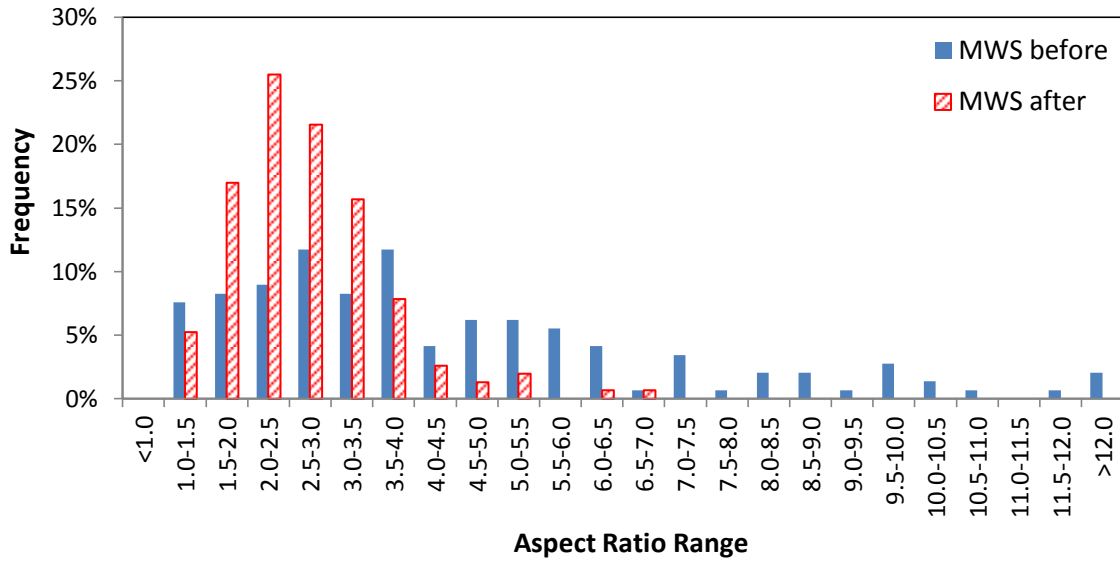
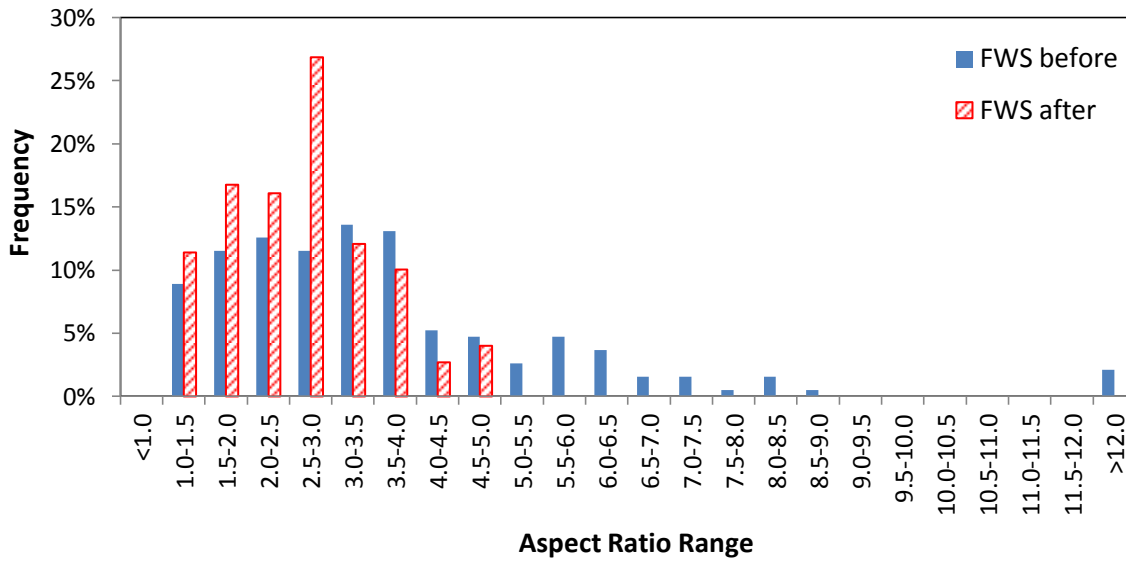


Figure A. 4 Length in mm of fine flax (FF) particles before and after processing



**Figure A. 5 Aspect ratio of medium wheat straw (MWS) particles before and after processing**



**Figure A. 6 Aspect ratio of fine wheat straw (FWS) particles before and after processing**

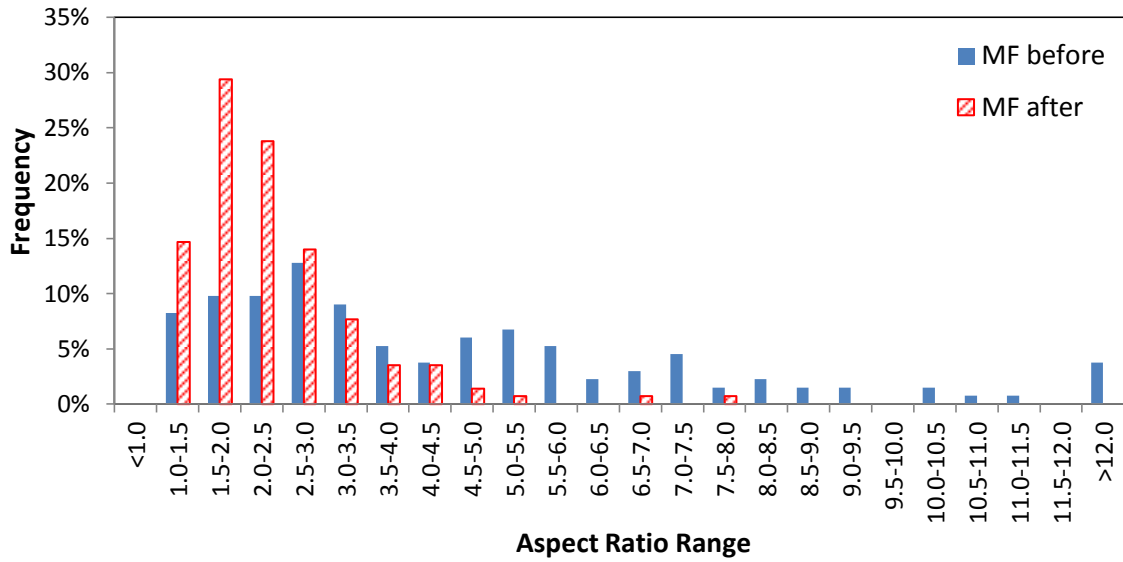


Figure A. 7 Aspect ratio of medium flax (MF) particles before and after processing

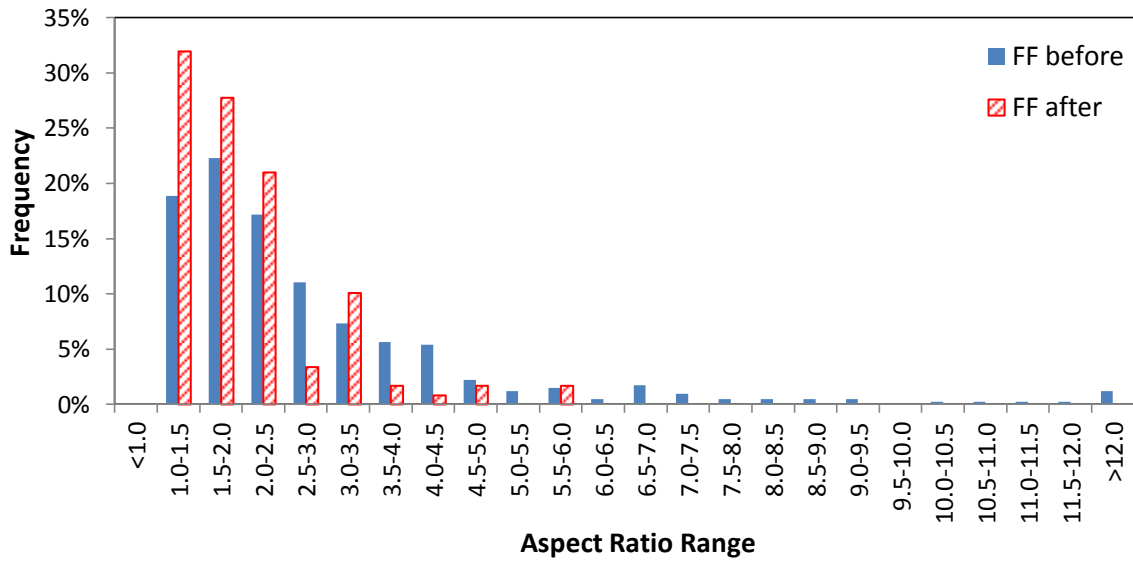
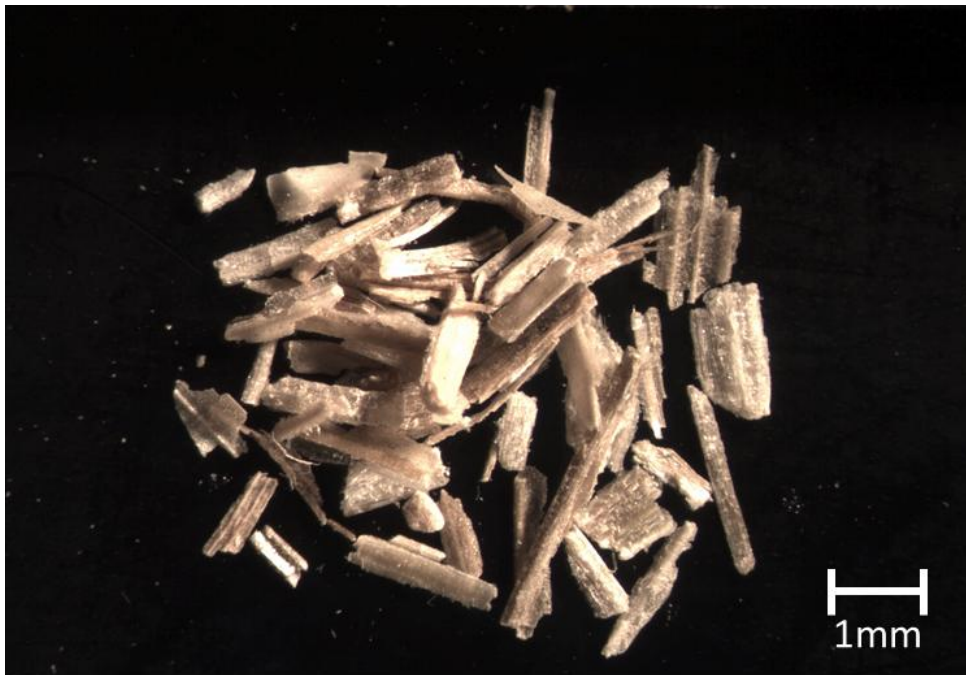


Figure A. 8 Aspect ratio of fine flax (FF) particles before and after processing

**Optical Microscopic Images of Fibres**



**Figure A. 9 Optical microscopic image of medium wheat straw (mws)**



**Figure A. 10 Optical microscopic image of fine wheat straw (fws)**



**Figure A. 11** Optical microscopic image of medium flax (mf)



**Figure A. 12** Optical microscopic image of fine flax (ff)

Scanned Electron Microscopic (SEM) Images

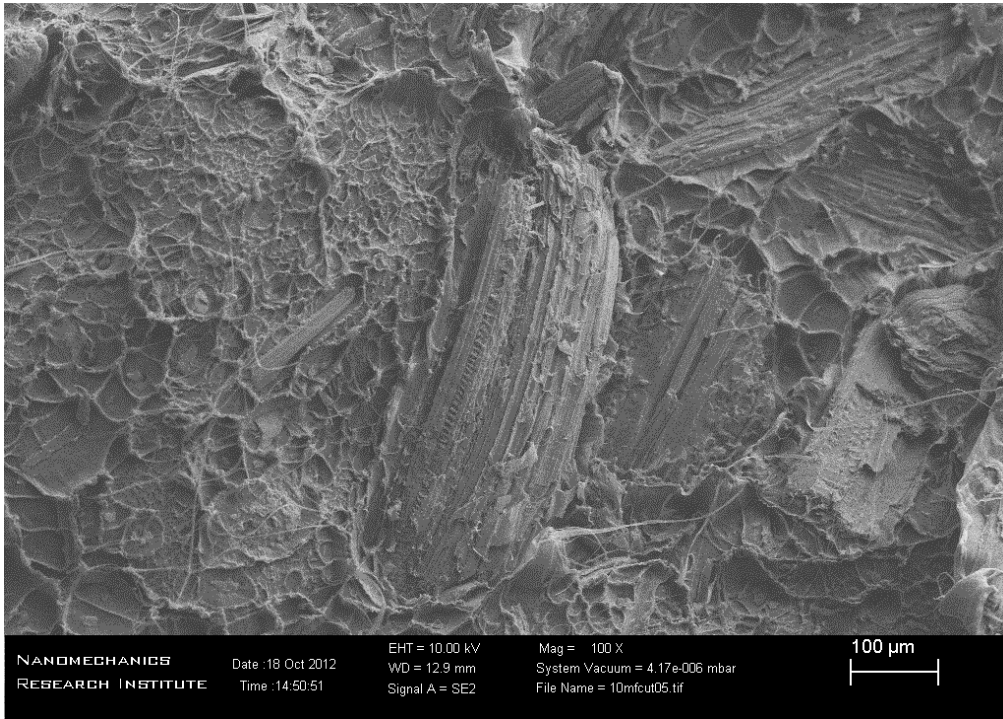


Figure A. 13 SEM image (100x, 10kV) of the fractured surface of PE-mf10

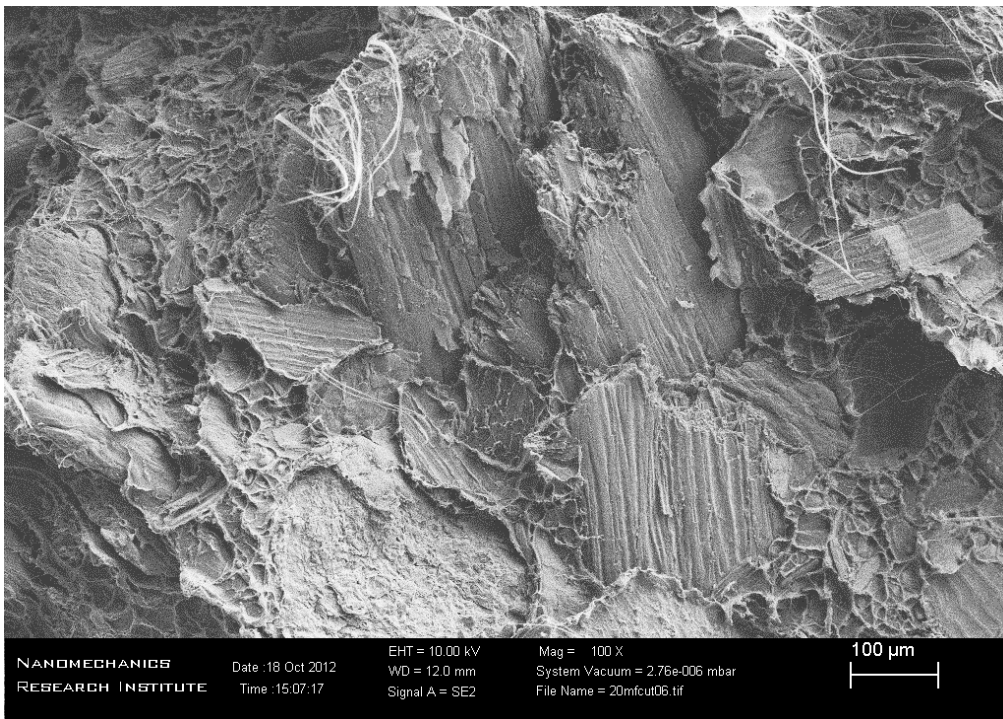
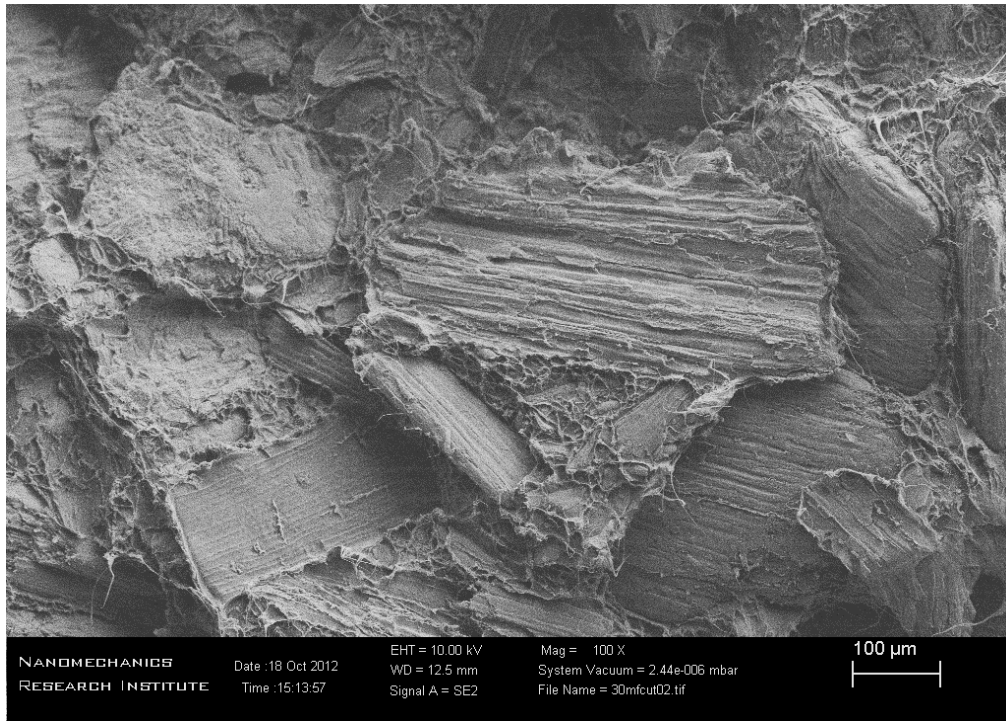
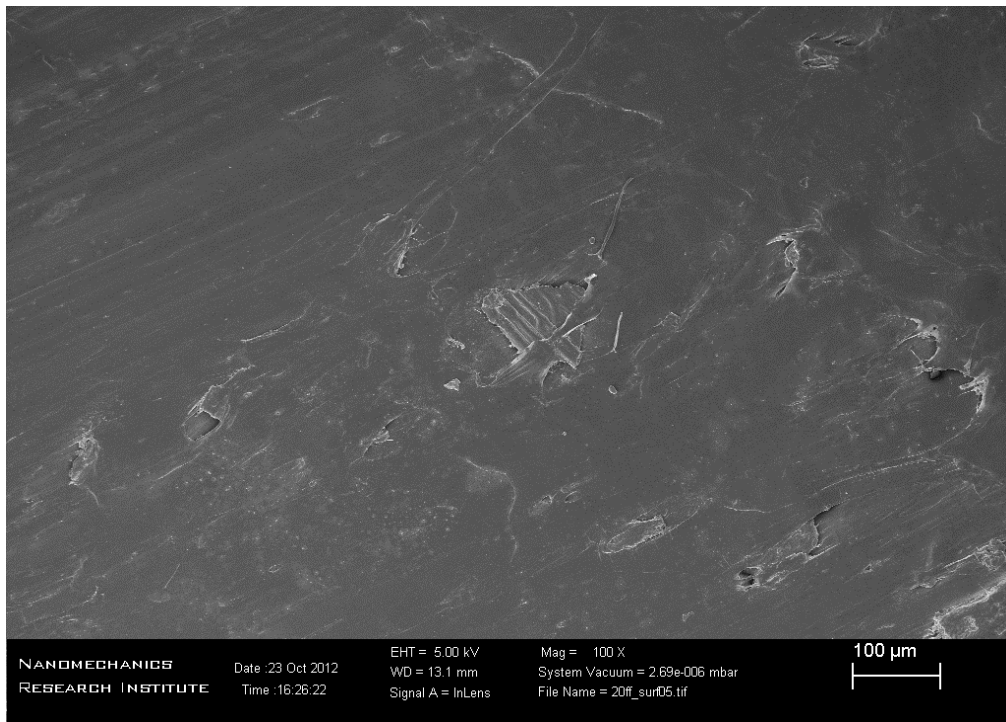


Figure A. 14 SEM image (100x, 10kV) of the fractured surface of PE-mf20





**Figure A. 15 SEM image (100x, 10kV) of the fractured surface of PE-mf30**



**Figure A. 16 SEM image (50x, 5kV) of the surface of PE-ff20**

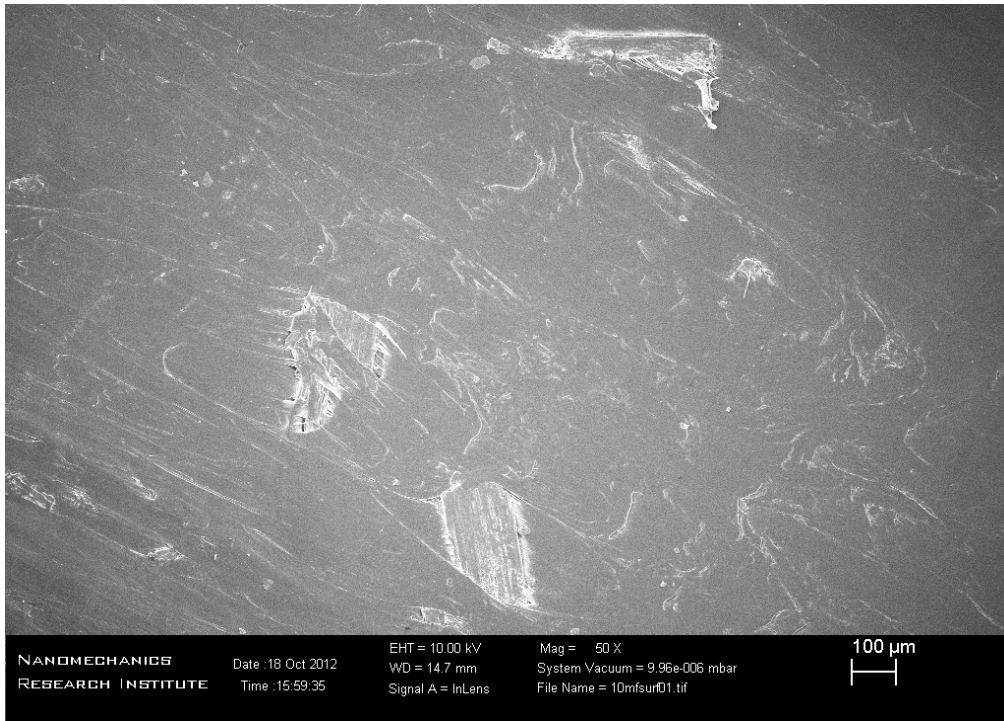


**Figure A. 17 SEM image (50x, 10kV) of the surface of PE-mf10**

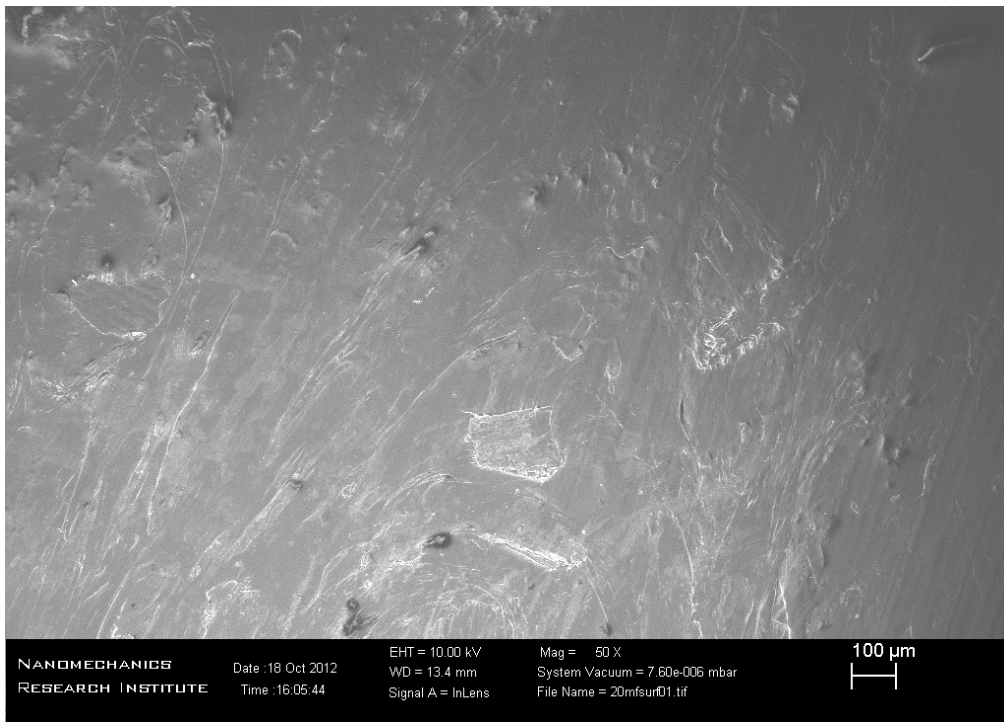



**Figure A. 18 SEM image (50x, 10kV) of the surface of PE-mf20**



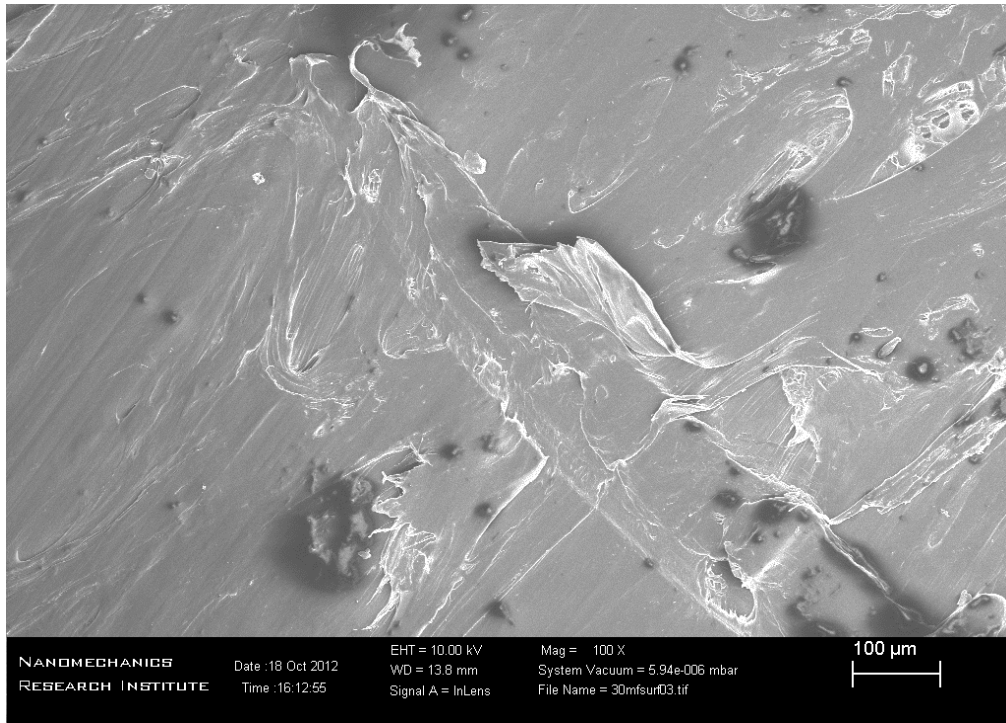


**Figure A. 19 SEM image (100x, 10kV) of the surface of PE-mf30**

	<p><b>AIB-VINÇOTTE International</b> s.a. / n.v.          SAFETY, QUALITY, ENVIRONMENT          Member of the Group AIB-VINÇOTTE          Head office : Boulevard A. Playens 80 - B-1020 Brussels / Belgium</p> <p><b>VINÇOTTE - CERTEST PRODUCTS</b>          Everest - Leuvensesteenweg 246 / B-1800 Vilvoorde / Belgium          Tel. : +32(0)2 674.57.50 - Fax : +32(0)2 674.57.85          E-Mail : okbiobased@vincotte.be</p>															
<p><b>CERTIFICATE FOR AWARDING AND USE OF THE          'OK BIOBASED' CONFORMITY MARK</b>          No. B 11-082-A</p> <p><b>Issued by AIB-VINÇOTTE International</b></p>																
<p><b>For the product(s) described hereafter :</b></p> <table border="0"> <tr> <td style="width: 30%;">Product Domain :</td> <td>Biobased Products</td> </tr> <tr> <td>Product Group :</td> <td>Raw material</td> </tr> <tr> <td>Product Family :</td> <td>Bio material</td> </tr> <tr> <td>Product Type :</td> <td>Granulates</td> </tr> <tr> <td>Trade mark :</td> <td>I'm green™</td> </tr> <tr> <td>Product description / Particularities :</td> <td><b>HDPE grades :</b> SGF 4950, SGF4950, SH47200, SHC7290, SHD7250LSL, SHE150, SGAM9450F</td> </tr> <tr> <td></td> <td>Color : natural translucent</td> </tr> </table>			Product Domain :	Biobased Products	Product Group :	Raw material	Product Family :	Bio material	Product Type :	Granulates	Trade mark :	I'm green™	Product description / Particularities :	<b>HDPE grades :</b> SGF 4950, SGF4950, SH47200, SHC7290, SHD7250LSL, SHE150, SGAM9450F		Color : natural translucent
Product Domain :	Biobased Products															
Product Group :	Raw material															
Product Family :	Bio material															
Product Type :	Granulates															
Trade mark :	I'm green™															
Product description / Particularities :	<b>HDPE grades :</b> SGF 4950, SGF4950, SH47200, SHC7290, SHD7250LSL, SHE150, SGAM9450F															
	Color : natural translucent															
<p><b>Class (between 1 &amp; 4):</b> The product is assigned to class 4, meaning: <b>80 % ≤ Biobased Carbon Content of the product ≤ 100 %</b>      <b>★ ★ ★ ★</b></p>																
<p><b>Conformity examination applied for by :</b> <b>BRASKEM SA</b>          Centro Prod. PPPE Triunfo          BR 386 - Rodovia Tabal-Canoas, lote 04, 850          Triunfo - RS - CEP 95653-000          Brazil</p>																
<p><b>Criteria for certification :</b></p> <ul style="list-style-type: none"> <li>• AVI Test Program 'OK biobased' with reference OK 20 edition A</li> <li>• Methodology conform to ASTM D 6866: "Standard Test Methods for Determining the Biobased Content of Solid, Liquid, and Gaseous Samples Using Radiocarbon Analysis"</li> </ul>																
<p><b>Validity of the certificate :</b> From 28 April 2011 till 28 April 2014</p>																
<p><b>Conclusions of the examination :</b> The products comply with the above mentioned certification criteria, as confirmed by the test report of AVI no. 09/ 60305554/ 104171p</p>																
<p><b>Applicable certification system :</b> Type examination followed by supervision through verification tests on samples from the distributor's stocks and/or of the market.          The conformity of the product is guaranteed by the procedures for awarding and use of the 'OK biobased' conformity mark. This only applies for specimen bearing the 'OK biobased' mark.</p>																
<p><b>Caution :</b> The use of OK biobased-certified polymers / materials is not a guarantee that intermediate or finished product into which it is incorporated complies with the requirements of the OK biobased programme.</p>																
<p>This certificate is issued in English.</p>		<p>Brussels, 28 April 2011</p>														
<p>L. TORDEUR          Contact Manager</p>	<p>For the Certification Committee          Ph. DEWOLFS          President of the Committee</p>															
<p><b>Annex</b></p>	<p>09-CERTOKR-e</p>															

**Polyethylene bio-based carbon content analysis report**

**SAFETY DATA SHEET**

**Product:** High Density Polyethylene – Green - Copolymer ethylene with 1-butene

**Revision:** 00      **Date:** 11.24.2011      **Page:** 1 /9      **FSP-0603-00089**

**1- IDENTIFICATION OF THE SUBSTANCE/MIXTURE AND COMPANY/ UNDERTAKING**

Product name:	SGM9450F
Company:	BRASKEM
Address:	Centro Prod. PE5 Triunfo BR 386 – Rodovia Tabai Canoas CEP 95853-200 Triunfo – RS – Brazil
Telephone number:	55(51) 3721-8600
Company:	BRASKEM
Address:	Escritório Eldorado SP Avenida Nações Unidas 8501 CEP 05425-070 São Paulo – SP – Brazil
Telephone number:	55(11) 3576-9000
Emergency telephone number:	55(51) 3721-8600 55(51) 3457-5500
Home Page:	<a href="http://www.braskem.com.br">www.braskem.com.br</a>

**2- HAZARDS IDENTIFICATION**

Most important hazards:	Not classified as hazardous.
Product effects	
Adverse effects to the human health:	In case of dust, Braskem suggests it to be treated as annoying dust or particulate, by international recommendations. Dust may cause respiratory irritation if inhaled.
Environmental effects:	It's expected that the product shows high persistence and slow degradability.
Physical and chemical hazards:	Not classified as physical hazards.
Classification of the substance or mixture:	Not classified as hazardous.
Label elements according to Regulation 1272:2008 (GHS)	
Symbol:	Not applicable.
Signal word:	Not applicable.
Hazard Statement:	Not applicable.

**MSDS of Polyethylene** – the rest of the data sheet can be found in Braskem web page



## ®IRGANOX 1010

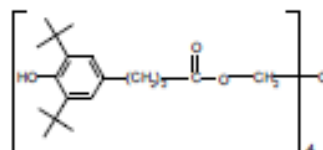
### Phenolic Primary Antioxidant for Processing and Long-Term Thermal Stabilization

**Characterization**    ®IRGANOX 1010 - a sterically hindered phenolic antioxidant - is a highly effective, non discoloring stabilizer for organic substrates such as plastics, synthetic fibers, elastomers, adhesives, waxes, oils and fats. It protects these substrates against thermo-oxidative degradation.

**Chemical Name**    Pentaerythritol Tetrakis(3-(3,5-di-tert-butyl-4-hydroxyphenyl)propionate)

**CAS Number**        6683-19-8

**Structure**            ®IRGANOX 1010



**Molecular weight**    1178

**Applications**        ®IRGANOX 1010 can be applied in polyolefins, such as polyethylene, polypropylene, polybutene and olefin copolymers such as ethylene-vinylacetate copolymers. Also, its use is recommended in other polymers such as polyacetals, polyamides and polyurethanes, polyesters, PVC, styrene homo- and copolymers, ABS, elastomers such as butyl rubber (IIR), SBS, SEBS, EPM and EPDM as well as other synthetic rubbers, adhesives, natural and synthetic tackifier resins, and other organic substrates.

**Features/ Benefits**    ®IRGANOX 1010 has good compatibility, high resistance to extraction and low volatility. It is odorless and tasteless.

The product can be used in combination with other additives such as costabilizers (e.g. thioethers, phosphites, phosphonites), light stabilizers and other functional stabilizers. The effectiveness of the blends of ®IRGANOX 1010 with ®IRGAFOS 168 (®IRGANOX B-blends) or with ®IRGAFOS 168 and HP-136 (®IRGANOX HP products) is particularly noteworthy.

<b>Product Forms</b>	Code:	Appearance:
	powder	white, free-flowing powder
	FF (C)	white, free-flowing granules
	DD	white to slightly green pellets

Distributed by

Wi

**Guidelines for Use** Already 500 ppm - 1000 ppm of <sup>®</sup>IRGANOX 1010 provide long-term thermal stability to the polymer. Concentrations up to several percent may be used depending on the substrate and the requirements of the end application.  
 In polyolefins the concentration levels for <sup>®</sup>IRGANOX 1010 range between 0.05% and 0.4% depending on substrate, processing conditions and long-term thermal stability requirements. The optimum level has to be determined application specific.  
 Concentration levels of <sup>®</sup>IRGANOX 1010 in hot melt adhesives range from 0.2% to 1%, in synthetic tackifier resins, <sup>®</sup>IRGANOX 1010 concentration ranges between 0.1% and 0.5%. Extensive performance data of <sup>®</sup>IRGANOX 1010 in various organic polymers and applications are available upon request.

**Physical Properties**

Melting Range (°C)	110-125
Flashpoint (°C)	297
Specific Gravity (20°C)	1.15 g/cm <sup>3</sup>
 Bulk density	 powder: 530 - 630 g/l
	FF (C): 480 - 570 g/l
	DD: 450 - 550 g/l
 Solubility (20°C)	 g/100g solution
Acetone	47
Chloroform	71
Ethanol	1.5
Ethylacetate	47
n-Hexane	0.3
Methanol	0.9
Methylene Chloride	63
Toluene	60
Water	<0.01

**Handling & Safety** In accordance with good industrial practice, handle with care and prevent contamination of the environment. Avoid dust formation and ignition sources.  
 For more detailed information please refer to the material safety data sheet.

**Registration** <sup>®</sup>IRGANOX 1010 is listed on the following inventories:

Australia: AICS	Canada: DSL	China: First Import
Europe: EINECS	Japan: MITI	Korea: ECL
Philippines: PICCS	USA: TSCA	

<sup>®</sup>IRGANOX 1010 is approved in many countries for use in food contact applications.  
 For detailed information refer to our Positive List or contact your local sales office.

**IMPORTANT:** The following supersedes Buyer's documents. SELLER MAKES NO REPRESENTATION OR WARRANTY, EXPRESS OR IMPLIED, INCLUDING OF MERCHANTABILITY OR FITNESS FOR A PARTICULAR PURPOSE. No statements herein are to be construed as inducements to infringe any relevant patent. Under no circumstances shall Seller be liable for incidental, consequential or indirect damages for alleged negligence, breach of warranty, strict liability, tort or contract arising in connection with the product(s). Buyer's sole remedy and Seller's sole liability for any claims shall be Buyer's purchase price. Data and results are based on controlled or lab work and must be confirmed by Buyer by testing for its intended conditions of use. The product(s) has not been tested for, and is therefore not recommended for, uses for which prolonged contact with mucous membranes, abraded skin, or blood is intended; or for uses for which implantation within the human body is intended.

Date first Edition: Product Name: <sup>®</sup>IRGANOX 1010  
 Printing Date: Aug-08

page 2  
 ©Ciba Specialty Chemicals, Inc.

**MSDS of Antioxidant IRGANOX1010**